DISSECTING NEUROFIBROMATOSIS TYPE 1 RELATED

VASCULOPATHY

Elisabeth A. Lasater

Submitted to the faculty of the University Graduate School
in partial fulfillment of the requirements
for the degree
Doctor of Philosophy
in the Department of Biochemistry and Molecular Biology
Indiana University

December 2009

Accepted by the Faculty of Indiana University, in partial
fulfillment of the requirements for the degree of Doctor of Philosophy.

_____
David A. Ingram, Jr., M.D., Chair

_____
Simon J. Conway, Ph.D.

Doctoral Committee

_____
Reuben Kapur, Ph.D.

September 28th, 2009

_____
D. Wade Clapp, M.D.

_____
Cynthia M. Hingtgen, M.D., Ph.D.

ACKNOWLEDGEMENTS

I would like to first acknowledge my mentor, Dr. David Ingram. Thank you for your patience and guidance throughout my graduate career. The knowledge I have gained during my time in your lab is immeasurable and you have been instrumental in shaping my scientific career. I truly appreciate all your time and help. I would also like to thank all the members of Dr. Ingram's lab, both past and current. Thank you for unending support. Each of you has contributed to my scientific career and as well as defining my time in Indiana.

I would like to acknowledge the members of my research committee, Drs. Simon J. Conway, D. Wade Clapp, Reuben Kapur and Cynthia M. Hingtgen. Thank you for your time and support throughout my graduate career. Your expertise and dedication shaped my thesis project and challenged me to grow as a scientist.

To the faculty and staff of the department of Biochemistry and Molecular Biology, I thank you for your assistance. Your knowledge and dedication to the program has provided me a solid platform from which to begin my own career. To the faculty and staff of the University Graduate School, thank you for your assistance and guidance throughout my term as a graduate student.

Finally, I would like to acknowledge my friends and family for their unending support. To my parents, Steve and Shelly, my sister, Sarah, and my grandparents, John and Joyce, thank you for always believing in me and for your encouragement through this journey. To Chris, thank you for being a graduate student with me and always believing that I could complete this task. Most

ABSTRACT

Elisabeth A. Lasater

DISSECTING NEUROFIBROMATOSIS TYPE 1 RELATED VASCULOPATHY

Neurofibromatosis type 1 (NF1) is a genetic disorder resulting from

mutations in the tumor suppressor gene *NF1*. *NF1* encodes the protein

neurofibromin, which functions to negatively regulate p21^{Ras} signaling. NF1 has

a wide range of clinical manifestations, including vascular disease, which is

characterized by neointima formation and subsequent vessel occlusion. Despite

numerous clinical observations of NF1 vasculopathy, the pathogenesis of

vascular lesion formation remains unclear. To determine the consequence of

Nf1 haploinsufficiency in vascular disease, we generated an *in vivo* model for

dissecting vascular lesion formation. In response to mechanical arterial injury,

Nf1$^{+/-}$ mice have significantly enhanced neointima formation characterized by an

accumulation of vascular smooth muscle cells (VSMCs) and excessive cellular

proliferation and Ras activation. Further, using the pharmacological antagonist,

imatinib mesylate, we identified that neointima formation in *Nf1*$^{+/-}$ mice was

directly dependent on Ras signaling through either the platelet derived growth

factor β receptor (PDGF-*β*R) and/or the C-kit receptor activation. These

observations identify a molecular mechanism of neointima formation given that

our group has previously demonstrated that *Nf1*$^{+/-}$ VSMCs have hyperactive Ras

signaling through PDGF-*β*R activation and *Nf1*$^{+/-}$ bone marrow derived cells

(BMDCs) have increased recruitment and survival in response to C-kit activation

compared to WT controls. In order to dissect the cellular contribution to

neointima formation, we utilized *cre/lox* technology and adoptive hematopoietic

stem cell transfer techniques to genetically delete one allele of *Nf1* in endothelial

cells, VSMCs or BMDCs individually to test which cell lineage is predominant in

NF1 vasculopathy. Surprisingly, in response to carotid artery injury,

heterozygous inactivation of *Nf1* in BMDCs alone was necessary and sufficient

for neointima formation. Specifically, *Nf1* haploinsufficiency in BMDCs resulted

in an infiltration of macrophages into the neointima, providing evidence of

"vascular inflammation" as factor in NF1 vasculopathy. Further, we demonstrate

for the first time that NF1 patients have evidence of chronic inflammation

determined by increased concentrations of circulating monocytes and pro-

inflammatory cytokines. In sum, we provide genetic and cellular evidence of

vascular inflammation in NF1 patients and $Nf1^{+/-}$ mice and provide a framework

for understanding the pathogenesis of NF1 vasculopathy and potential

therapeutic and diagnostic interventions.

David A. Ingram, Jr., M.D.

TABLE OF CONTENTS

LIST OF FIGURES

LIST OF ABBREVIATIONS

*α*SMA	Alpha-Smooth Muscle Actin
ATP	Adenosine Triphosphate
BM	Bone Marrow
BMDCs	Bone Marrow Derived Cells
cAMP	Cyclic Adenosine 3',5'-Monophosphate
CPDL	Cumulative Population Doubling Level
DNA	Deoxyribonucleic Acid
ECs	Endothelial Cells
eNOS	Endothelial Nitric Oxide Synthase
Erk	Extracellular Signal-Related Kinase
FGF	Fibroblast Growth Factor
GAP	GTPase Activating Protein
GDP	Guanosine Diphosphate
GFP	Green Fluorescent Protein
GM-CSF	Granulocyte/Macrophage Colony Stimulating Factor
GRD	GAP Related Domain
GTP	Guanosine Triphosphate
H&E	Hematoxylin and Eosin
IFN-γ	Interferon gamma
I/M	Intima-to-Media Ratio
ICAM	Intracellular Adhesion Molecule
IL	Interleukin
MCP-1	Monocyte Chemoattractant Protein 1
M-CSF	Macrophage Colony Stimulating Factor
MMP	Matrix Metalloproteinase
MNC	Mononuclear Cell
NF1	Neurofibromatosis Type 1
NIH	National Institutes of Health
OPN	Osteopontin
PBS	Phosphate Buffered Saline
PCR	Polymerase Chain Reaction
PDGF	Platelet Derived Growth Factor
PDT	Population Doubling Time
PKA	Protein Kinase A
RNA	Ribonucleic Acid
SCF	Stem Cell Factor
SEM	Standard Error of the Mean
shRNA	Short Hairpin RNA
TNFα	Tumor Necrosis Factor α
VCAM	Vascular Cell Adhesion Molecule
VEGF	Vascular Endothelial Growth Factor
VSMCs	Vascular Smooth Muscle Cells
WT	Wildtype

INTRODUCTION

Neurofibromatosis Type 1.

Neurofibromatosis type 1 (NF1) is an autosomal dominate disorder that affects 1 in 3500 individuals (1). NF1 results from mutations in the tumor suppressor gene *NF1*, which encodes the protein product neurofibromin (2). The *NF1* gene, originally described in 1990 (3-5), spans 350 kilobases of DNA on chromosome 17 and contains 60 exons (6). Although NF1 is generally considered a familial disorder, approximately fifty-percent of patients do not have an affected parent. Consistent with this finding, the *NF1* gene has been described as having one of the highest mutation rates in humans (7, 8), with over 240 different mutations described throughout the gene (9). Mutations described to date include insertions, duplications, substitutions, nonsense mutations, frameshift mutations, and gene deletions (10), resulting in little or no protein product. The germline mutations that cause NF1 affect only one allele of the *NF1* gene (11), however, loss of heterozygosity has been described in from primary tumor samples taken from NF1 patients, indicating the role of *NF1* as a tumor suppressor gene (12).

NF1 is a complete penetrance genetic disorder and manifestation of the disease varies greatly among patients as well as with age. Clinical diagnosis of NF1 is confirmed if a patient meets two or more of the criteria established by the National Institutes of Health (NIH) (13) which is defined as: 1) the presence of six or more café-au-lait macules over 5 millimeters (mm) in diameter for prepubertal

individuals or 15mm in greatest diameter for postpubertal individuals, 2) two or more neurofibromas or one plexiform neurofibroma, 3) axillary or inguinal freckling, 4) optic glioma, 5) two or more Lisch nodules, 6) distinctive osseous abnormality, or 7) a first degree relative diagnosed with NF1 by the NIH criteria (13). Additional manifestations of NF1 which complicate clinical management include learning disabilities, malignant peripheral nerve sheath tumors, myeloid leukemias, and vascular lesions.

NF1 and Vascular Disease.

One of the least studied complications of NF1 involves disorders of the cardiovascular system. Although the exact frequency of vascular lesions is unknown, vasculopathy is an under-recognized complication of the disease and contributes to excess morbidity and mortality particularly among younger patients (14-17). NF1 vasculopathy was first described in 1945 (18) and was further classified in 1974 based on the size of the lesion and the vessel effected (19). Specifically, NF1 patients develop aneurysms, stenosis and arterial occlusions that result in cerebral and visceral infarcts (14-17, 20). NF1 vascular lesions are characterized by an accumulation of vascular smooth muscle cells (VSMCs) in the intima area of the vessel (termed neointima formation) resulting in lumen occlusion (14, 21, 22).

In 2001, an analysis of 3,253 death certificates of persons with NF1 indicated that the median age of death for NF1 patients was fifteen years less that of the general population (16). In this report, a diagnosis suggestive of NF1

vasculopathy was listed 7.2 times more often than expected among NF1 patients less than 30 years old at time of death and 2.2 times more often than expected among patients 30 to 40 years old at the time of death (16). Another study demonstrated that 2.5% of children with NF1 who had undergone brain MRI were found to have cerebrovascular system abnormalities including narrowed vessels, moya-moya, vascular stenosis and aneurysm (17). Although rare, sudden death in individuals with NF1 has been reported in both adults and children and vascular lesions have been identified in these patients. Most recently, a 22-month old male was found to have 33% luminal reduction in the left main coronary artery and left anterior descending coronary artery at the time of death (22). In an unrelated patient, an adolescent male had 90% luminal occlusion of the left main coronary artery and left anterior descending coronary artery at the time of death (22). Vascular lesions described in both patients were consistent with NF1 vasculopathy with histopathology including intimal hyperplasia and VSMC proliferation (21). Despite numerous clinical observations, the molecular mechanism that underlies the cardiovascular complications of NF1 is virtually unknown. In 2002, the NF1 Cardiovascular Task Force made research recommendations with included the development of a valid experimental model of NF1 vasculopathy in a laboratory animal or an *in vitro* system to dissect the molecular basis of NF1-associated cardiovascular disease in order to improve care for patients (14). Therefore, studies outlined in this project developed an expandable *in vivo* murine model of NF1 vasculopathy to test the hypothesis that:

1. *Nf1$^{+/-}$* mice have increased neointima formation in response to vascular injury compared to wildtype (WT) controls.

2. Heterozygous inactivation of *Nf1* in VSMCs directly leads to increased neointima formation in response to vascular injury compared to WT controls.

3. Increased neointima formation in *Nf1$^{+/-}$* mice compared to WT controls is a result of hyperactive signaling through the PDGF-receptor.

Neurofibromin.

Neurofibromin, the product encoded by *NF1*, is a 2818 amino acid protein (23) that contains 60 exons (6). Neurofibromin is expressed in all cell lineages analyzed to date, including neurons, glial cells, Schwann cells, leukocytes, astrocytes, vascular smooth muscle cells (VSMCs), endothelial cells (ECs) and fibroblasts (24-28). *In vivo* studies have demonstrated that at least some neurofibromin expression is required for normal development in mice. Germline homozygous deletion of *Nf1* is embryonic lethal around day 13.5 and dissection of *Nf1$^{-/-}$* mutants determined that embryonic lethality was due to cardiac malformation (29, 30). Specifically, the absence of neurofibromin during development results in a condition in which the pulmonary artery and aorta both emerge from the right ventricle. However, *Nf1$^{+/-}$* embryos are viable and development normally with no sign of cardiac malformation. Adult *Nf1$^{+/-}$* mice do not develop neurofibromas, café-au-lait macules or Lisch nodules and therefore are phenotypically the same to WT mice. However, in prolonged studies over a

period of 27 months, $Nf1^{+/-}$ mice did show a predisposition to tumor formation as well as myeloid leukemia (30). These observations, along with genetic studies that indicate NF1 is caused from mutations within a single allele provide evidence that *NF1* is a tumor suppressor gene (31). While, loss of heterozygosity has been described in some tumors isolated from NF1 patients (32-34), haploinsufficiency of *NF1* is sufficient for many of the clinical manifestations of NF1 (35-39).

The most extensively studied role of neurofibromin, to date, is its function regulating $p21^{Ras}$ (Ras) signaling. Neurofibromin has been demonstrated to have a catalytic domain with sequence homology to the mammalian Ras guanosine triphosphate accelerating protein (GAP), p120 Ras-GAP, and the yeast Ras inhibitors IRA1 and IRA2 (2, 40-42). The activity of Ras proteins is tightly controlled by cycling between an activated guanosine triphosphate bound state (Ras-GTP) and an inactivated guanosine diphosphate bound state (Ras-GDP)(43-45). GAP proteins, including neurofibromin, accelerate the hydrolysis of GTP to GDP, converting active Ras-GTP to inactivate Ras-GDP (Figure 1) and negatively regulating Ras signaling (2, 44, 46). The GAP domain of neurofibromin spans exons 20 through 27 and introduction of only this GAP related domain (GRD) is sufficient to stimulate GTP hydrolysis of Ras in yeast (2, 40, 42). Further experiments have also shown that the GRD domain of neurofibromin functions as effectively as a Ras-GAP as the full length protein (47). Consistent with its function, primary cells isolated from both NF1 patients

and *Nf1*$^{+/-}$ mice have hyperactivated Ras signaling pathways, including ECs and

VSMCs (48, 49), which are important in maintaining vascular health.
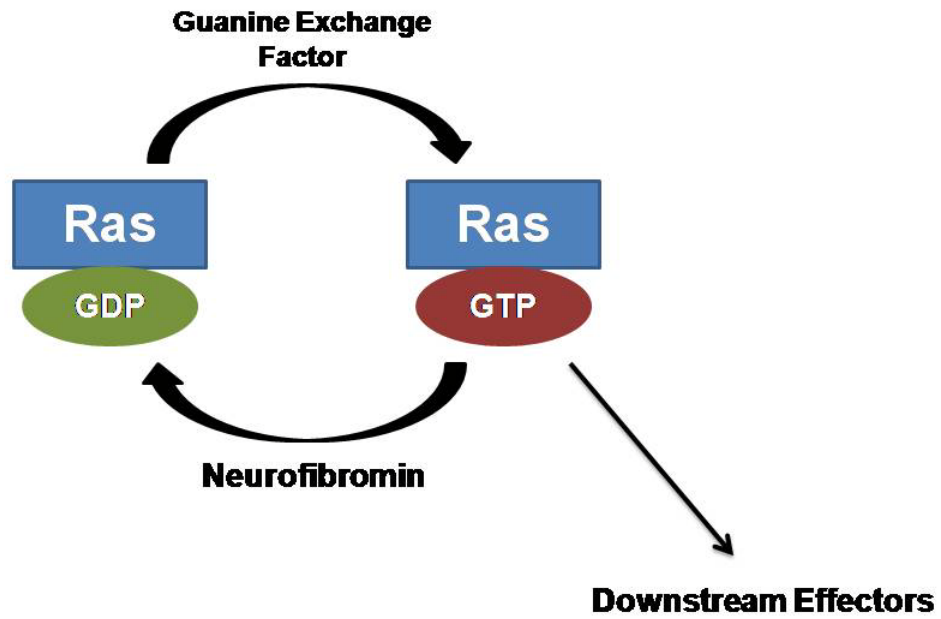
Figure 1. Schematic of Ras signaling.

While neurofibromin functioning as a Ras-GAP can be attributed to many of the *in vitro* and *in vivo* observations described in NF1, the GAP domain only accounts for 10% of the NF1 gene (50), indicating additional roles of neurofibromin in cellular function. Studies in *Drosophila* have demonstrated that neurofibromin positively regulates adenylyl cyclase (51-53) (Figure 2) and mutations within NF1 result in reduced cyclic adenosine 3',5'-monophosphate (cAMP) production and downregulation of protein kinase A (PKA) signaling (51, 52). Homozygous *NF1* mutant *Drosophila* present with small size and decreased lifespan (51, 53) that was not recapitulated by upregulation of the Ras-Raf signaling axis. However, these studies identified that mutation of adenylyl cyclase, the enzyme which produces cAMP from adenosisne triphosphate (ATP), also results in small size and decreased lifespan (53). Further, the *NF1* null phenotype is corrected by mutation of cAMP phosphodiesterase, which inhibits cAMP degradation, as well as constitutive activation of PKA (53). Along with identifying the signaling axis, Tong et al. (53) demonstrated that loss of neurofibromin resulted in increased mitochondrial oxidative stress. These studies suggest that neurofibromin is a regulator of adenylyl cyclase-cAMP-PKA signaling. These observations in *Drosophila* have encouraged the interrogation of neurofibromin-adenylyl cyclase signaling in mammalian cells. Dasgupta et al. (54) have identified that neurofibromin positively regulates adenylyl cyclase activity in astrocytes regulating cellular proliferation. Interestingly, Kim et al. (55) have demonstrated that neurofibromin negatively regulates cAMP production in Schwann cells. These conflicting observations reveal that the function of

neurofibromin in regulating cAMP production is dependent on cell lineage and additional studies need to be completed to determine the role of neurofibromin and cAMP in NF1 manifestations. To this point, *in vitro* studies in Dr. Ingram's lab have demonstrated the ECs transduced with short hairpin RNA (shRNA) directed against NF1 have reduced levels of cAMP compared to control ECs (Figure 3). The cellular consequence of reduced cAMP levels in neurofibromin deficient ECs needs to be further investigated to determine if this signaling axis is involved in NF1 vasculopathy.
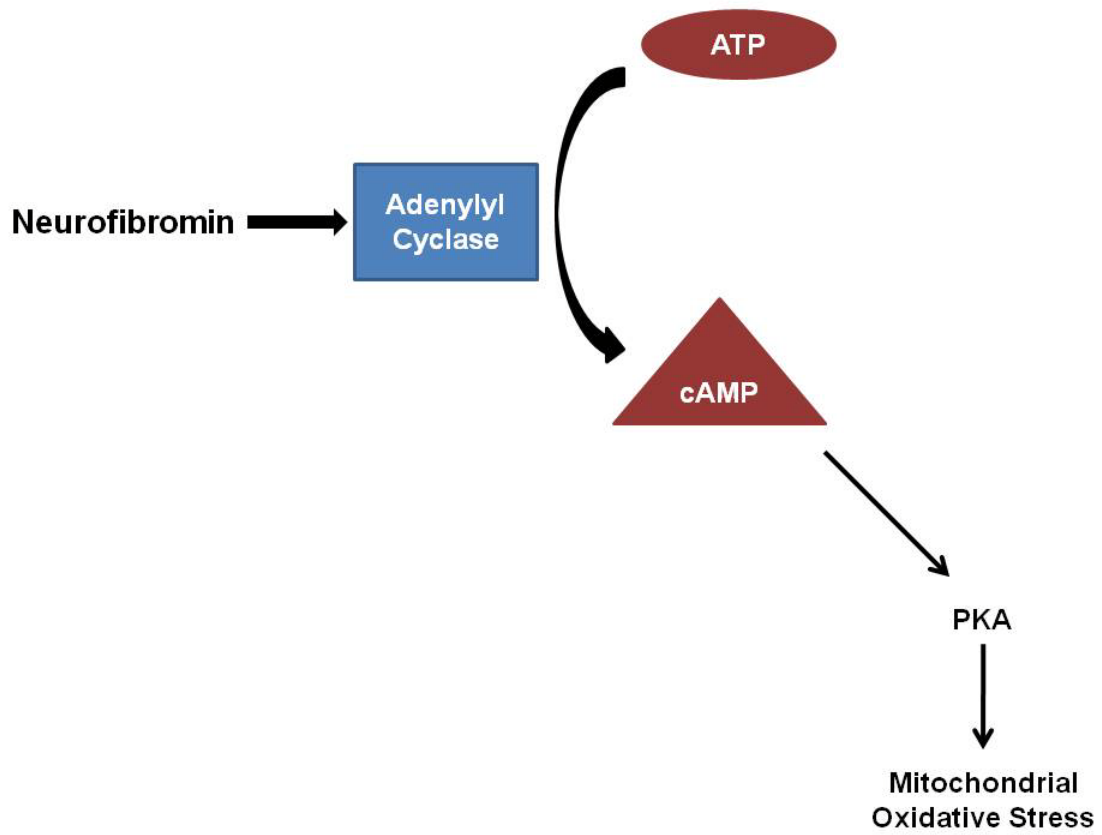
Figure 2. Simplified schematic of positive regulation of adenylyl cyclase activity by neurofibromin.
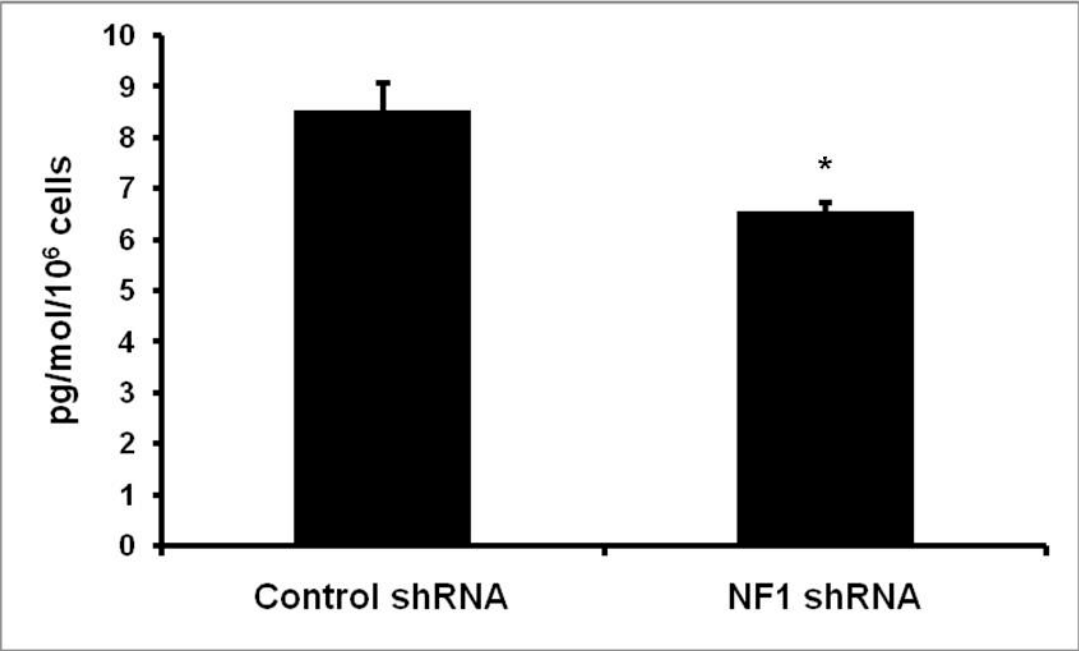
Figure 3. Quantitative analysis of cAMP levels in control and neurofibromin deficient ECs. Cytoplasmic cAMP levels in ECs transduced with either scrambled shRNA (Control shRNA) or shRNA targeted against NF1 (NF1 shRNA) in pg/mol per 10^6 cells. Data represents the mean cAMP levels ± SEM, n=3, *p=0.0245.

Vascular Smooth Muscle Cells, Ras Activation and Neointima Formation.

Arteries are composed of three primary regions, the intima, media and adventitia. The intima area is the innermost region of the artery and consists of a monolayer of ECs resting on a basement membrane within the internal elastic lamina. The ECs function as a barrier between the blood and VSMCs within the vessel wall regulating the transmigration of cells into the vessel (56, 57). Further, ECs produce nitric oxide, which is important for regulating vascular tone and a potent inhibitor of VSMC proliferation (58). The media area of the vessel, the interior region between the internal elastic lamina and external elastic lamina, is composed primarily of quiescent VSMCs and extracellular matrix. The adventitia is the outermost region of the vessel and is composed of fibroblasts and connective tissue (Figure 4). Vascular homeostasis requires a controlled interaction between the three regions to inhibit the infiltration cells into the vessel wall from either the lumen or adventitia, as well as maintain the VSMCs within the media in a quiescent state.

A
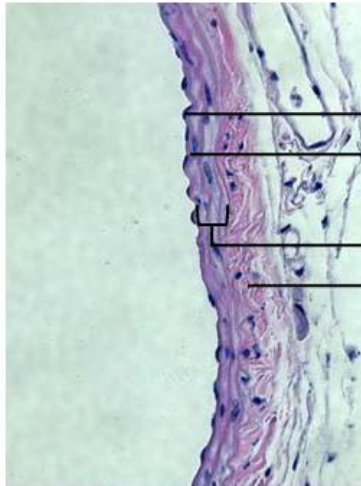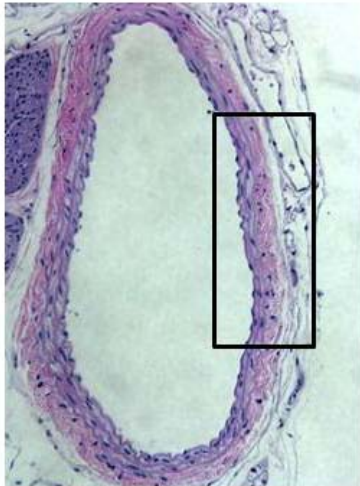
Endothelium

Internal Elastic Lamina

Media

Adventitia

B
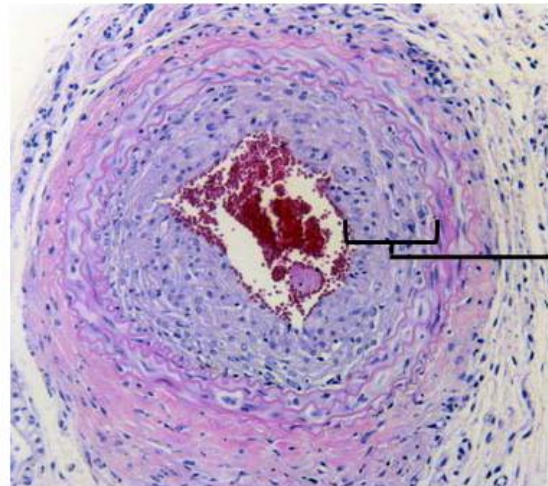
Neointima Formation

Figure 4. Schematic of an arterial cross-section and neointima formation.

A) Cross-section of a normal murine carotid artery that has been stained with

Hematoxylin/Eosin (H&E) to identify nuclei (blue) and cellular cytoplasm (pink).

Black box identifies area magnified in the right panel. B) Cross-section of

murine carotid artery with neointima formation.

Vascular occlusive disease is characterized by an accumulation of VSMCs within the intima area of the vessel (neointima formation), which results in lumen occlusion. Studies by others have demonstrated that in response to injury, VSMCs from the media migrate into the intima in response to platelet derived growth factor BB (PDGF-BB) where they proliferate and produce extracellular matrix, forming the neointima (59-61). Arterial injury results, initially, in the accumulation of platelets at the sites of exposed collagen due to loss of the endothelium. Platelets are a potent source of PDGF-BB which serves as a necessary stimulant for medial VSMCs to migrate into the intima area in response to injury (61, 62). Further, the importance of PDGF-BB signaling through the PDGFβ-receptor (PDGFβ-R) has been elucidated in a number of *in vivo* models where mice harboring genetic mutations that increase signaling through the PDGFβ-R-Ras-Erk signaling axis develop exaggerated neointimal hyperplasia and arterial occlusive disease reminiscent of the vascular complications which develop in some NF1 patients (63-72).

Ras proteins regulate the growth, survival and differentiation of many cell types by functioning as a molecular switch that relays signals from the extracellular environment to the nucleus (45, 73-76). Therefore, based on the global control of Ras signaling in regulating cell function, deficiency of neurofibromin in VSMCs could contribute to neointima formation. Neurofibromin is expressed in human and murine VSMCs and has been demonstrated to function as a Ras GAP, negatively regulating Ras signaling (28, 48). *In vitro* data from our laboratory demonstrated that neurofibromin deficient human and murine

VSMCs have increased proliferation and migration in response to PDGF-BB and that the hyperactivation is abrogated by pre-incubation of the cells with either the Mek inhibitor PD98059 or imatinib mesylate (48). Further, stimulation of $Nf1^{+/-}$ VSMCs demonstrated increased Erk phosphorylation in response to PDGF-BB stimulation compared to WT VSMCs with no difference detected in Akt phosphorylation between $Nf1^{+/-}$ and WT VSMCs (48). This data identifies the canonical Ras-Raf-Mek-Erk (Ras-Erk) signaling pathway as the primary axis for the increased proliferation and migration of the $Nf1^{+/-}$ VSMCs, therefore studies outlined in this project will focus on Ras-Erk signaling *in vivo*. Understanding the role of neurofibromin in VSMCs gives potential insights into NF1 vasculopathy given the emerging paradigm in vascular biology where tight control of the PDGF-BB-Ras-Erk signaling axis in VSMCs is critical for maintaining in blood vessel homeostasis and preventing premature development of vascular occlusive disease (68-72, 77, 78).

Traditionally, the role of Ras signaling in neointima formation has centered on activating Ras mutations or mutation of proteins within the Ras signaling scaffold. For example, Grb2 is a critical adapter molecule required for the activation of Ras by receptor tyrosine kinases, including the PDGFR-βR (72). $Grb2^{+/-}$ mice are resistant to neointima formation in response to mechanical arterial injury compared to WT controls (72). Consistent with this result, *in vitro* studies indicate that murine $Grb2^{+/-}$ VSMCs have decreased proliferation and migration in response to PDGF-BB compared to WT controls (72). Similar results were obtained through the use of a pharmacological inhibitor of Mek in

17

rats (79), as well as the adenoviral mediated transfer of a dominant negative H-Ras into VSMCs (68), both of which prevent the development of stenotic lesions after mechanical arterial injury by inhibiting the proliferation and migration of VSMCs. In 2004, Chen et al. (65) demonstrated that the loss of a negative regulator of Ras activity resulted in neointima formation in response to vascular injury. The protein product of hyperplasia suppressor gene (*HSG*) directly binds to Ras, inhibiting the activation of the Ras-Erk signaling axis and inducing cell cycle arrest (65). HSG protein and mRNA expression is dramatically reduced in hyperproliferative VSMCs *in vitro* as well as in response to mechanical arterial injury. This finding supports the hypothesis that increased Ras-Erk signaling in VSMCs through the loss of a negative regulator is sufficient to drive neointima formation in response to injury. Based on these observations, we hypothesize that *Nf1*^{+/-} VSMCs would have increased migration in response to arterial injury, resulting in enhanced neointima formation.

Endothelial Cells, Ras Activation and Neointima Formation.

Neurofibromin has a critical role in regulating EC function. Complete germline inactivation of *Nf1* results in midgestation lethality due to cardiovascular malformations (29, 30). Lineage specific inactivation has shown that expression of *Nf1* in ECs is essential for normal embryonic development (80). Utilizing transgenic mice that express conditional *Nf1* alleles that are susceptible to *cre* mediated recombination, Gitler et al. demonstrated that complete ablation of *Nf1* in ECs driven by the EC promoter, *Tie2,* recapitulates the phenotype of the *Nf1*^{-/-}

embryo (80). These results indicate that neurofibromin plays a critical role in normal cardiovascular development and therefore we hypothesize that neurofibromin also has an important role in maintaining vessel homeostasis.

ECs derived from NF1 patients have reduced neurofibromin expression consistent with heterozygous inactivation of *NF1* (49). Decreased neurofibromin expression results in increased Ras activation *in vitro*, determined by increased Erk phosphorylation, in response to vascular endothelial growth factor (VEGF) and basic fibroblast growth factor (bFGF). Further, we have shown that primary human ECs derived from NF1 patients have increased proliferation and migration in response to VEGF and bFGF through hyperactivation of the Ras-Erk signaling axis (49). The effects of prolonged activation of Ras in ECs in NF1 patients are unknown; although oncogenic Ras signaling in ECs has been linked to cellular senescence *in vitro* (81). This observation is intriguing given that EC senescence has been associated with vascular disease in other patient populations (58, 82).

Cellular senescence is an irreversible growth arrest that is generally attributed to telomere shortening and chromosome instability (83). This form of senescence, termed replicative senescence, limits the proliferative potential of a cell (84-86). Another form of senescence, termed stress-induced or premature senescence, is independent of telomere shortening and can be induced by a number of challenges, including DNA damage, oxidative stress or oncogenic transformation (58, 87). The functional consequences of EC senescence, either replicative or premature, include decreased production of nitric oxide, decreased

repair ability in response to injury and increased expression of cellular adhesion molecules which could predispose patients to vascular lesion formation (58).

The endothelium forms a continuous monolayer that lines the lumen side of the vasculature and is essential for maintaining the integrity of the vessel wall. Normal functioning ECs produce nitric oxide, a multi-functional compound which regulates vascular tone, inhibits VSMC proliferation, and has anti-inflammatory effects (58). Endothelial nitric oxide synthase (eNOS), a constitutively expressed EC enzyme, produces nitric oxide through the conversion of L-arginine to L-citrulline. A hallmark of senescence and subsequent endothelial dysfunction is reduced nitric oxide production, which has been associated *in vitro* with decreased eNOS activity (88, 89). Reduction in eNOS activity has been attributed to reduced telomerase activity (88), oxidative stress (90, 91) and changes in shear stress (92). Endothelial dysfunction mediated by changes in shear stress or increased oxidative stress implicates the role of premature senescence in vascular disease (58, 93, 94) because the anti-inflammatory effects of nitric oxide function to inhibit platelet aggregation and adherence to ECs (95-97) as well as regulate the expression of leukocyte adhesion molecules, such as intracellular adhesion molecule 1 (ICAM-1) *in vitro* (98). This is an interesting observation given that recruitment of circulating inflammatory cells to the vessel wall can result in increased oxidative stress and EC activation, perpetuating an inflammatory response.

EC activation by inflammatory mediators has been linked to vascular disease in patient populations with lesions reminiscent of NF1 vasculopathy.

Increased serum levels of the pro-inflammatory cytokines tumor necrosis factor α

(TNFα) and interleukin 6 (IL-6) have been associated with atherosclerosis and

coronary artery disease (99-103). Endothelial activation by inflammatory

mediators upregulates the expression of leukocyte adhesion molecules, including

ICAM-1 and vascular cell adhesion molecule 1 (VCAM-1) as well as the

chemokine monocyte chemoattractant protein 1 (MCP-1) (104). These leukocyte

adhesion molecules and chemokines mediate the recruitment and binding of

leukocytes to the endothelium, facilitating the transmigration of cells into the

vessel wall (105). The infiltration of monocytes/macrophages, natural killer (NK)

cells, dendritic cells, T cells, B cells and mast cells have all been described in

vascular lesion formation (106, 107). *In vivo* models utilizing antibody blockade

of adhesion molecules or genetic ablation of leukocyte receptors have

determined that transmigration of inflammatory cells into the vessel wall is

essential for neointima formation in response to arterial injury (108-111). These

observations provide a potential mechanism through which EC senescence

results in a recruitment of circulating inflammatory cells to the vessel wall,

initiating vascular lesion formation.

Recent unpublished studies from Dr. Ingram's laboratory show that ECs

isolated from NF1 patients' peripheral blood and expanded *ex vivo* undergo

premature senescence compared to healthy donors (Figure 5). Specifically,

these primary cells have increased population doubling time (Figure 5b) and

show reduced growth kinetics compared to ECs derived from healthy adult

controls (Figure 6). However, targeted reduction of neurofibromin in ECs by

shRNA does not result in premature senescence or reduced growth kinetics compared to controls (Figure 6), indicating that premature senescence detected in primary NF1 ECs is not cultural artifact and is potentially a result of increased stress *in vivo*. Preliminary studies utilizing ECs derived from NF1 patients and age-matched healthy controls showed that NF1 ECs have increased oxidative DNA damage compared to control ECs, determined by expression of the oxidative DNA adduct 8-oxo-deoxyguanosine (Figure 5c). Inflammatory cells, specifically monocytes and macrophages are potent sources of reactive oxygen species. Recruitment of these cells to the vessel wall either through vascular injury, changes in shear stress, or endothelial activation by inflammatory cytokines could result in stress-induced premature senescence of ECs that line the vessel wall in NF1 patients (56, 112, 113). Therefore, cellular dysfunction as a consequence of haploinsufficiency of *NF1* would result in transmission of migratory and proliferative signals to VSMCs, and/or increased expression of inflammatory markers on the endothelium, promoting vascular lesion formation.

A Control Adult ECs   NF Patient ECs

B

C
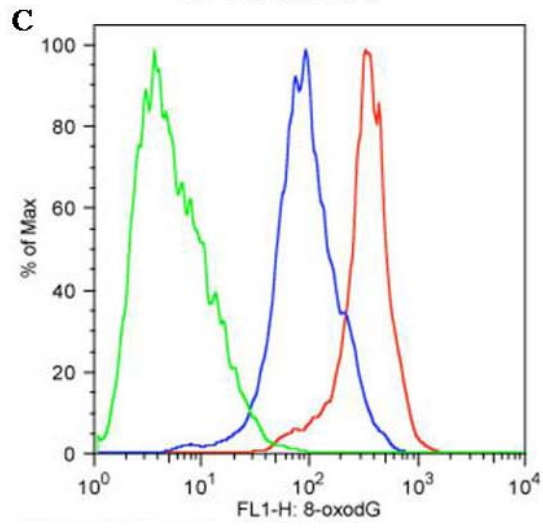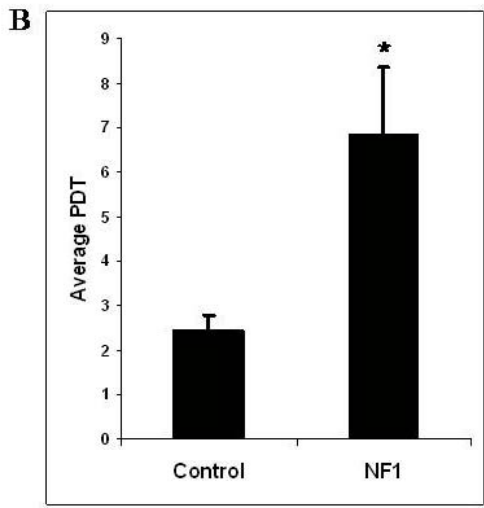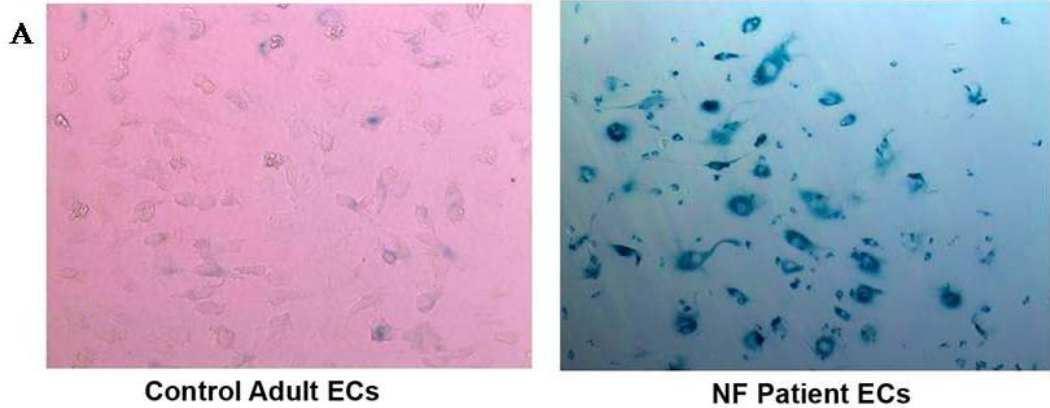
**Figure 5. Identification of premature senescence of peripheral blood
derived ECs from NF1 patients.** A) Representative photomicrographs of
senescence associated beta-galactosidase stain of age and passage matched
ECs derived from the peripheral blood of healthy adult controls (left panel) or
NF1 patients (right panel). Blue staining indicates cellular senescence.
Photomicrographs are representative of 6 independent observations. B)
Quantification of average population doubling time (PDT) of ECs derived from
healthy controls and NF1 patients. Data represents average PDT ± SEM, n=6,
*p=0.031 by Student's unpaired t test with Welch correction. C) Histogram of 8-
oxo-deoxyguanine expression in cultured ECs derived from healthy adult control
(blue line) or NF1 patient (red line). Green line represents negative control.

A
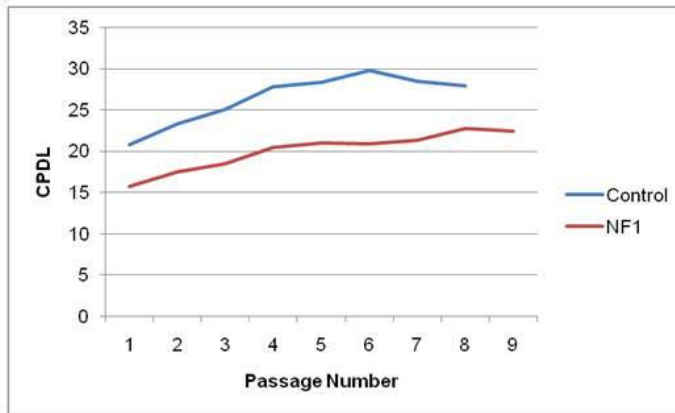
B
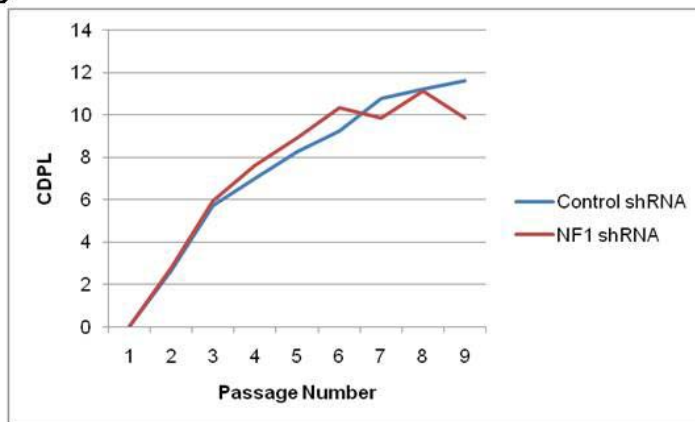
Figure 6. Growth kinetics of peripheral blood derived ECs and shRNA transduced ECs. A) Representative growth kinetics curve of cultured ECs derived from sex and age matched healthy adult control (blue line) and NF1 patient (red line) peripheral blood indicating reduced cumulative population doubling level (CPDL) of NF1 patient ECs. B) Representative growth kinetics curve of human microvascular cells transduced with control shRNA (blue line) or NF1 shRNA (red line), n=3.

Bone Marrow Derived Cells and Neointima Formation.

Bone marrow derived cell (BMDCs) are mobilized in response to vascular injury and are required for repair and remodeling (114, 115). Although neointima formation after injury has been described as local proliferation of VSMCs, recent data demonstrates that bone marrow derived inflammatory cells directly contribute to neointima initiation and progression (111, 115-119). Leukocyte transmigration into the vessel wall in response to vascular injury is essential for neointima formation. The requirement for the infiltration of BMDCs in neointima formation has been demonstrated through genetic ablation of receptors known to facilitate leukocyte transmigration, including *Mac-1* (111) and *CCR2* (120). Along with the requirement for leukocyte attachment and transmigration into the vessel wall in neointima formation, a recent study indicates that neointima formation is dependent, at least in part, on activation of the C-kit signaling pathway (115). Wang et al demonstrated that C-kit deficient mice have reduced neointima formation in response to arterial injury (115). Further, bone marrow transplantation of the C-kit deficient mice with WT bone marrow restored neointima formation in response to injury.

Stem cell factor (SCF) is the ligand for the C-kit receptor and activation of C-kit by SCF has been shown to regulate hematopoietic stem cell proliferation, survival and recruitment (121-124). *In vivo*, circulating levels of SCF were shown to be increased in response to vascular injury, peaking at three days post injury (115). Further, SCF deficiency attenuated neointima formation in response to injury (115). This observation is intriguing given that our group provided the first

genetic data that $Nf1^{+/-}$ myeloid cells have increased proliferation, survival and migration mediated through SCF activation of the C-kit-Ras signaling compared to WT controls (125-127). Along with SCF stimulation, $Nf1^{+/-}$ BMDCs have increased Ras activation in response to granulocyte/macrophage colony stimulating factor (GM-CSF) (128-130). As with SCF, GM-CSF has been shown to directly influence the accumulation of BMDCs within the neointima in response to injury. GM-CSF stimulation increases the adhesion of monocytes to the endothelium (131, 132) and activates macrophages, stimulating pro-inflammatory cytokine production (133), which contributes to neointima formation. *In vivo,* GM-CSF$^{-/-}$ mice have reduced macrophage infiltration and PDGF-BB expression within the neointima in response to arterial injury compared to controls (134). The reduced accumulation of macrophages due to GM-CSF deficiency is hypothesized to account for the reduction in neointima size. Given the role of SCF and GM-CSF in neointima formation and the observation that $Nf1^{+/-}$ BMDCs are hypersensitive to activation by these factors, we predict that $Nf1^{+/-}$ mice have increased contribution of BMDCs to neointima formation.

The observation that GM-CSF deficiency attenuates neointima formation through the reduced infiltration of macrophages identifies a potential bone marrow derived lineage that directly contributes to neointima formation. Along with traditional phagocytic properties, macrophages produce a variety of growth factors and cytokines that have been implicated in neointima formation, including PDGF-BB which stimulates VSMC migration into the intima area of the vessel in response to injury (60, 61, 77, 135, 136). VSMC migration from the media area

into the intima area of the vessel is an essential process in neointima formation (59-61) and the release of VSMCs from the extracellular matrix of the media is required for this migration. Macrophages are an important source of matrix proteases, which degrade extracellular matrix in the vessel wall, releasing the VSMCs to migrate in response to chemotactic stimuli. *In vivo*, arterial injury induces the expression and activity of the matrix metalloproteinases MMP-2 and MMP-9 in the vessel wall (137). Both VMSCs and macrophages produce and secrete MMP-2 and MMP-9 (138-140) and inflammatory cytokines have been shown to upregulate the activity of these enzymes (140, 141). Further, Bendeck et al. demonstrated that treating rats with an MMP inhibitor significantly reduced neointima formation without effecting the proliferation of medial VSMCs in response to injury (137). In a murine model of neointima formation by flow cessation, Godin et al. demonstrated that MMP-9 expression is significantly upregulated in ligated carotid arteries as early as 24 hours post ligation and remains significantly elevated through day seven post injury (142). The expression of MMPs in neurofibromin deficient VSMCs and macrophages has not been investigated, however we hypothesize that hyperactivation of Ras signaling in these cells results in increased production/secretion of the proteases, mediating neointima formation. Further, we hypothesize that heterozygous inactivation of *Nf1* in macrophage results in increased production of growth factors and inflammatory cytokines. This increased macrophage activation would subsequently produce an environment for vascular inflammation in both $Nf1^{+/-}$ mice and NF1 patients.

Vascular Inflammation and Cardiovascular Disease

Vascular inflammation has been identified in numerous patient populations with vascular lesions reminiscent of NF1 vasculopathy. Vascular homeostasis requires a tightly controlled interaction between vascular ECs, VSMCs and circulating inflammatory cells. In response to activation by inflammatory cytokines, ECs increase their expression of chemoattractant proteins and cellular adhesion molecules, promoting the recruitment and transmigration of monocytes into the vessel wall (112, 143-145). In circulation, the pro-inflammatory monocytes identified by CD14 and CD16 cell surface expression ($CD14^+CD16^+$) are a major source of inflammatory cytokines, including tumor necrosis factor α (TNFα), which is known to induce the expression of cellular adhesion molecules on the endothelium (146). In patients with coronary artery disease, Schlitt et al. demonstrated that patients had higher levels of $CD14^+CD16^+$ monocytes in circulation compared to healthy controls and that there was a positive correlation between the frequency of $CD14^+CD16^+$ monocytes and the severity of disease (102). Further, this report identified a significant increase in circulating TNFα levels that was associated with increased severity of coronary artery disease (102). This observed increase in TNFα in relation to the severity of disease is consistent with another report that has demonstrated that levels of TNFα correlate with the progression of atherosclerosis (103). Further, TNFα expression has been identified in atherosclerotic lesions and sites of vascular injury (99, 147-149) while TNFα deficiency in mice protects against neointima

formation in response to injury (150). These observations identify increased expression of pro-inflammatory cytokines as mediators of vascular disease.

Along with the production of pro-inflammatory cytokines, CD14$^+$CD16$^+$ monocytes effectively undergo endothelial attachment and transmigration under normal flow conditions due to the expression of the fractalkine receptor CX3CR1 (151, 152). CD14$^+$CD16$^+$ monocytes express high levels of CX3CR1 compared to other monocyte populations and tightly adhere the vessel wall upon binding to fractalkine (153, 154). Fractalkine is a membrane bound chemokine that expressed on ECs activated by inflammatory cytokines, including TNFα and IL-1(143). Fractalkine and CX3CR1 produce a high-affinity interaction that allows for the transmigration of inflammatory monocytes into the vessel wall. *In vivo*, CX3CR1 deficiency significantly reduces monocyte infiltration into the vessel wall and protects against neointima formation in response to injury (155). To date, the role of inflammation in NF1 vasculopathy has not been determined. However, observations in other patient populations provide a mechanism for interrogating and understanding the development of vascular lesions in NF1.

MATERIAL AND METHODS

Animals.

All protocols for this study were approved by the Indiana University Laboratory Animal Research Center. $Nf1^{+/-}$ mice were obtained from Tyler Jacks at the Massachusetts Institute of Technology (Cambridge, MA) in a C57BL/6.129 background and backcrossed for 13 generations into the C57BL/6J strain. WT C57BL/6 mice were obtained from Harlan Laboratories. C57BL/6 WT and $Nf1^{+/-}$ mice were utilized for the mechanical arterial injury studies. For the carotid ligation studies, $Nf1^{flox/flox}$ mice were obtained from Luis Parada (University of Texas Southwestern) and back-crossed 13 generations into the 129SvJ strain. $Rosa26R$ $lacZ$ reporter (stock #3474), GFP (stock #3291), $SM22cre$ (stock #4746) and $Tie2cre$ (stock #4128) mice were purchased from Jackson Laboratory (Bar Harbor, ME) and maintained on the C57BL/6 strain. $Nf1^{flox/flox}$ mice were crossed with either $SM22cre$ or $Tie2cre$ mice to generate C57BL/6 x 129SvJ pups. $Nf1^{flox/+};SM22cre$ and $Nf1^{flox/+};Tie2cre$ mice were used for experiments. $Nf1^{+/-}$ and WT controls were generated by crossing $Nf1^{flox/flox}$ 129SvJ mice with $Nf1^{+/-}$ C57BL/6 mice. $Rosa26R$ reporter mice were crossed with $Nf1^{flox/flox}$ mice to generate $Nf1^{flox/flox};Rosa26R$ reporter mice that were crossed with either $SM22cre$ or $Tie2cre$ mice. $Nf1^{+/-}$ mice that ubiquitously express GFP were generated by crossing GFP mice with $Nf1^{+/-}$ mice. Only male mice, at least 12 weeks of age were used for experiments.

Genotyping of Mice.

DNA was extracted from tail clippings by Proteinase K (Roche) digestion followed by ethanol extraction. The *Nf1* allele was genotyped by identifying the neomycin resistance gene (neo) expression cassette that has been inserted into exon 31 of the *Nf1* gene (30). The 3' primer, TTCAATACCTGCCCAAGG, is complementary to a 3' region of exon 31 the *Nf1* gene. The 5' primer, CACCTTTGTTTGGAATATATGACT, is complimentary to exon 31 of the *Nf1* gene. The 5' *Nf1* primer and 3' *Nf1* primer identify the WT allele and produce a 230 basepair (bp) fragment. The 5' neo primer, ATTCGCCAATGACAAGAC, along with the 3' *Nf1* primer identify the mutant allele and produce a 350-bp fragment (127). The polymerase chain reaction (PCR) program for identifying the mutant *Nf1* allele is: 95° Celsius (C) for 5 minutes, then 34 cycles of 95°C for 30 seconds, 55°C for 1 minute and 72°C for 1 minute followed by 72°C for 7 minutes and held at 4°C.

Nf1$^{flox/+}$*;SM22cre* and *Nf1*$^{flox/+}$*;Tie2cre* mice were genotyped for *cre* expression by the forward primer 5'- CATTTGGGCCAGCTAAACAT-3' and the reverse primer 5'- CCCGGCAAAACAGGTAGTTA-3' which yield a 450-bp fragment. The PCR program for identifying *cre* is: 94°C for 4 minutes, 27 cycles of 94°C for 20 seconds, 65°C for 20 seconds and 72°C for 20 seconds followed by 72°C for 2 minutes and held at 4°C. The conditional *flox* alleles were identified by using three primers. Two primers, from intron 30 of the *Nf1* allele yield a 480-bp fragment identifying a WT allele. The sequence of primer 1 is 5'-CTTCAGACTGATTGTTGTACCTGA-3' and the sequence of primer two is 5'-

ACCTCTCTAGCCTCAGGAATGA-3'. The third primer, 5'-TGATT

CCCACTTTGTGGTTCTAAG-3' along with primer one yields a 350-bp fragment.

The PCR program for identifying the conditional *Nf1* allele is: 94°C for 3 minutes,

35 cycles of 94°C for 1 minute, 55°C for 2 minutes and 72°C for 3 minutes

followed by 72°C for 4 minutes and held at 4°C. This reaction for the *Nf1*^{flox/+}

mouse yields two fragments, one at 480-bp and the other at 350-bp.

Expression of the *Rosa26R* allele was identified by the combination of

three primers with sequence 5'-AAAGTCGCTCTGAGTTGTTAT-3',

5'-GCGAAGAGTTTGTCCTCAACC-3' and 5'-GGAGCGGGAGAAATGGATATG-

3'. The PCR program 94°C for 4 minutes, 43 cycles of 94°C for 30 seconds,

67°C for 30 seconds and 72°C for 30 seconds and held at 4°C yields 2

fragments, one that is 600-bp and that is 275-bp. A single 600-bp band indicates

WT alleles, one 600-bp fragment and one 275-bp fragment indicates a *Rosa26R*

heterozygous genotype and a single 275-bp fragment indicates a *Rosa26R*

homozygous genotype.

Mechanical Wire Carotid Artery Injury.

The carotid arteries of 12-15 week old C57BL/6 WT and *Nf1*^{+/-} male mice

were mechanically injured by use of a beaded guidewire as previously described

with minor modifications (72, 167). In brief, animals were anesthetized by

inhalation of isoflurane (2%)-oxygen (98%) mixture. Under a dissecting

microscope (Leica, Bannockburn, IL), the entire left carotid artery was exposed

via an anterior incision of the neck. Microvascular clamps were used to

temporarily occlude the common and internal carotid artery and a 6/O silk ligature was used to tie off the distal external carotid artery. An epoxy resin-beaded probe (0.45 mm to 0.6 mm diameter beads) was introduced through a transverse arteriotomy in the external carotid artery. The probe was inserted and withdrawn into the common carotid artery three times with rotation to denude the endothelium and stretch the artery approximately 2 fold. The external carotid artery was immediately ligated proximal to the arteriotomy site. Microvascular clamps were removed and normal blood flow through the common carotid and internal carotid artery was reestablished. The skin was closed with running 6/O suture. The mice recovered for 21 days with no sign of stroke or surgical complications.

Imatinib Mesylate Administration

When stated, imatinib mesylate (50 mg/kg/day; Novartis International AG, Basel, Switzerland) was administrated once per day by intraperitoneal (I.P.) injection. Imatinib mesylate treatment began 3 days prior to carotid injury and continued through day 7 post injury. Mice recovered to 21 days post injury. Phosphate buffered saline (PBS; Invitrogen, Grand Island, NY) was given in an equivalent volume as described for imatinib mesylate as a control.

Histopathology and Immunohistochemistry for Mechanical Wire Carotid Injury.

Twenty-one days after carotid injury, mice were anesthetized with 1.25% Avertin (Sigma-Aldrich, St. Louis, MO) and were perfusion fixed *in situ* with PBS for 5 minutes followed by 4% paraformaldehyde in PBS (pH 7.3) for 10 minutes at a constant pressure of 100 mmHg. The injured left and control uninjured right common carotid arteries were excised under a dissecting microscope, fixed in 4% paraformaldehyde for 8-12 hours at 4°C and embedded in paraffin or snap-frozen in O.C.T. (Sakura Finetek U.S.A., Inc. Torrance, CA) in liquid nitrogen. Serial 5 μm cross-sections were made at 100 μm intervals across the length of the artery. Hematoxylin/Eosin (H&E) staining was conducted according to standard methods (Anatech, Ltd., Battle Creek, MI).

For immunostaining, de-waxed and hydrated sections were blocked for endogenous peroxidase activity with 3% hydrogen peroxide in PBS following antigen retrieval in Antigen Unmasking Solution (Vector Laboratories, Berlingame, CA) at 95°C. Sections were blocked in 3% bovine serum albumin (BSA; Sigma, St. Louis, MO) for 1 hour at room temperature and were stained for smooth muscle cells (anti-α-SMA; Sigma, 1:400), cellular proliferation (anti-Ki67; DAKO Corp, Carpinteria, CA, 1:50), or Erk phosphorylation (anti-phospho-Erk; Cell Signaling, Danvers, MA, 1:100) for 1 hour at room temperature. Purified class- and species-matched immunoglobulins (BD Pharmingen, San Jose, CA) were used for isotype controls. Sections were incubated with the appropriate biotinylated secondary antibody (Vector Laboratories) followed by incubation with

either 3,3′-Diaminobenidine (DAB; Vector Laboratories) for 5 min and counterstained with hematoxylin, or were mounted in 90% glycerol/10% PBS, pH 8.0, containing, 6-diamidino-2-phenylindole dihydrochloride (DAPI; Sigma) to permit nuclear identification. Sections were examined and images of sections were collected using a Zeiss Axioskop microscope (Carl Zeiss, Chester, VA) with a 20X or 40X CP-ACHROMAT/0.12NA objective. Images were acquired using a SPOT RT color camera (Diagnostic Instruments, Sterling Heights, MI).

Percent positive Ki67 cells in the neointima was calculated as: (total number Ki67 positive cells in neointima/total cell number in neointima)*100. Percent positive phospho-Erk cells in the neointima was calculated as (total number phospho-Erk positive cells in neointima/total cell number in neointima)*100.

Carotid Artery Ligation.

Carotid artery injury was induced by complete ligation of the left common carotid artery as previously described (161). Briefly, mice were anesthetized by inhalation of isoflurane (2%)-oxygen (98%) mixture. Under a dissecting scope (Leica), the entire left carotid artery was exposed through a midline incision of the neck. The common carotid artery was completely ligated just proximal to the bifurcation using 6-O silk suture (Fine Science Tools, Foster City, CA). Mice recovered without for 28 days with no sign of stroke or complication.

Bone Marrow Transplantation.

Femurs and tibias from WT and *Nf1*$^{+/-}$ mice that ubiquitously express GFP were flushed with Iscove's Modified Dulbeccos Medium (IMDM, Invitrogen, Carlsbad, CA). Whole, unfractionated bone marrow was collected and washed and re-suspended in IMDM. Male, 12 week old recipient WT and *Nf1*$^{+/-}$ mice were conditioned by lethal irradiation (1100 rads) given at a 700 rad dose followed by a 400 rad dose 4 hours later. Unfractionated bone marrow cells (5x10^6 cells) were injected via tail vein into conditioned recipients. After a four month reconstitution period, peripheral blood was collected via tail vein bleed to determine percent engraftment. Red blood cells were lysed (Qiagen, Germantown, MD) and mononuclear cells (MNCs) were re-suspended and analyzed by flow cytometry using FACS Calibur (BD, Franklin Lakes, NJ) and data was analyzed using FlowJo software, version 8.7.3 (Tree Star, Ashland, OR). MNCs isolated from a non-transplant control were used for a negative control and only mice with greater than 85% engraftment were used for experiments.

Histopathology and Immunohistochemistry for Carotid Artery Ligation.

Twenty-eight days post ligation, whole ligated and contralateral uninjured carotid arteries were harvested from mice. Mice were anesthetized with 1.25% Avertin (Sigma-Aldrich, St. Louis, MO) and were perfusion fixed at constant pressure (100mmHg) with 10 mL of 0.9% sodium chloride followed by Z-fix solution (Anatech) for 5 minutes at a constant pressure of 100 mmHg. Under a

dissecting scope, whole carotid arteries were excised then subsequently fixed overnight at 4°C in Z-fix solution and paraffin embedded. Serial, 5 μm arterial cross-sections were collected every 200μm across the length of the carotid artery. H&E staining was performed according to standards methods (Anatech). Animals that showed sign of clot or thrombus formation due to carotid ligation were excluded from the study.

For immunohistochemistry, paraffin-embedded sections were de-waxed followed by enzymatic (20μg/mL Proteinase K, Roche, Indianapolis, IN) antigen retrieval for 10 minutes at 37°C. Sections were blocked with Protein Block (Dako, Carpinteria, CA) for 1 hour at room temperature followed by incubation with anti-GFP (Abcam, Cambridge, MA, 1:1000), or anti-Mac3 (BD Pharmingen, San Jose, CA, 1:50) primary antibodies. Sections were incubated with the appropriate secondary antibody (Vector Laboratories) and visualized DAB development and counterstained with hematoxylin.

For immunofluoresence co-staining, paraffin-embedded sections were de-waxed followed by enzymatic antigen retrieval at 37°C for 10 minutes. Sections were blocked with M.O.M. reagents according to manufacturer's recommendations (Vector Laboratories) and incubated with anti-GFP (Abcam, 1:1000) primary antibody followed by the appropriate biotinylated secondary antibody. The sections were then co-incubated with anti-α-SMA (Sigma, 1:400) and AlexaFluor 546 strepavidin conjugated antibody (BD Pharmingen) and mounted with ProLong Gold antifade mounting media containing DAPI (Invitrogen).

Sections were visualized on a Leica DM4000 B microscope with a 20X or 40X objective and images were captured using a SPOT RT color camera.

Morphometric Analysis.

For morphometric analyses, images of H&E stained cross-sections of injured and control arteries were analyzed using Metamorph 6.1 (Universal Imaging System Corp, Westerchester, PA). Lumen area, area inside internal elastic lamina (IEL) and area inside external elastic lamina (EEL) were measured for each cross-section. The neointima area was calculated by subtracting the lumen area from the IEL area and the media area was calculated by subtracting the IEL area from the EEL area. The intima-to-media (I/M) ratio was calculated as intima area divided by media area(165). For mechanical wire injury, 5-10 sections along the length of each artery, 100 µm apart were measured by a person blinded to animal genotypes. The average neointima area and average I/M ratio were calculated for both the uninjured and injured artery. An average was neointima area and I/M ratio was calculated for each genotype. Percent lumen stenosis was calculated as: (intima area/IEL area)*100. For the carotid ligation model, H&E stained arterial cross-sections at 400 µm, 800 µm, and 1200 µm proximal to the ligation were measured for neointima area and I/M ratio as described. The measurements from the three sections were averaged for each animal and an average neointima area and I/M ratio were calculated for each genotype.

40

Identification of Murine Monocytes by Flow Cytometry.

Peripheral blood from WT and *Nf1+/-* mice was collected via tail vein bleed into EDTA microtainer tubes (BD). Peripheral blood was diluted 1:10 with PBS followed by red blood cell lysis (Qiagen). MNCs were washed in PBS and blocked with mouse FcR Blocking Reagent (Milltenyi Biotec, Auburn, CA) for 30 minutes at 4°C. MNCs were incubated with anti-Cd11b phycoerythrin (PE; BD Pharmingen) and anti-F4/80 fluoroscein isothyocyanate (FITC, Invitrogen) for 30 minutes at 4°C. Stained MNCs were acquired on a FACS Calibur (BD). 50,000 events were collected per sample and analyzed using FlowJo software, version 8.7.3.

Quantification of Cytokine and Chemokine Levels in Murine Peripheral Blood.

Peripheral blood from WT and *Nf1+/-* mice was collected via tail vein bleed into EDTA microtainer tubes (BD). Samples were centrifuged at 2,000g for 20 minutes at 4°C. Plasma was isolated and stored at -80°C until use. IL-1β, IL-6, IL-10, TNFα, IFN-γ, GM-CSF, MCP-1 and M-CSF were quantified by using a custom Milliplex Cytokine kit (Millipore, Billerica, MA) according to manufacturer's recommendations. Samples were analyzed by a Luminex200 version 2.3 and the StatLIA Immunoassay Analysis Software (Brendan Technologies, Inc., Carlsbad, CA) with a 5-parameter logistic curve fitting method was used to calculate sample concentrations. Concentrations below the minimum detectable concentration were set equal to the minimum detectable concentration.

Patient Recruitment.

NF1 patients were recruited through the Indiana University Neurofibromatosis Clinic at Riley Hospital for Children. All patients had a medical history and physical examination performed to confirm the diagnosis of NF1 using standard NIH clinical criteria (193). Patients with a personal history of cancer, currently using anti-cancer drugs or patients who were pregnant were excluded from the study. All patients gave informed consent prior to their participation in the study.

PFC Analysis of Peripheral Blood MNCs.

Blood samples were collected from NF1 patients (37.6±9.7 years) and age and sex-matched healthy controls (40.2±8.1 years) into EDTA Vacutainer tubes (BD Biosciences). MNCs were isolated from 16 mLs of peripheral blood by density centrifugation using Ficoll-Paque Plus (GE Healthcare, Pittsburgh, PA) as previously described (194). A total of 10 million MNCs were resuspended in PBS with 2% FBS and incubated with human FcR Blocking Reagent (Miltenyi Biotec, Auburn, CA) for 10 minutes at 4°C. Following blocking, MNCs were incubated for 30 minutes at 4°C with the following primary conjugated monoclonal antibodies: anti-human CD14 PECy5.5 (Abcam), anti-human CD45 allophycocyanin (APC)-AlexaFluor 750 (Invitrogen), and anti-human CD16 PECy7 (BD Pharmigen) as well as the live/dead marker ViVid (Invitrogen). Following staining, MNCs were washed 2 times with PBS with 2% FBS and fixed in 1% formaldehyde (Sigma-Aldrich) for a minimum of 24 hours. Stained MNC

samples were acquired on a BD LSRII flow cytometer (BD, Franklin Lakes, NJ, USA) equipped with a 405nm violet laser, 488nm blue laser and 633nm red laser. At least 300,000 events were collected for each sample. Data was collected uncompensated and analyzed using FlowJo software, version 8.7.3 (Tree Star, Inc., Ashland, OR, USA). The Institutional Review Board at the Indiana University School of Medicine approved all protocols.

Quantification of Cytokines in Patient Plasma Samples.

Blood samples were collected from NF1 patients (17±2 years, n=6) and healthy age-matched controls (18.5±3.4 years, n=7) EDTA Vacutainer tubes (BD Biosciences). Plasma was isolated from 3 mLs of blood by centrifugation at 900g for 10 minutes at 4°C. Plasma was aliquoted and stored at -80°C until use. IL-1β, IL-6, IL-10, TNFα, GM-CSF, MCP-1, IFN-γ and fractalkine were quantified by using a custom Milliplex Cytokine kit (Millipore, Billerica, MA) according to manufacturer's recommendations. Only plasma samples that had not undergone a freeze/thaw cycle were analyzed. Samples were analyzed by a Luminex200 version 2.3 and the StatLIA Immunoassay Analysis Software (Brendan Technologies, Inc., Carlsbad, CA) with a 5-parameter logistic curve fitting method was used to calculate sample concentrations. Concentrations below the minimum detectable concentration were set equal to the minimum detectable concentration. The Institutional Review Board at the Indiana University School of Medicine approved all protocols.

Statistical Analyses.

All values are presented as mean ± S.E.M. Intima area and I/M ratio analysis was assessed by One-way ANOVA with a Tukey post-test was performed using GraphPad InStat version 3.00 (GraphPad Software, San Diego California USA). Percent lumen stenosis and percent Ki67 positive cells analysis were assessed by Student's unpaired t test with Welch correction. Percent phopsho-Erk positive cells were assessed by Student's unpaired t test. Percent GFP positive cells were analyzed by One-way ANOVA with a Tukey post-test. Patient and control plasma concentrations of IL-1β were assessed by the non-parametric Mann-Whitney test. Patient and control plasma concentrations of IL-6 were log-transformed for normal distribution and assessed by Student's unpaired t test. Fractalkine levels were assessed by Student's unpaired t test with Welch correction. p values <0.05 were considered significant.

RESULTS

Development of an *In Vivo* Model of NF1 Vasculopathy.

In order to fully understand NF1 vasculopathy, an *in vivo* model needed to be developed that recapitulated the human phenotype. The following criteria was established to ensure an expandable model murine was developed to interrogate NF1 vasculopathy:

1. The genotype of the animal or cell lineage being investigated must agree with experimental findings described in NF1 patients.

2. The established model must be reproducible and provide consistent results.

3. The vascular phenotype identified in the experimental model must recapitulate the vascular lesions described in NF1 patients.

NF1 patients are heterozygous for *NF1* and loss of heterozygosity has not been described in ECs or VSMCs. Therefore, we utilized $Nf1^{+/-}$ mice which are genetically similar to NF1 patients, having one functional allele of the *Nf1* gene. $Nf1^{+/-}$ mice develop normally and are phenotypically similar to WT mice. The vasculature of $Nf1^{+/-}$ mice shows no vascular lesion formation without external manipulation. To induce neointima formation, two well-established models of arterial injury have been described which include a mechanical injury model and a hemodynamic injury model. The mechanical injury model mimics vascular lesion formation by denuding the endothelium through the insertion of either a balloon catheter (156) or a flexible wire (157) into the artery. In this model, the

loss of the endothelium results in platelet aggregation on the exposed extracellular matrix followed by leukocyte recruitment (157). Platelets are a potent source of PDGF-BB (158, 159), which stimulates VSMC migration from the media into the intima area (61, 62, 160). As originally described, VSMC proliferation is at the highest rate 1-2 weeks post injury and reendothelialization of the artery is complete within 3 weeks (157). This model is technically challenging with the caveat that breaking of the internal elastic lamina during injury can result in robust neointima formation mediated through a different mechanism than that of just endothelial denudation. The second injury model, a ligation model, induces neointima formation through changes in hemodynamic forces (161). In this model, the artery is ligated to stop the net forward flow of blood. Changes in shear stress activate the endothelium to express adhesion molecules which facilitate leukocyte transmigration. Further, the near static conditions in the ligated artery allow for platelet aggregation on the endothelium that can stimulate VSMC migration and proliferation into the intima. The ligation model is technically easier and more consistent than the mechanical injury model and mimics vascular lesion formation that has been described in areas of low or altered shear stress in patient populations (162, 163).

The vascular injury models described have been utilized in numerous genetically engineered mice to demonstrate the role of adhesion molecules, signaling molecules, growth factors etc. in vascular lesion formation. Along with information about the mechanism of neointima formation, these models have identified that murine strain and sex have a direct role in the size of vascular

lesion formation in response to injury. Strain dependent studies have been conducted with carotid artery injury using both the mechanical wire injury model and arterial ligation model (164, 165). In both studies, the C57BL/6 strain had one of the lower responses in terms of neointima area and intima-to-media (I/M) ratio and the 129/SvJ strain had an intermediate response. In order to determine which strain is appropriate to identify the role of a specific protein in neointima formation, it is important to understand whether the mutant mouse will have a larger or smaller response than the WT controls. When using the C57BL/6 strain, the injured artery from the WT mouse does not have a significantly larger neointima area than the uninjured artery, therefore this strain is a poor choice if a reduction in neointima is the expected result from genetic manipulation. Further, in response to vascular injury, female mice have been shown to have reduced neointima area compared to male mice of the same genotype and strain (166). Tolbert et al. reported that ovariectomy of the female mice corrected the sex-dependent difference and that exogenous estrogen attenuated neointima formation in these mice (166). Therefore, the use of male mice eliminates the variation in response to vascular injury due to the effects of estrogen.

Nf1 $^{+/-}$ Mice Have Increased Neointima Formation and Vessel Lumen Occlusion in Response to Mechanical Arterial Injury.

Heterozygous inactivation of *Nf1* increases VSMC proliferation and migration in response to PDGF-BB stimulation *in vitro* (48), which are cellular functions linked to neointima formation *in vivo* (63, 64, 68-72). Therefore, based on these prior studies, we tested whether *Nf1*$^{+/-}$ mice had increased neointima

formation in response to mechanical arterial injury *in vivo* compared to WT

controls utilizing a well established surgical model (167). The C57BL/6 murine

strain was utilized for these experiments since previous studies indicate that

C57BL/6 mice are more resistant to neointima formation in response to injury

compared to other strains (165). Therefore, we hypothesized that use of

C57BL/6 mice would allow us to interrogate whether *Nf1* haploinsufficiency would

enhance neointima formation on a relatively resistant murine genetic strain.

Briefly, the endothelium of the common carotid artery of WT and *Nf1*$^{+/-}$ mice

was denuded using a beaded wire and the mice were allowed to recover for 21

days postoperatively. Whole carotid arteries were then harvested and analyzed

to quantify the animal's response to injury (Figure 7). For each animal, the

contralateral carotid artery served as an uninjured control compared to the

injured vessel. To quantitate differences between the two experimental

genotypes, morphometric analysis on arterial cross-sections was completed by

measuring lumen, intima and media area. From these measurements, the I/M

ratio was calculated for the injured and uninjured arteries. The I/M ratio is a

widely used measurement to predict the development of cardiovascular morbidity

(168). Of note, animals in which the internal elastic lamina was damaged by the

mechanical injury were excluded from the study.

C57BL/6 WT vs *Nf1*^{+/-}

Carotid Injury

21 days

Experimental Readouts

Morphometric Analysis
· I/M ratio

Cell Proliferation
· Ki67

Identification of VSMC
· α-SMA

Ras Activation
· phospho Erk
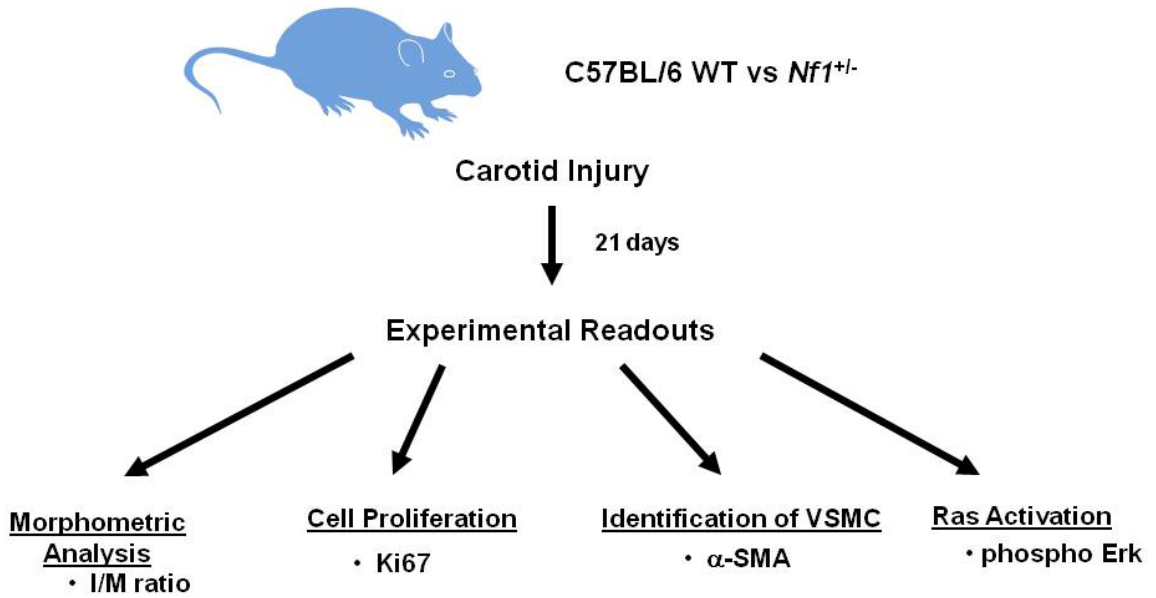
Figure 7. Schematic of experimental strategy for assessing neointima formation in *Nf1*^{+/-} and WT mice in response to mechanical injury of the carotid artery.

Histological examination of the uninjured carotid arteries from WT and $Nf1^{+/-}$ mice demonstrated the absence of neointima formation and revealed no structural differences in vessel architecture between the two experimental genotypes (Figure 8A). However, in response to arterial injury, $Nf1^{+/-}$ mice had increased vessel occlusion compared to WT controls (Figure 8A). A representative low and high power image of a hematoxylin-eosin (H&E) stain of an arterial cross section of uninjured and injured vessels harvested from WT and $Nf1^{+/-}$ mice is shown in Figure 8A. Detailed morphometric analysis revealed that the injured arteries isolated from $Nf1^{+/-}$ mice had a five-fold increase in intima area compared to WT controls (Figure 8B). No significant difference was observed in the media area in response to injury between the two genotypes (Figure 9) indicating $Nf1^{+/-}$ mice have increased accumulation of cells in the intima area resulting in partial lumen occlusion. Of note, the C57/BL6 WT mice formed a small neointima after arterial injury, which is similar to previously published reports utilizing this murine strain(165). Based on intima and media area measurements, the average I/M ratio of the injured arteries harvested from $Nf1^{+/-}$ mice was 3.5 fold higher than WT controls (Figure 8C). Further, $Nf1^{+/-}$ mice had a six fold increase in percent lumen stenosis in response to injury compared to WT mice (Figure 8D). Therefore, this data clearly demonstrates that heterozygous inactivation of $Nf1$ greatly accelerates neointima formation and vessel lumen occlusion after arterial injury.
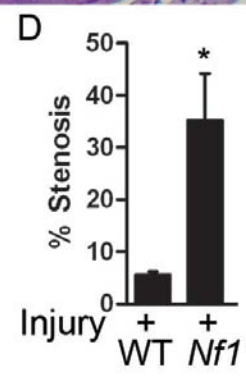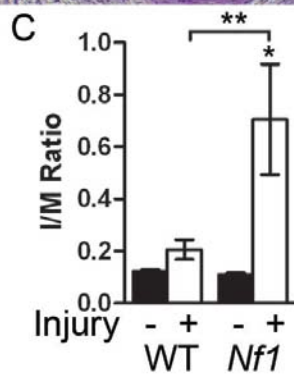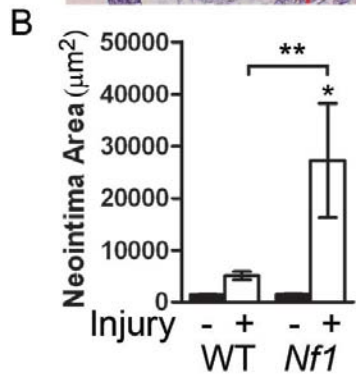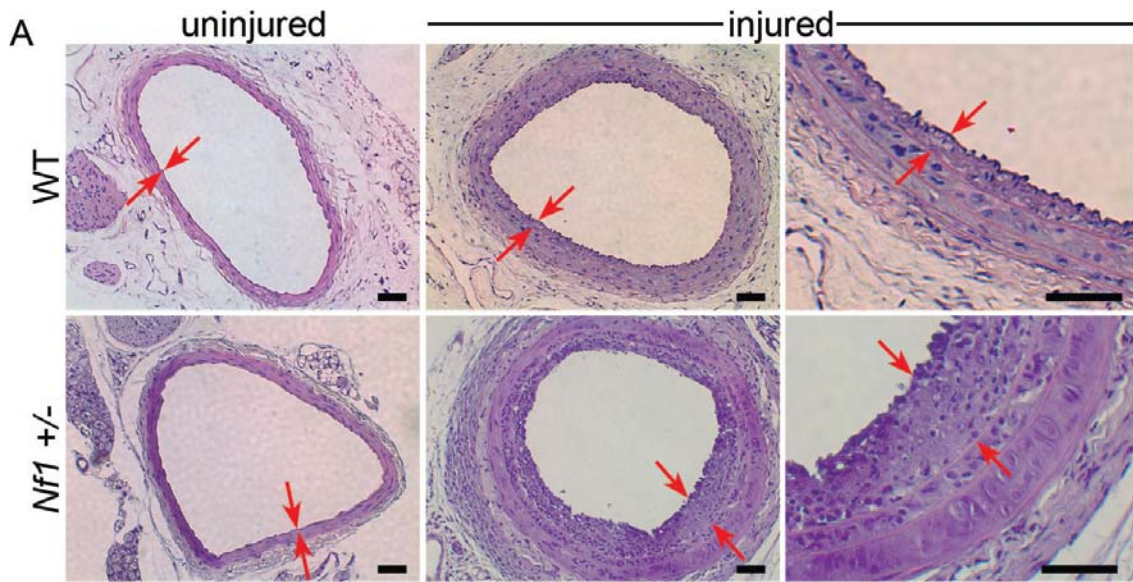
Figure 8. Histological and morphometric analysis of neointima formation in WT and *Nf1*⁺/⁻ mice. A) Representative H&E stained carotid artery cross-sections from WT (top panel) and *Nf1*⁺/⁻ mice. Red arrows indicate neointima boundaries. Scale bars represent 50 µm. B) Quantification of neointima area of uninjured and injured carotid arteries from WT and *Nf1*⁺/⁻ mice. Data represent mean neointima formation of 5 cross-sections ± SEM, n=5. For *Nf1*⁺/⁻ uninjured vs. injured, *p<0.05, and for WT injured vs. *Nf1*⁺/⁻ injured, **p<0.05 by one way ANOVA. C) Quantification of I/M ratio of uninjured and injured carotid arteries from WT and *Nf1*⁺/⁻ mice. Data represent mean I/M formation of 5 cross-sections ± SEM, n=5. For *Nf1*⁺/⁻ uninjured vs. injured, *p<0.01, and for WT injured vs. *Nf1*⁺/⁻ injured, **p<0.05 by one way ANOVA. D) Quantification of percent carotid artery stenosis for injured WT and *Nf1*⁺/⁻ mice. Data represent the mean percent stenosis of 5 cross-sections ± SEM, n=5, *p<0.04 by Student's unpaired t test with Welch correction.
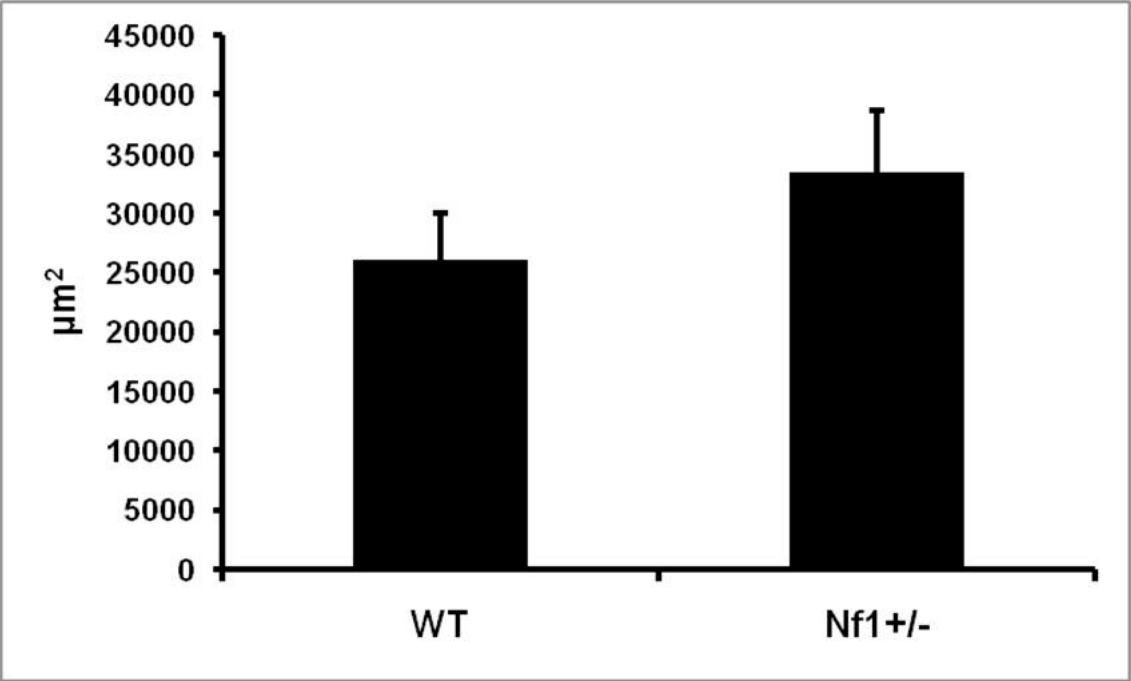
Figure 9. Morphometric analysis of media area in WT and *Nf1*^{+/-} mice.

Quantitative analysis of media area of injured carotid arteries from WT and *Nf1*$^{+/-}$

mice. Data represent mean media area of 5 arterial cross-sections ± SEM, n=5.

Nf1 $^{+/-}$ Mice Have Increased Numbers of VSMCs in the Evolving Neointima.

PDGF-BB binding to its receptor activates both the Ras-Erk and PI-3 kinase-Akt signaling pathways, which regulate the proliferation and migration of VSMCs (169-171). Our previous data demonstrates that heterozygous inactivation of *Nf1* increases both murine and human VSMC proliferation and migration via hyperactivation of the canonical Ras-Erk pathway and not the Ras-PI-3 kinase-Akt pathway *in vitro* (48). Therefore, in order to better understand the mechanism of increased neointima formation in *Nf1*$^{+/-}$ mice, we utilized immunohistochemistry to identify VSMCs within the neointima, proliferating resident neointima cells, and Erk activation after arterial injury.

In response to arterial injury, the evolving neointima in both WT and *Nf1*$^{+/-}$ mice was composed primarily of VSMCs, as detected by immunohistochemical staining of cells with an anti-alpha smooth muscle actin (*α*-SMA) antibody in arterial cross sections (Figure 10). For both WT and *Nf1*$^{+/-}$ mice, VSMCs accounted for at least 75 percent of the cells in the neointima, which is consistent with previously published reports (78, 172). This may be an underestimation of VSMCs in the neointima because vascular injury produces phenotypic change in VSMCs from a quiescent, differentiated cell to a cell with enhanced proliferation and migration which downregulates the expression of certain proteins, including *α*-SMA (173). The accumulation of VSMCs within the intima area of recapitulates the phenotype described in case reports from NF1 patients with vascular lesions (14, 22).

Uninjured　　　　**Injured**

WT

Nf1+/-
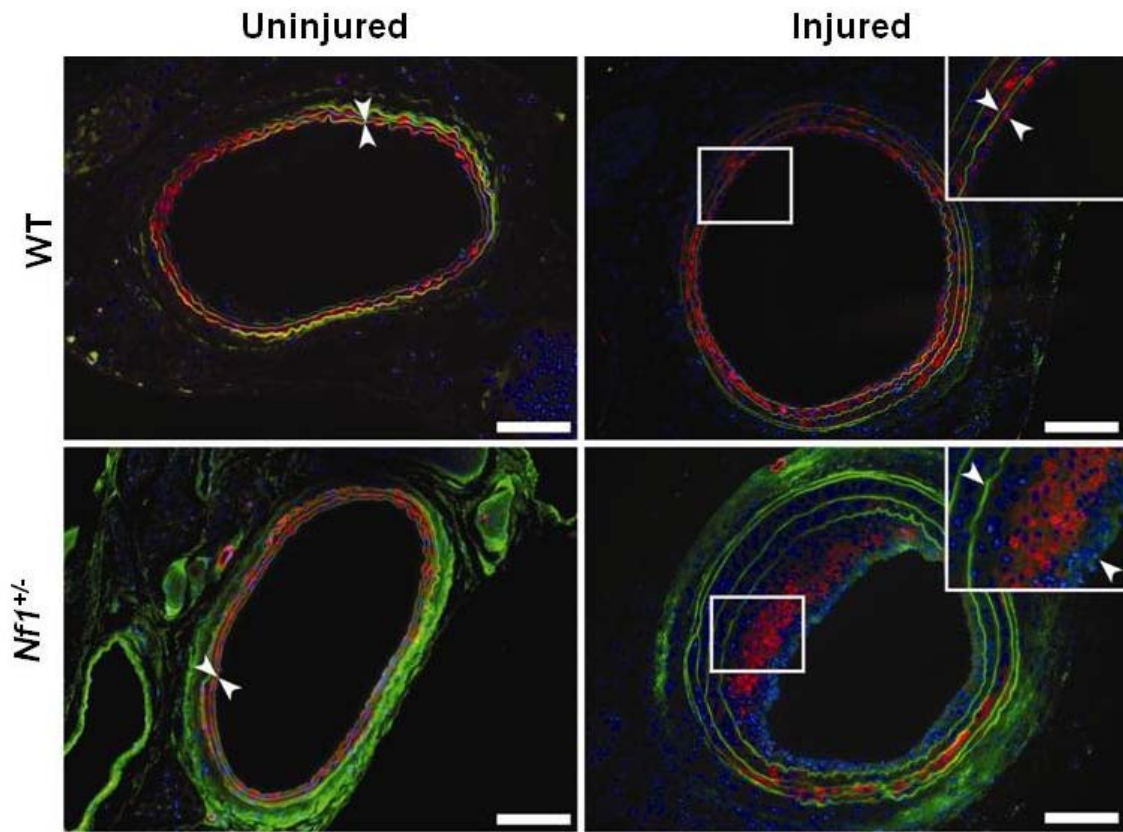
Figure 10. *α*-SMA analysis of carotid arteries from WT and *Nf1$^{+/-}$* mice.

Representative photomicrographs of uninjured (left panel) and injured (right panel) carotid arteries from WT (top panel) and *Nf1$^{+/-}$* (bottom panel) mice stained with *α*-SMA (red). Cell nuclei are counterstained with DAPI (blue) and tissue autofluorescence is visible (green). White arrows indicate neointima boundaries. White boxes indicate areas magnified in inset. Scale bars represent 100 μm. Results are representative of 5 independent experiments.

_Nf1_ ^{+/-} Mice Have Increased Cellular Proliferation in the Evolving Neointima.

Intimal hyperplasia in response to arterial injury requires the migration of VSMCs from the media area of the vessel in to the intima area where they proliferate. To determine if $Nf1^{+/-}$ VSMCs had increased proliferation in response to arterial injury, cellular proliferation in the neointima was determined by immunohistochemical staining of arterial cross-sections for the presence of Ki67, a nuclear protein that is expressed in all cells active in cell cycle (174). The injured vessels harvested from $Nf1^{+/-}$ mice had increased cellular proliferation in the neointima compared to WT controls (Figure 11A). Specifically, $Nf1^{+/-}$ injured vessels had an approximately 20 fold increase in the percent of proliferating cells in the neointima, which expressed the Ki67 antigen, compared to WT controls 21 days post injury (Figure 11B). Since the majority of the cells within the neointima are VSMCs, the increased neointima area in $Nf1^{+/-}$ mice compared to WT mice can be attributed to increased proliferation of VSMCs in response to mechanical injury. Of note, there was little cellular proliferation detected in the uninjured arteries from either $Nf1^{+/-}$ or WT mice indicating that in the absence of a stimulus $Nf1^{+/-}$ VSMCs are not hyperproliferative in the mouse model.
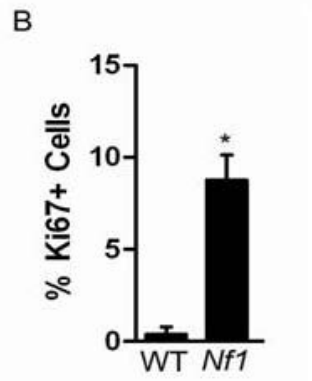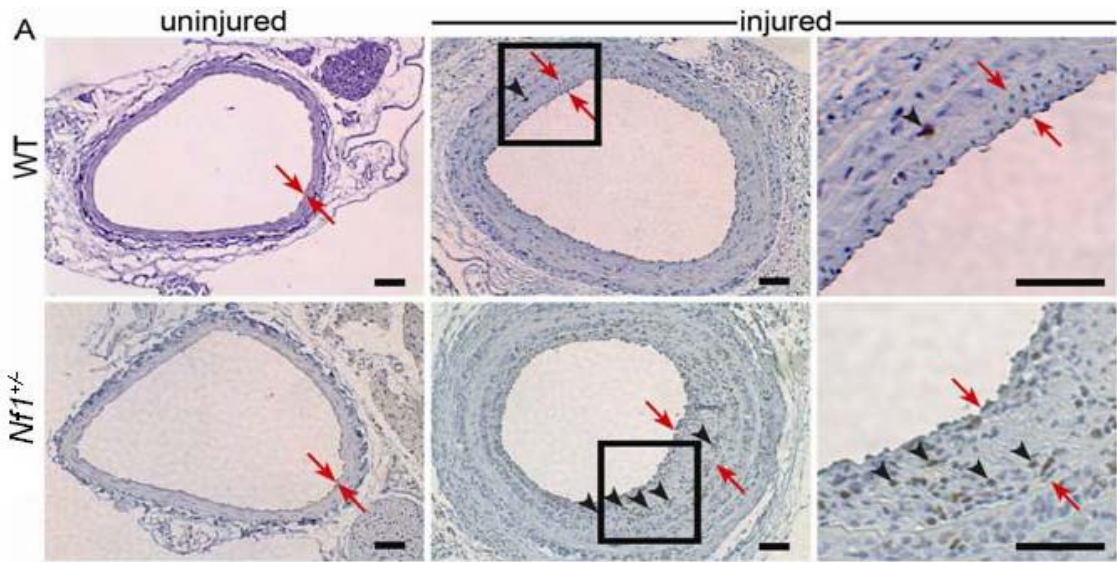
Figure 11. Analysis of cellular proliferation within the neointima of injured carotid arteries from WT and *Nf1$^{+/-}$* mice. A) Representative photomicrographs of uninjured (left panel) and injured (right panels) carotid arteries from WT (top panels) and *Nf1$^{+/-}$* (bottom panels) stained with anti-Ki67 (brown) and hematoxylin (blue). Black boxes in middle panel indicate areas that are magnified in far right panels. Red arrows indicate neointima boundaries. Black arrows represent positive Ki67 staining of proliferating cells. Scale bars represent 50 μm. Results are representative of 5 independent experiments. B) Quantification of percent Ki67 positive cells within the neointima of injured carotid arteries from WT and *Nf1$^{+/-}$* mice calculated as (total Ki67 positive cells in neointima/total number of cells in neointima)*100. Data represent the mean percentage of Ki67 positive cells in the neointima ± SEM, n=3, *p<0.005 by two-tailed Student's unpaired t test.

_Nf1_ ^{+/-} Mice Have Increased Erk Phosphorylation in the Evolving Neointima.

The increased proliferation detected 21 days post-injury in the _Nf1_^{+/-} mice

suggests that the cells within the neointima have hyperactive Ras-ERK signaling,

a pathway known to control cellular proliferation. Activation of the Ras-Erk

pathway _in vivo_ in response to arterial injury was determined by staining injured

arterial cross sections with an antibody directed against phosphorylated-Erk.

Consistent with increased numbers of VSMCs and cellular proliferation in the

neointima, _Nf1_^{+/-} mice had increased Erk phosphorylation compared to WT

controls 21 days after arterial injury (Figure 12). Similar to results seen with

cellular proliferation, baseline levels of Erk phosphorylation were minimal in the

uninjured arteries and there was no difference detected between the WT and

_Nf1_^{+/-} mice. The hyperactivation of the Ras-Erk pathway in response to arterial

injury provides a molecular target for understanding the mechanism of NF1

vascular lesion formation.

A

B
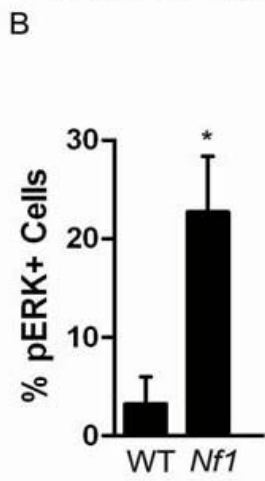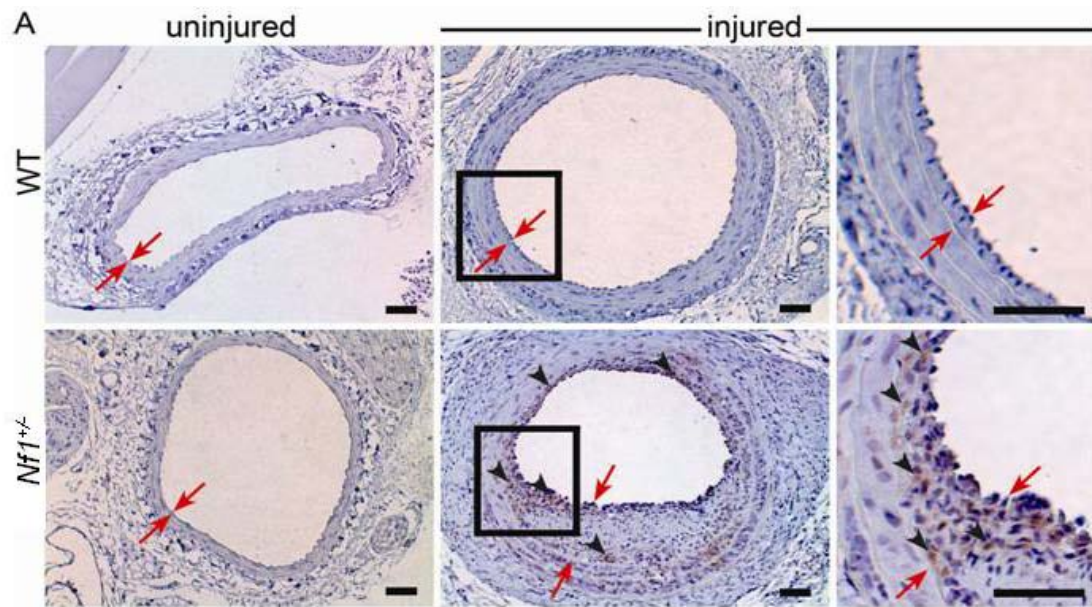
Figure 12. Analysis of Erk phosphorylation within the neointima of injured carotid arteries of WT and *Nf1*⁺/⁻ mice. A) Representative photomicrographs of uninjured (left panels) and injured (right panels) carotid arteries from WT (top panels) and *Nf1*⁺/⁻ (bottom panels) mice stained with anti-phospho-Erk (brown) and counterstained with hematoxylin (blue). Black boxes in middle panel indicate areas magnified in far right panel. Red arrows indicate neointima boundaries. Black arrowheads represent positive phosphor-Erk staining. Data represent 5 independent experiments. Scale bars represent 50 µm. B) Quantification of percent phosphorylated-Erk positive cells within the neointima of injured carotid arteries of WT and *Nf1*⁺/⁻ mice. Data represent mean percentage of phosphorylated-Erk positive cells in the neointima ± SEM, n=3, *p<0.04 by two-tailed Student's unpaired t test.

Administration of Imatinib Mesylate Inhibits Neointima Formation in *Nf1* ⁺/⁻ Mice After Mechanical Arterial Injury.

Imatinib mesylate is a potent inhibitor of the PDGF-BB signaling axis in VSMCs and prevents neointima formation and aneurysms *in vivo* in mice genetically predisposed to diverse vasculopathies (63). Given our prior experimental observations implicating hyperactivation of the PDGF-BB-Ras-Erk signaling pathway in the neointima formation in *Nf1*⁺/⁻ mice, we tested whether pre-administration of imatinib mesylate would inhibit neointima formation in *Nf1*⁺/⁻ mice after arterial mechanical injury (Figure 13). We utilized an imatinib mesylate treatment protocol which had previously been shown to prevent neointima formation in other murine models of vascular disease (115). Specifically, either phosphate buffered saline (PBS) or 50 mg/kg imatinib mesylate was administered daily to WT and *Nf1*⁺/⁻ mice intraperitoneally beginning 3 days prior to arterial injury and continued for 7 days post injury. Mice were then sacrificed 21 days postoperatively for analysis.

In response to carotid injury, imatinib mesylate treatment greatly reduced neointima formation in *Nf1*⁺/⁻ mice compared to PBS treatment (Figure 14A). Specifically, imatinib mesylate treated *Nf1*⁺/⁻ mice had a four-fold reduction in I/M ratio compared to PBS treated *Nf1*⁺/⁻ mice (Figure 14B) in response to carotid injury. No significant difference was seen in response to injury in the I/M ratios of WT mice when comparing PBS to imatinib mesylate treatment. This is consistent with the fact that C57BL/6 WT mice are resistant to neointima formation in response to mechanical injury (165, 172). Further, immunohistochemistry

indicates that imatinib mesylate treatment reduced cellular proliferation as well as Erk phosphorylation in $Nf1^{+/-}$ mice in response to injury compared to PBS treatment (Figure 15). Thus, this data indicates that enhanced neointima formation in $Nf1^{+/-}$ in response to vascular injury is mediated via an imatinib mesylate sensitive pathway. While we have identified a pharmacological antagonist of neointima formation in $Nf1^{+/-}$ mice, the cellular mechanism of neointima formation is unknown because imatinib mesylate inhibits more than one receptor. Therefore, to fully understand NF1 vasculopathy, the predominate cell lineage(s) involved in neointima formation in $Nf1^{+/-}$ mice need to be identified.
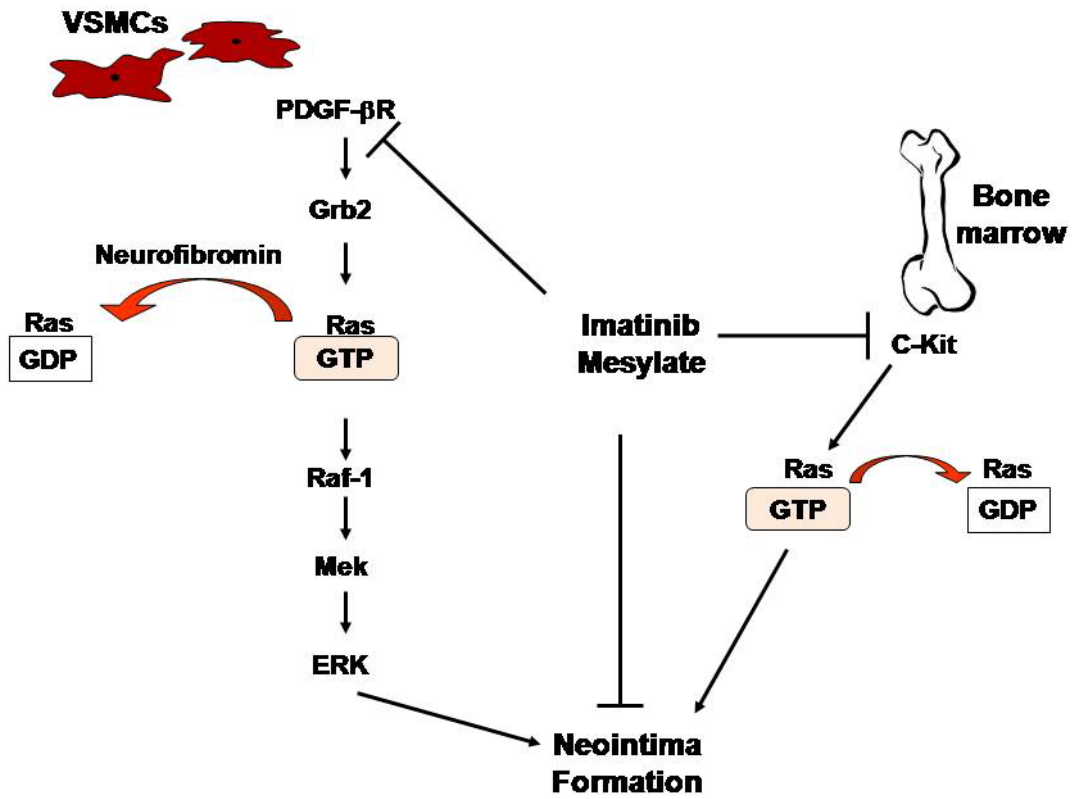
Figure 13. Schematic of imatinib mesylate inhibition of neointima formation.

A

| | uninjured PBS | injured PBS | injured Imatinib Mesylate |

WT

Nf1⁺/⁻

B
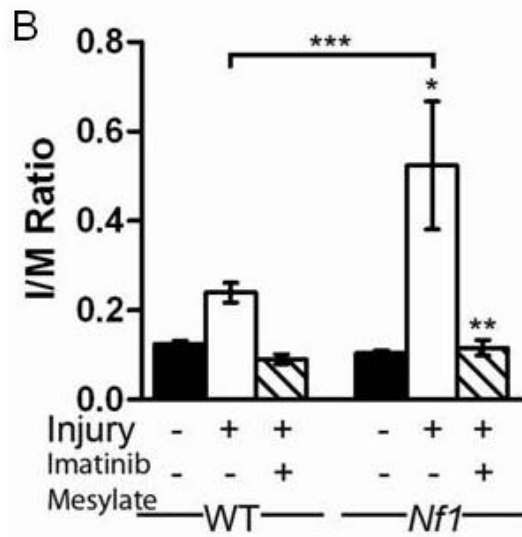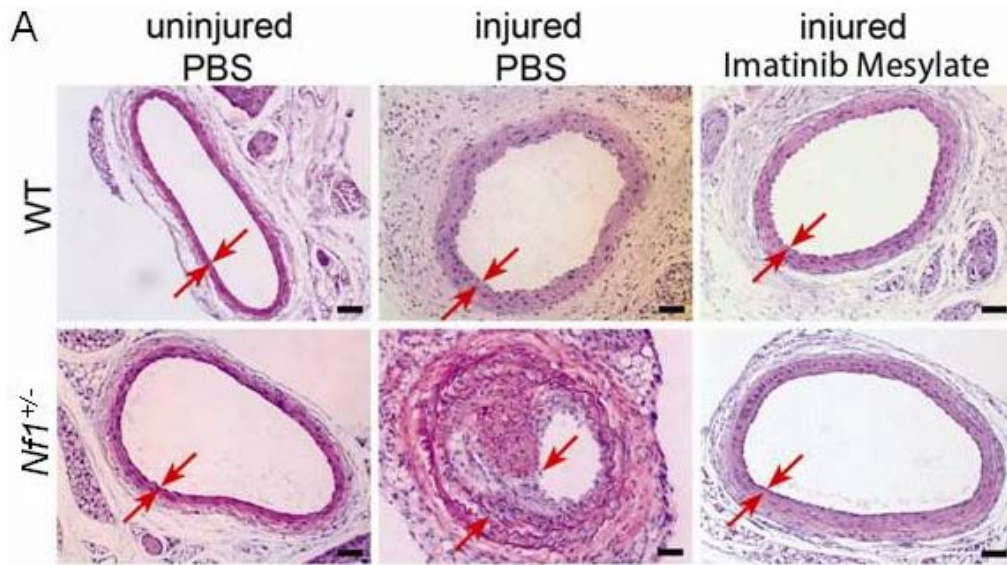
Figure 14. Histological and morphometric analysis of injured carotid arteries from imatinib mesylate-treated WT and *Nf1*⁺/⁻ mice. A) Representative photomicrographs of H&E-stained carotid arteries from WT (top panels) and *Nf1*⁺/⁻ (bottom panels) mice 21 days following no injury and PBS treatment (left panels), injury and PBS treatment (middle panels), or injury and imatinib mesylate treatment (right panels). Red arrows indicate boundary of neointima. Scale bars represent 50 μm. Results are representative of 5 independent experiments. B) I/M ratio of injured carotid artery cross-sections from PBS and imatinib mesylate-treated WT and *Nf1*⁺/⁻ mice. Data represent mean I/M ratio of 5 cross-sections ± SEM, n=4 to 6 mice. For *Nf1*⁺/⁻ uninjured vs. injured with PBS treatment, *$p<0.001$; for *Nf1*⁺/⁻ injured with PBS vs. injured with imatinib mesylate treatment, **$p<0.001$; and for WT injured with PBS treatment vs. *Nf1*⁺/⁻ injured with PBS treatment, ***$p<0.05$ by one-way ANOVA with Tukey post-test.

	α-SMA	Ki67	pERK
PBS			
Imatinib Mesylate			
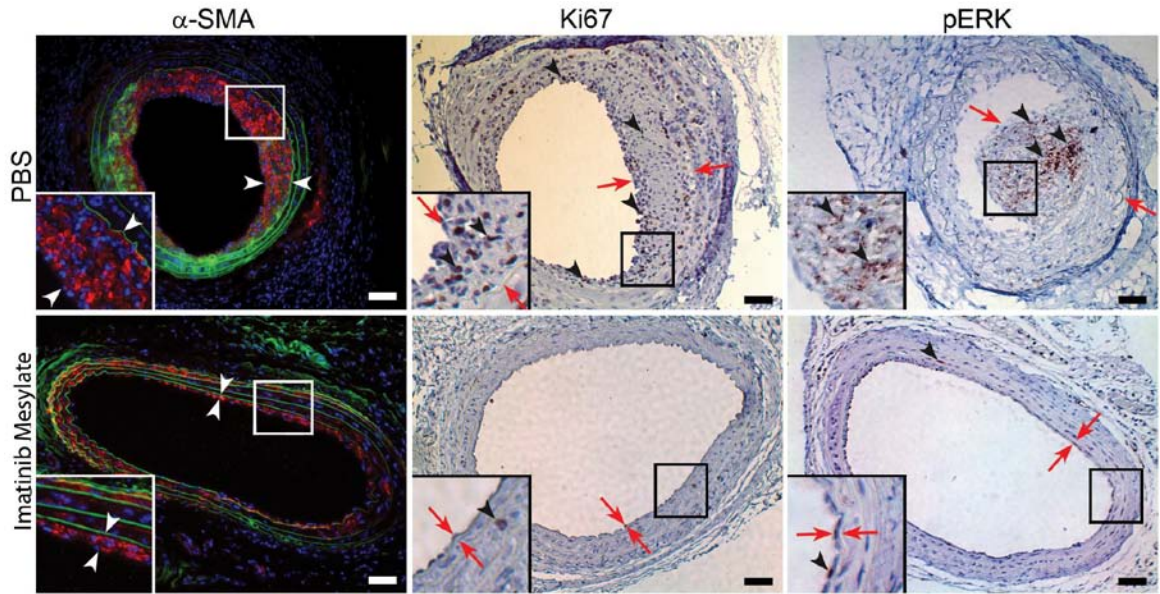
Figure 15. Analysis of *α*-SMA, Ki67, and Erk phosphorylation within the neointima of injured carotid arteries from imatinib mesylate-treated *Nf1$^{+/-}$* mice. Representative photomicrographs of *α*-SMA staining (left panels) of carotid artery cross-sections from injured *Nf1$^{+/-}$* PBS-treated (top panels) and *Nf1$^{+/-}$* imatinib mesylate-treated (bottom panels) mice. *α*-SMA staining is seen in red, DAPI nuclear dye is blue and murine tissue autofluorescence is green. White arrows indicate neointima boundary. White boxes indicate area magnified in inset. Representative images of Ki67 (middle panels) and phoshophorylated-Erk (right panels) staining of carotid artery cross-sections counter-stained with hematoxylin (blue). Red arrows indicate neointima boundary. Black arrowheads represent positive Ki67 or phosphorylated-Erk staining (brown). Black boxes indicate areas magnified in insets. Results are representative of 5 independent experiments. Scale bars represent 50 *μ*m.

Heterozygous Inactivation of *Nf1* in ECs and VSMCs Alone is Insufficient to Recapitulate Neointima Formation of *Nf1*$^{+/-}$ Mice.

In order to determine the cellular mechanism of NF1 vasculopathy, we initially generated mice, utilizing *cre/lox* technology, that were heterozygous for *Nf1* in ECs alone or VSMCs alone. Briefly, *Nf1*$^{flox/flox}$ mice, which contain conditional *Nf1* alleles susceptible to Cre mediated recombination, were crossed with either *Tie2cre* or *SM22cre* mice to generate *Nf1*$^{flox/+}$*;Tie2cre* and *Nf1*$^{flox/+}$*;SM22cre* progeny (Figure 16). *Tie2cre* mice express Cre recombinase under the control of the *Tek* promoter, which is expressed uniformly in ECs resulting in deletion of floxed sequences in ECs (175). In the *SM22cre* mice, Cre recombinase expression is driven by the smooth muscle cell specific promoter, transgelin, resulting in deletion of floxed sequences in smooth muscle cells, including VSMCs in the carotid artery (176). Cre expression was mapped utilizing the *Rosa26* reporter mouse, which expresses *lacZ* in response to Cre expression (177) to demonstrate the generation of experimental mice that are heterozygous for *Nf1* only in ECs (*Nf1*$^{flox/+}$*;Tie2cre*) or VSMCs (*Nf1*$^{flox/+}$*;SM22cre*) with all other cell lineages containing both *Nf1* alleles (Figure 16).

To interrogate the role of *Nf1* in ECs and VSMCs, *Nf1*$^{flox/+}$*;Tie2cre* and *Nf1*$^{flox/+}$*;SM22cre* mice, respectively, underwent carotid artery ligation and analysis for neointima formation along with experimental controls. Carotid artery ligation is a well-established model that induces neointima formation through changes in hemodynamic forces (161). Briefly, the common carotid artery was completely ligated proximal to the bifurcation and the mice recovered for 28 days

post-operatively. Whole ligated carotid arteries along with the contralateral uninjured carotid arteries were harvested from each animal and analyzed for neointima formation as previously described (161).

Histological analysis of H&E stained arterial cross-sections from the uninjured carotid artery demonstrated that WT, $Nf1^{+/-}$, $Nf1^{flox/+};Tie2cre$ and $Nf1^{flox/+};SM22cre$ are not structurally different and showed no sign of neointima formation (Figure 17). Analysis of the ligated carotid arteries indicated that only $Nf1^{+/-}$ mice have significantly enhanced neointima formation in response to arterial injury (Figure 17 and 18) with no difference in neointima formation detected between WT, $Nf1^{flox/+};Tie2cre$ and $Nf1^{flox/+};SM22cre$ mice. Specifically, $Nf1^{+/-}$ mice have a five-fold increase in I/M ratio compared with WT, $Nf1^{flox/+};Tie2cre$ and $Nf1^{flox/+};SM22cre$ mice (Figure 17c). This data demonstrates that heterozygous inactivation of $Nf1$ in ECs or VSMCs alone is insufficient for neointima formation in $Nf1^{+/-}$ mice after vascular injury.
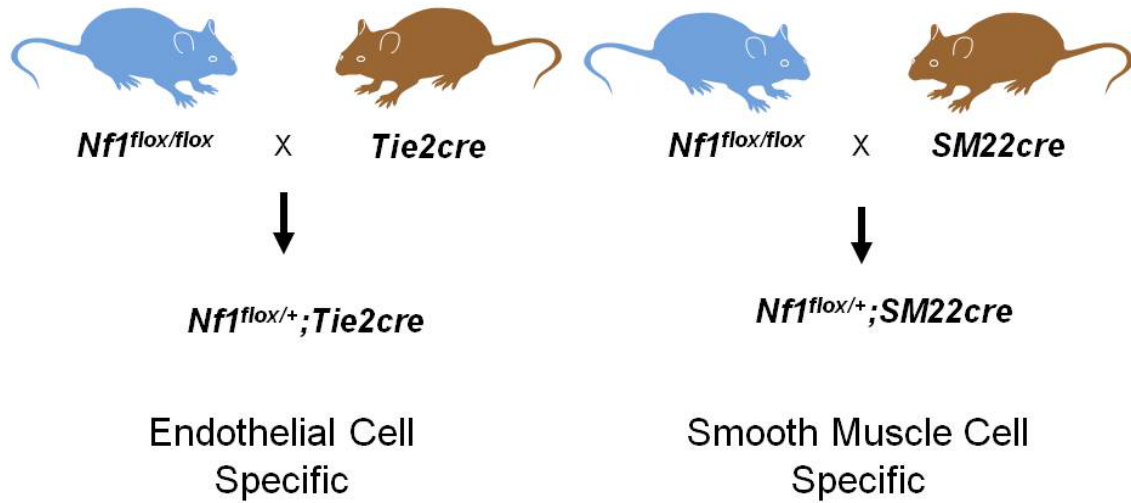
Figure 16. Breeding scheme for the generation of _Nf1^{flox/+};Tie2cre_ and _Nf1^{flox/+};SM22cre_ mice.

*
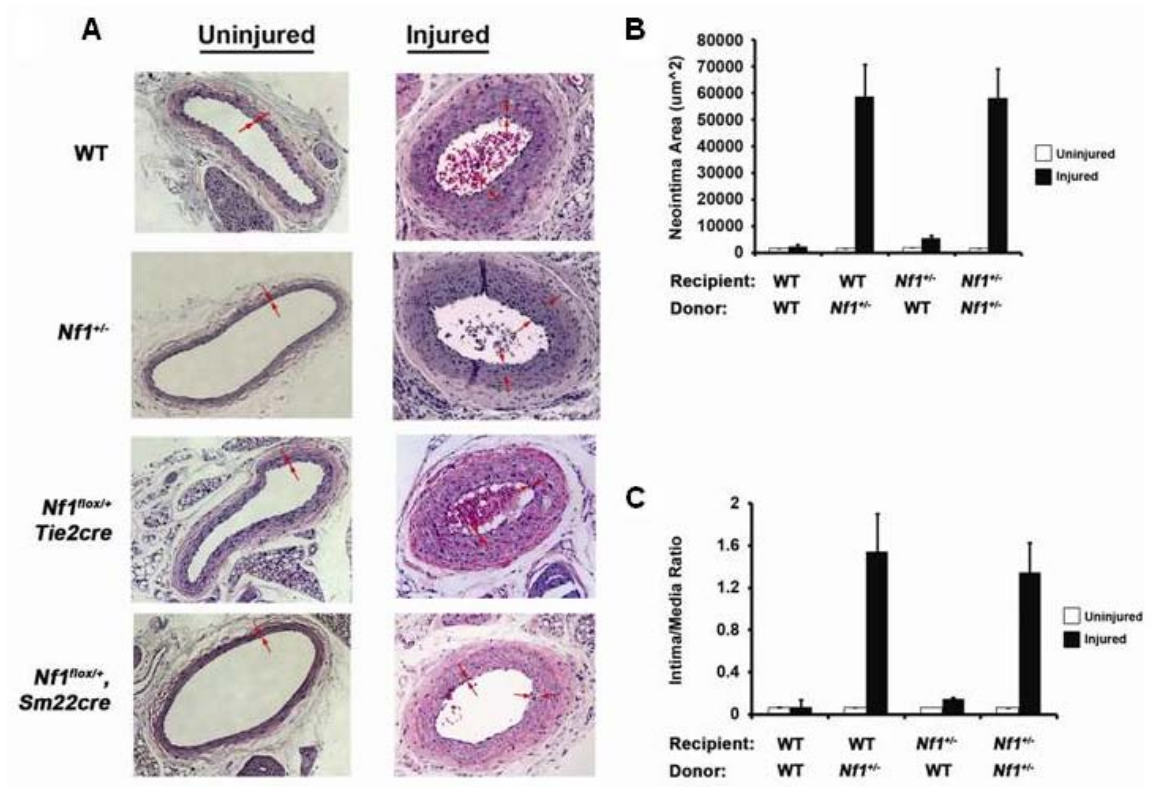
Figure 17. Histological and morphometric analysis of WT, *Nf1⁺/⁻*,

***Nf1^flox/+^;Tie2cre* and *Nf1^flox/+^;SM22cre* mice.** A) Representative H&E stained

cross-sections uninjured (left panel) and injured (right panel) carotid arteries from

WT, *Nf1⁺/⁻*, *Nf1^flox/+^;Tie2cre* and *Nf1^flox/+^;SM22cre* mice. Red arrows indicate

neointima boundaries. B) Quantification of neointima area of uninjured (open

bars) and injured (black bars) carotid arteries from WT, *Nf1⁺/⁻*, *Nf1^flox/+^;Tie2cre*

and *Nf1^flox/+^;SM22cre* mice. Data represent the mean neointima area of 3 arterial

cross-sections (400 μm, 800 μm and 1200 μm proximal to the ligation) ± SEM,

n=4-7, *p<0.001 for *Nf1+/-* uninjured vs. *Nf1+/-* injured and *Nf1+/-* injured vs. WT

injured, *Nf1^flox/+^;Tie2cre* injured and *Nf1^flox/+^;SM22cre* injured by one-way

ANOVA. C) Quantification of I/M ratio of uninjured (open bars) and injured

(black bars) carotid arteries from WT, *Nf1⁺/⁻*, *Nf1^flox/+^;Tie2cre* and

Nf1^flox/+^;SM22cre mice. Data represent the mean I/M ratio of 3 arterial cross-

sections (400 μm, 800 μm and 1200 μm proximal to the ligation) ± SEM, n=4-7,

*p<0.001 for *Nf1+/-* uninjured vs. *Nf1+/-* injured and *Nf1+/-* injured vs. WT injured,

Nf1^flox/+^;Tie2cre injured and *Nf1^flox/+^;SM22cre* injured by one-way ANOVA with

Tukey post-test.

WT

Nf1^{+/-}

**Nf1^{flox/+}
Tie2cre**

**Nf1^{flox/+},
Sm22cre**

Figure 18. Histological analysis of WT, *Nf1⁺ᐟ⁻*, *Nf1ᶠˡᵒˣᐟ⁺;Tie2cre* and

***Nf1ᶠˡᵒˣᐟ⁺;SM22cre* mice.** Representative H&E stained arterial cross-sections

from injured *Nf1⁺ᐟ⁻*, *Nf1ᶠˡᵒˣᐟ⁺;Tie2cre* and *Nf1ᶠˡᵒˣᐟ⁺;SM22cre* mice (left panel). Black

box indicates area magnified in right panel. Red arrows indicate neointima

boundaries.

***Nf1*^{+/-} Bone Marrow Derived Cells Are Necessary and Sufficient for**

Neointima Formation.

Previous reports demonstrate that infiltration of BMDCs, especially

leukocytes and macrophages, significantly contributes to neointima formation

(108, 110, 111). We have previously reported that *Nf1*^{+/-} BMDCs have increased

migration and proliferation in response to multiple growth factors implicated in

neointima formation (125-127). Therefore, to test the hypothesis that *Nf1*^{+/-}

BMDCs enhanced neointima formation, we utilized adoptive hematopoietic stem

cell transfer techniques. BMDCs isolated from *Nf1*^{+/-} or WT mice that

ubiquitously express green fluorescent protein (GFP) were transplanted into

conditioned *Nf1*^{+/-} or WT recipients to generate *Nf1*^{+/-} mice with either WT or

Nf1^{+/-} GFP bone marrow (BM) and WT mice with either WT or *Nf1*^{+/-} GFP BM

(Figure 19). Bone marrow engraftment was determined after four months by

determining the percent of GFP positive mononuclear cells in peripheral blood by

flow cytometric analysis. Mice with greater than 85% engraftment (Figure 20)

underwent carotid artery ligation as previously described.
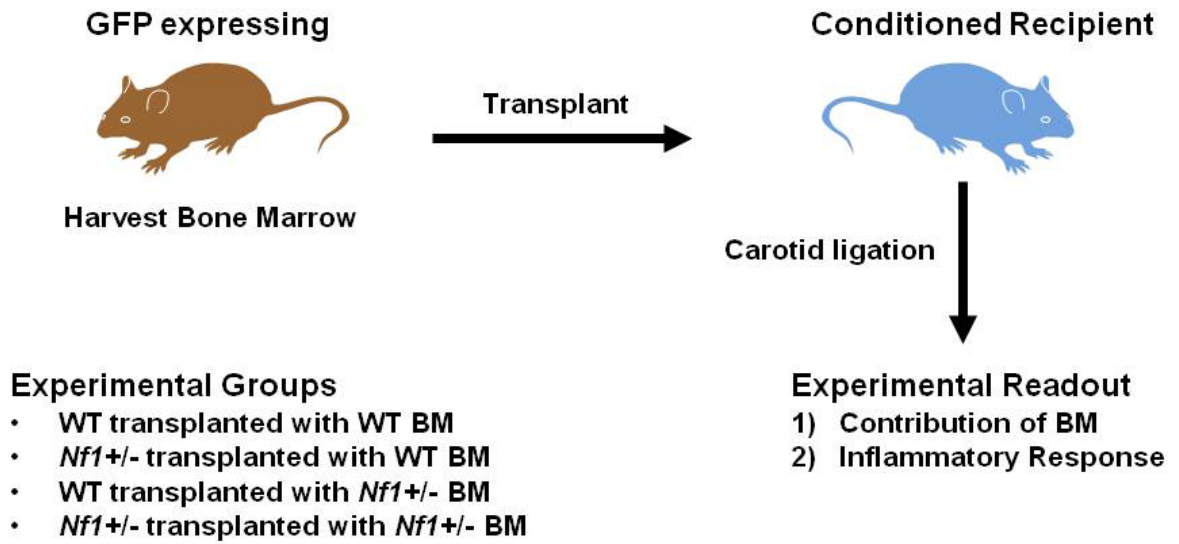
Figure 19. Experimental strategy for adoptive hematopoietic stem transfer.
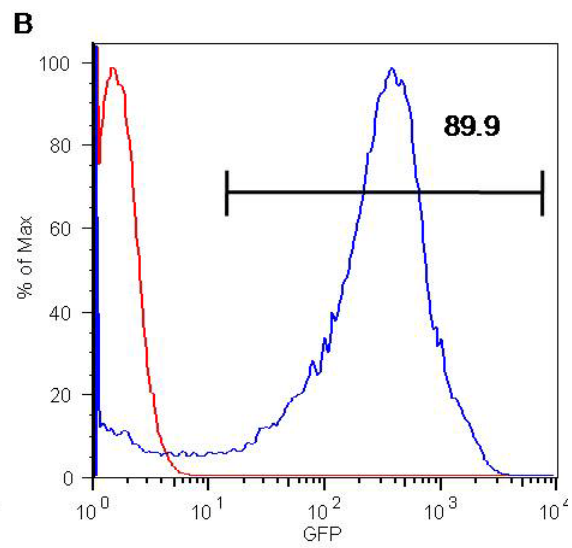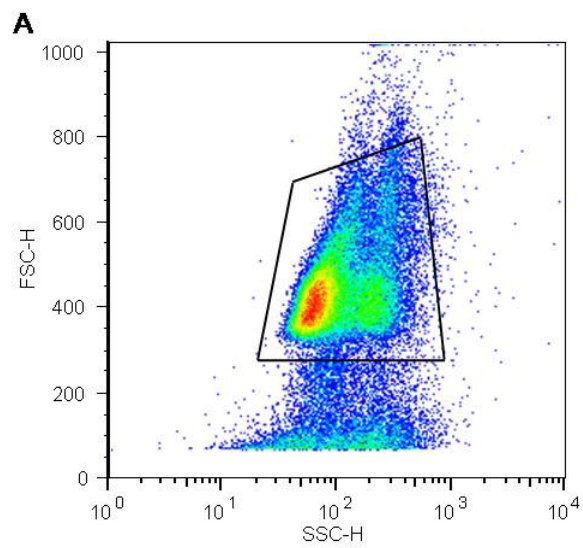
Figure 20. Determination of percent bone marrow engraftment.

A) Representative forward-scatter (FSC-H) side-scatter (SSC-H) profile of whole MNCs from murine peripheral blood. Black box represents live events gated for GFP expression analysis. B) Representative histogram of percent GFP expression in MNCs. Red line represents GFP negative control. Blue line represents MNCs from a mouse transplanted with GFP positive bone marrow.

Uninjured arteries from each transplant group were morphologically similar and showed no evidence of neointima formation (Figure 21). In response to carotid artery ligation, $Nf1^{+/-}$ mice transplanted with WT BM had a 10 fold reduction in neointima area (Figure 21a-b and 22) and a 9 fold reduction in I/M ratio compared to $Nf1^{+/-}$ mice reconstituted with $Nf1^{+/-}$ BM (Figure 21c). Further, WT mice transplanted with $Nf1^{+/-}$ BM had a 20 fold increase in neointima area (Figure 21b) and I/M ratio (Figure 21b) compared to WT mice reconstituted with WT BM. The observation that transplantation of WT BM into $Nf1^{+/-}$ mice completely abrogates neointima formation indicates that heterozygous inactivation of $Nf1$ in BMDCs is necessary and sufficient for neointima formation in response to vascular injury.

A

Uninjured   Injured

WT BM   *Nf1⁺ᐟ⁻* BM   WT BM   *Nf1⁺ᐟ⁻* BM

WT

Nf1⁺ᐟ⁻

B

Neointima Area (um^2)

☐ Uninjured
■ Injured

Recipient: WT   WT   *Nf1⁺ᐟ⁻*   *Nf1⁺ᐟ⁻*
Donor: WT   *Nf1⁺ᐟ⁻*   WT   *Nf1⁺ᐟ⁻*

C

Intima/Media Ratio

☐ Uninjured
■ Injured

Recipient: WT   WT   *Nf1⁺ᐟ⁻*   *Nf1⁺ᐟ⁻*
Donor: WT   *Nf1⁺ᐟ⁻*   WT   *Nf1⁺ᐟ⁻*

83
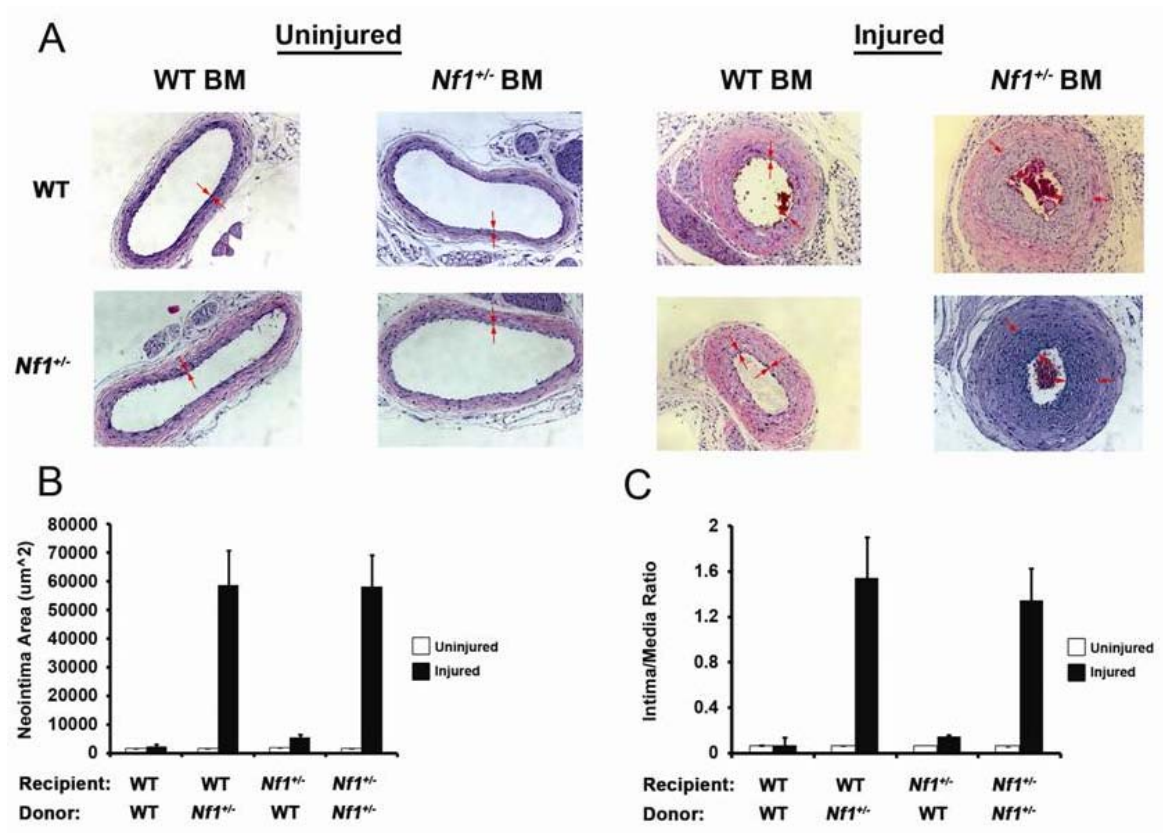
Figure 21. Histological and morphometric analysis of WT and *Nf1*^{+/-} mice transplanted with WT and *Nf1*^{+/-} bone marrow. A) Representative H&E stained cross-sections of uninjured (left panels) and injured (right panels) carotid arteries from WT (top panels) and *Nf1*$^{+/-}$ (bottom panels) mice transplanted with WT or *Nf1*$^{+/-}$ BM. Red arrows indicate boundaries of neointima. B) Quantification of neointima area of uninjured (open bars) and injured (black bars) carotid arteries from WT or *Nf1*$^{+/-}$ recipients transplanted with WT or *Nf1*$^{+/-}$ BM. Data represent the mean neointima area of 3 arterial cross-sections (400 μm, 800 μm and 1200 μm distal to the ligation) ± SEM, n=5-8. *p<0.001 for WT mice transplanted with *Nf1*$^{+/-}$ BM uninjured vs. WT mice transplanted with *Nf1*$^{+/-}$ BM injured and *Nf1+/-* mice transplanted with *Nf1+/-* BM uninjured vs. *Nf1+/-* mice transplanted with *Nf1+/-* BM injured, and **p<0.001 for WT mice transplanted with *Nf1*$^{+/-}$ BM and *Nf1+/-* mice transplanted with *Nf1+/-* BM vs. WT mice transplanted with WT BM and *Nf1+/-* mice transplanted with WT BM injured by one-way ANOVA with Tukey post-test. C) Quantification of I/M ratio of uninjured (open bars) and injured (black bars) carotid arteries from WT or *Nf1*$^{+/-}$ recipients transplanted with WT or *Nf1*$^{+/-}$ BM. Data represent the mean I/M ratio of 3 arterial cross-sections (400 μm, 800 μm and 1200 μm distal to the ligation) ± SEM, n=5-8. *p<0.001 for WT mice transplanted with *Nf1*$^{+/-}$ BM uninjured vs. WT mice transplanted with *Nf1*$^{+/-}$ BM injured and *Nf1+/-* mice transplanted with *Nf1+/-* BM uninjured vs. *Nf1+/-* mice transplanted with *Nf1+/-* BM injured, and **p<0.001 for WT mice transplanted with *Nf1*$^{+/-}$ BM and *Nf1+/-* mice transplanted with *Nf1+/-*

BM vs. WT mice transplanted with WT BM and *Nf1+/-* mice transplanted with WT

BM injured by one-way ANOVA with Tukey post-test.

Donor BM: WT | WT | Nf1+/- | Nf1+/-

Recipient Genotype: WT | Nf1+/- | WT | Nf1+/-

Figure 22. Histological analysis of WT and *Nf1*^{+/-} mice transplanted with WT and *Nf1*^{+/-} bone marrow. Representative H&E stained arterial cross-sections from injured WT and *Nf1*^{+/-} mice that have been transplanted with either WT or *Nf1*^{+/-} bone marrow (BM). Black box indicates area magnified in lower panel. Red arrows indicate neointima boundaries.

_Nf1^{+/-}_ Mice Have Evidence of Vascular Inflammation.

To further understand the cellular mechanism of $Nf1^{+/-}$ BMDCs in neointima formation, we identified BMDCs within the neointima in response to injury. Utilizing immunohistochemistry, uninjured and injured carotid artery cross-sections from each transplant group were co-stained with an anti-GFP antibody, to identify BMDCs, and an $α$-SMA antibody, to identify VSMCs. We utilized an anti-GFP antibody given the amount of autofluorescence inherent in murine tissue. Uninjured carotid arteries for each transplant group showed no accumulation of BMDCs within the vessel (Figure 23a). In response to injury, WT mice transplanted with $Nf1^{+/-}$ BM had a 12 fold increase in the accumulation of GFP positive BMDCs within the neointima compared to WT mice reconstituted with WT BM (Figure 23). Similarly, $Nf1^{+/-}$ mice transplanted with $Nf1^{+/-}$ BM had a 14 fold increase in the number of GFP positive BMDCs within the neointima compared to $Nf1^{+/-}$ mice transplanted with WT BM (Figure 23b). Surprisingly, despite no difference in neointima size, $Nf1^{+/-}$ mice transplanted with $Nf1^{+/-}$ BM had a two fold increase in the number of GFP positive BMDCs within the neointima compared to WT mice transplanted with $Nf1^{+/-}$ BM in response to carotid ligation (Figure 23b) with no difference in the total number of cells within the neointima. This observation indicates that heterozygous inactivation of $Nf1$ in other cell lineages enhances the recruitment/survival of BMDCs in $Nf1^{+/-}$ mice transplanted with $Nf1^{+/-}$ BM. Of note, arterial cross-sections showed no colocalization of GFP positive cells with $α$-SMA positive cells (Figure 23a)

indicating that the VSMCs within the neointima are locally derived and not bone

marrow derived VSMCs.

A

Uninjured   Injured

Donor BM: WT   *Nf1+/-*   WT   *Nf1+/-*

Recipient Genotype

WT

Nf1+/-

B

GFP + Cells in Neointima

| Recipient: | WT | WT | *Nf1+/-* | *Nf1+/-* |
| Donor: | WT | *Nf1+/-* | WT | *Nf1+/-* |

90
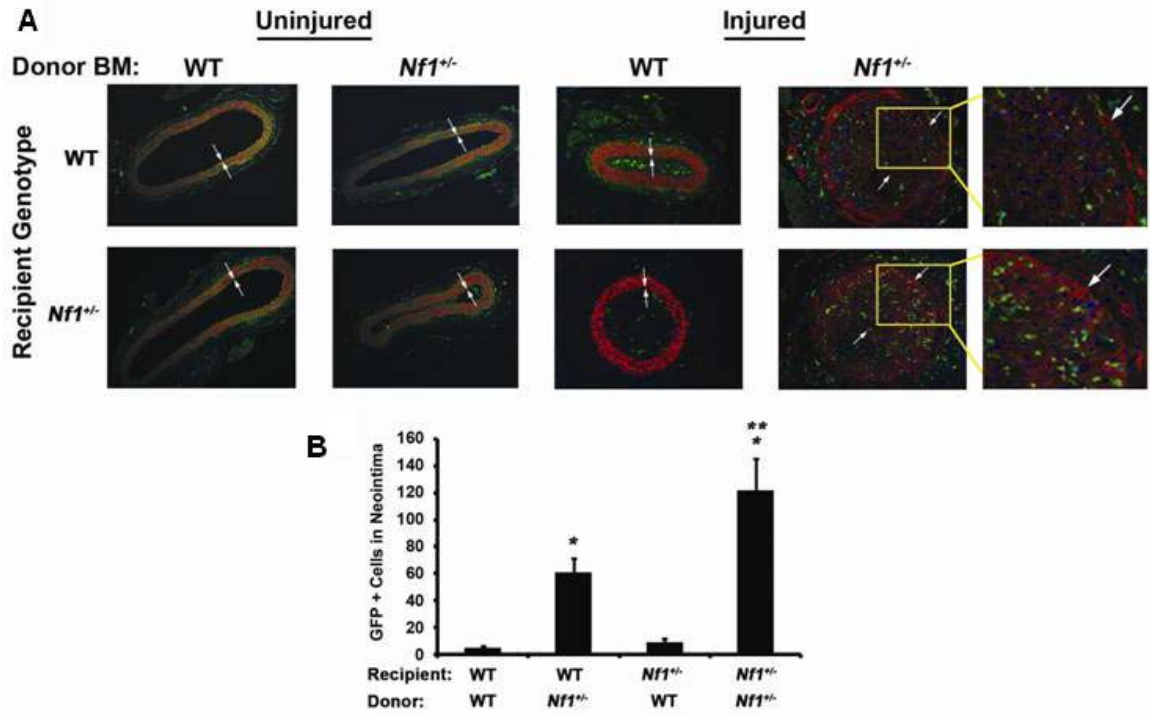
Figure 23. Identification of VSMCs and BMDCs within the neointima of WT and _Nf1_$^{+/-}$ mice transplanted with WT and _Nf1_$^{+/-}$ bone marrow. A) Representative photomicrographs of uninjured (left panels) and injured (right panels) carotid arteries from WT (top panels) and _Nf1_$^{+/-}$ (bottom panels) mice transplanted with either WT or _Nf1+/-_ bone marrow (BM). VSMCs are stained with anti-α-SMA (red) and anti-GFP (green). Cell nuclei are visible by DAPI stain (blue) and some tissue autofluorescence is visible (green). White arrows indicate neointima boundaries. Yellow boxes identify area of injured WT and _Nf1_$^{+/-}$ mice transplanted with _Nf1_$^{+/-}$ BM magnified in the far right panel. B) Quantification of the total number of GFP positive cells within the neointima of WT and _Nf1_$^{+/-}$ recipient mice after carotid ligation. Data represents the mean GFP positive cells within the neointima 600 μm distal to the ligation ± SEM, n=6. *$p<0.05$ for injured WT mice transplanted with WT BM vs. injured WT mice transplanted with _Nf1_$^{+/-}$ BM and injured _Nf1_$^{+/-}$ mice transplanted with WT BM vs. injured _Nf1_$^{+/-}$ mice transplanted with _Nf1_$^{+/-}$ BM and **$p<0.05$ for injured WT mice transplanted with _Nf1_$^{+/-}$ BM vs. injured _Nf1_$^{+/-}$ mice transplanted with _Nf1_$^{+/-}$ BM by one-way ANOVA with Tukey post-test.

Heterozygous Inactivation of *Nf1* in VSMCs and BMDCs Increased the Accumulation of BMDCs Within the Neointima Compared to WT VSMCs.

In order to determine if heterozygous inactivation in an additional cell lineage increased the accumulation of BMDCs in the neointima, we generated *Nf1^{flox/+};SM22cre* mice reconstituted with *Nf1^{+/-}* BM.   In response to carotid artery ligation, the *Nf1^{flox/+};SM22cre* mice transplanted *Nf1^{+/-}* BM had similar neointima formation to both *Nf1^{+/-}* and WT mice transplanted *Nf1^{+/-}* BM. Further, immunohistochemistry demonstrated that *Nf1^{flox/+};SM22cre* mice reconstituted with *Nf1^{+/-}* BM had equivalent accumulation of BMDCs as the *Nf1^{+/-}* mice transplanted with *Nf1^{+/-}* BM (Figure 24). This observation indicates that heterozygous inactivation of *Nf1* in VSMCs enhanced the recruitment/survival of *Nf1^{+/-}* BMDCs to the site of vascular injury in *Nf1^{+/-}* mice transplanted with *Nf1^{+/-}* BM compared to WT mice transplanted with *Nf1^{+/-}* BM. In future studies in Dr. Ingram's lab, the role of neurofibromin in the production of chemokines and cytokines from *Nf1^{+/-}* VSMCs will be determined *in vitro* and *in vivo*.

A

WT   Nf1+/-   Nf1^{flox/+};SM22cre

Nf1+/- BM

B

GFP+ Cells in Neointima

Recipient: WT   Nf1+/-   Nf1^{flox/+};SM22cre
Donor: Nf1+/-   Nf1+/-   Nf1+/-
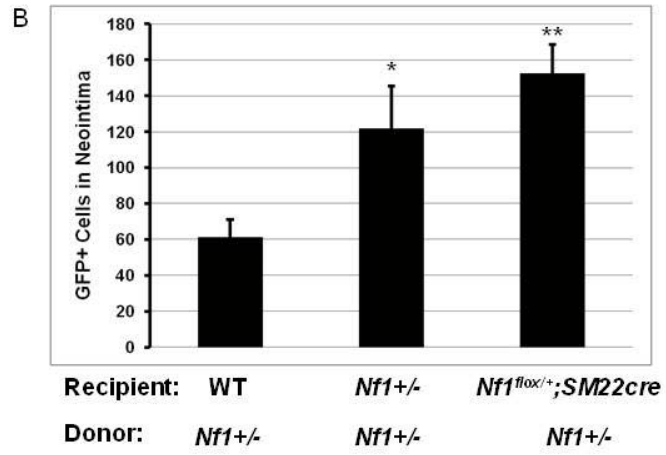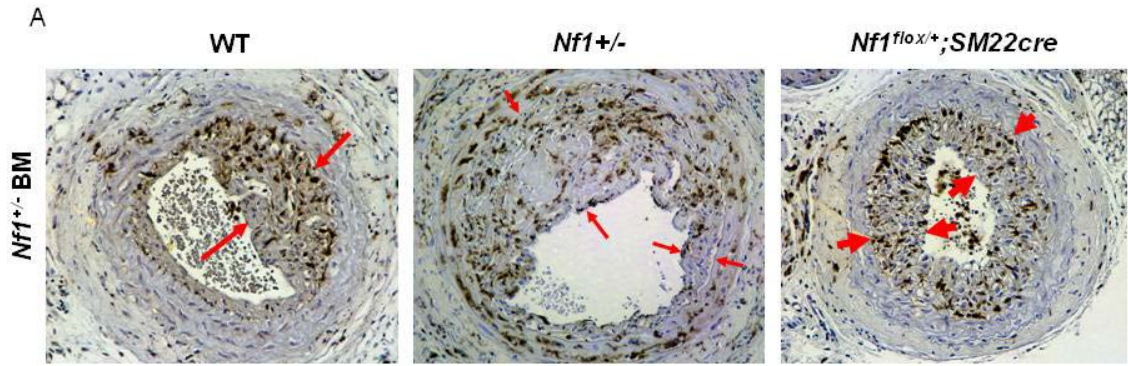
Figure 24. Identification of GFP positive BMDCs within the neointima or WT, *Nf1$^{+/-}$* and *Nf1$^{flox/+}$;SM22cre* mice transplanted with *Nf1$^{+/-}$* BM. A) Representative photomicrographs of injured carotid arteries from WT (left panel), *Nf1$^{+/-}$* (middle panel) and *Nf1$^{flox/+}$;SM22cre* (right panel) mice transplanted with *Nf1$^{+/-}$* bone marrow (BM) stained with anti-GFP (brown) and counterstained with hematoxylin (blue). Red arrows indicate neointima boundaries. B) Quantification of the total number of GFP positive cells within the neointima of WT, *Nf1$^{+/-}$* and *Nf1$^{flox/+}$;SM22cre* mice transplanted with *Nf1$^{+/-}$* bone marrow. Data represents the mean total number of GFP positive cells within the neointima 600 µm distal to the ligation ± SEM, n=3-6. *p<0.05 for *Nf1$^{+/-}$* vs. WT and **p<0.01 for *Nf1$^{flox/+}$;SM22cre* vs. WT by one-way ANOVA with Tukey post-test.

Heterozygous Inactivation of *Nf1* in BMDCs Leads to Vascular Inflammation in Response to Injury.

Carotid artery ligation results in the deposition of platelets and leukocytes on the endothelium and the transmigration of leukocytes into the vessel wall. Specifically, monocytes and macrophages have been shown to play an essential role in neointima formation. To further define the cellular mechanism of neointima formation in WT and *Nf1$^{+/-}$* mice reconstituted with *Nf1$^{+/-}$* BM, we utilized immunohistochemistry to identify the lineage of BMDCs within the neointima. Anti-CD45 immunohistochemistry demonstrated that the BMDCs within the neointima were leukocytes (Figure 25). To further identify the BMDCs within the neointima, carotid artery cross-sections were analyzed for the presence of lymphocytes and macrophages. Lymphocytes and macrophages are inflammatory cells, which secrete growth factors and cytokines that have been implicated in neointima formation in response to injury (178-183). Further, our group has demonstrated that neurofibromin is a critical regulator of Ras activation in both lymphocytes and mast cells *in vitro* and *in vivo* (126, 184). Based on immunohistochemistry, lymphocytes (Figure 26) did not significantly accumulate in the neointima or vessel wall of injured arteries in any of the experimental genotypes. However, anti-Mac3 staining of injured carotid arteries demonstrated that the majority (>80%) of the GFP positive cells within the neointima of all transplant groups were macrophages (Figure 27). Consistent with the results of anti-GFP immunohistochemistry, WT and *Nf1$^{+/-}$* mice transplanted with WT BM had minimal accumulation of macrophages within the

intima area compared with WT and $Nf1^{+/-}$ mice reconstituted with $Nf1^{+/-}$ BM in response to injury (Figure 27). This observation suggests that $Nf1^{+/-}$ BMDCs contribute to neointima formation through increased recruitment and/or survival of monocytes into the vessel wall where they differentiate into macrophages and drive enhanced neointima formation.

WT Recipient   *Nf1*^{+/-} Recipient
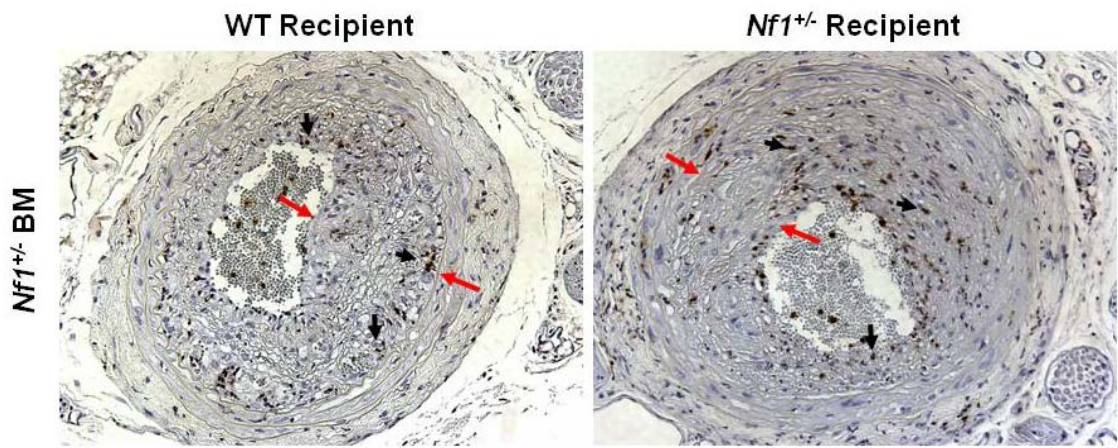
Nf1^{+/-} BM

Figure 25. Immunohistochemical analysis of CD45 positive cells within the neointima. Representative photomicrographs of injured carotid arteries from WT (left panel) and $Nf1^{+/-}$ (right panel) recipient mice transplanted with $Nf1^{+/-}$ BM stained with an anti-CD45 antibody (brown) and counterstained with hematoxylin (blue). Red arrows indicate neointima boundaries. Black arrows represent positive staining.

	WT BM	Nf1^{+/-} BM
WT Recipient		
Nf1^{+/-} Recipient		

99
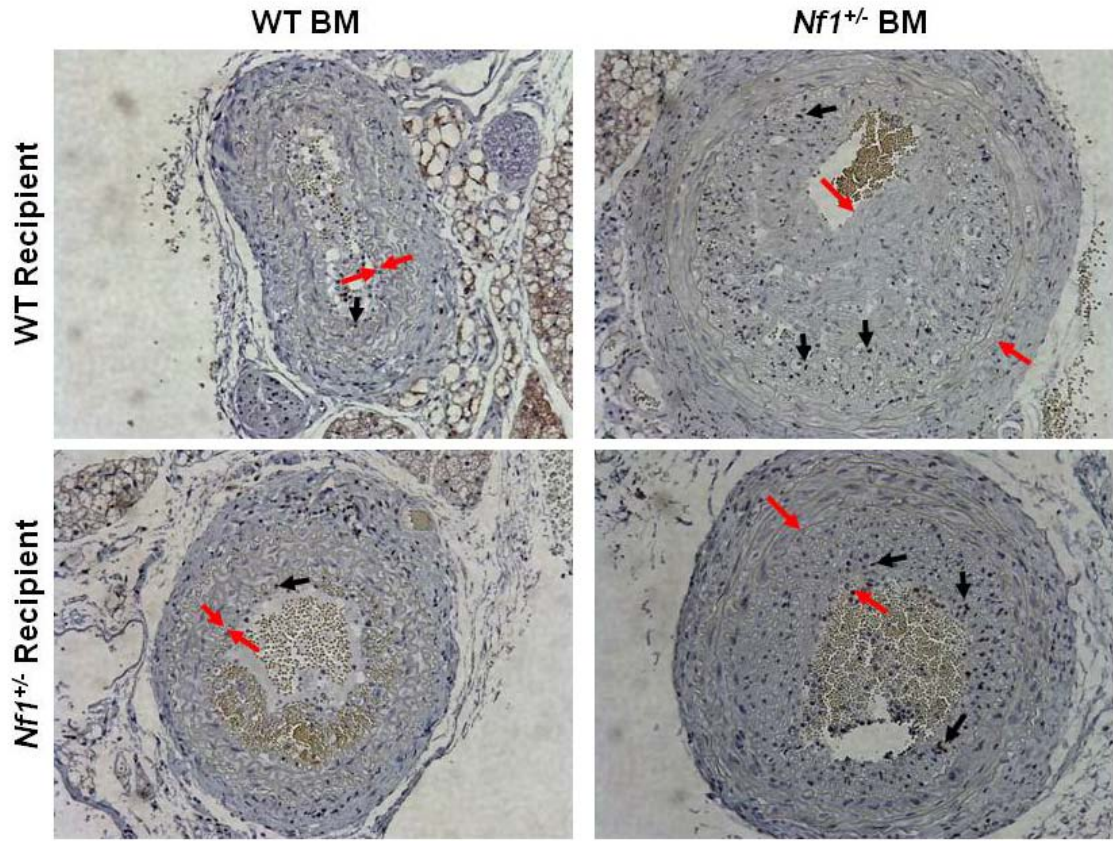
Figure 26. Immunohistochemical analysis of CD3 positive cells within the neointima. Representative photomicrographs of injured carotid arteries from WT (top panels) and *Nf1*$^{+/-}$ (bottom panels) recipient mice transplanted with WT BM (left panels) or *Nf1*$^{+/-}$ BM (right panels) stained with an anti-CD3 antibody (brown) and counterstained with hematoxylin (blue). Red arrows indicate neointima boundaries. Black arrows represent positive staining.
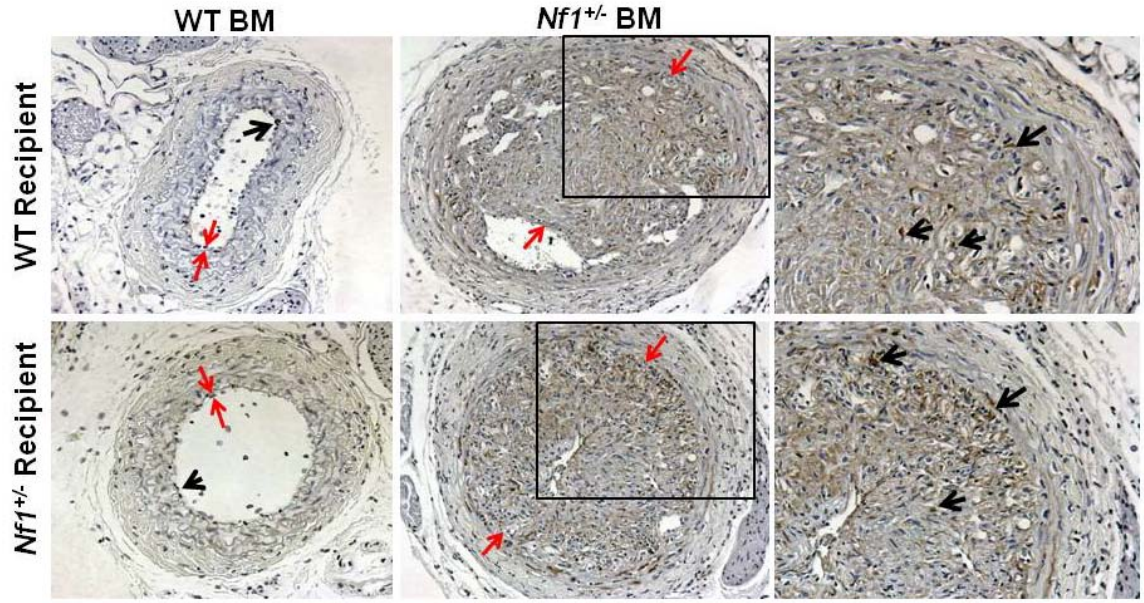
Figure 27. Identification of macrophage accumulation within the neointima of WT and *Nf1*$^{+/-}$ mice transplanted with *Nf1*$^{+/-}$ bone marrow. Representative photomicrographs of injured carotid artery cross sections from WT (top panels) and *Nf1*$^{+/-}$ (bottom panels) mice transplanted with WT (left panels) or *Nf1*$^{+/-}$ BM (middle and right panels) stained with anti-Mac3 antibody (brown) and counterstained with hematoxylin (blue). Red arrows indicate neointima boundaries. Black arrows represent positive Mac3 staining. Black boxes identify area of injured WT and *Nf1*$^{+/-}$ mice transplanted with *Nf1*$^{+/-}$ BM that is magnified in the far right panel.

Based on this observation, we investigated whether heterozygous inactivation of *Nf1* leads to increased numbers of circulating monocytes. Peripheral blood samples were taken from uninjured WT and $Nf1^{+/-}$ mice and complete blood count analysis completed. At baseline, $Nf1^{+/-}$ mice have a 1.5 fold increase in the percentage of circulating monocytes compared to WT mice (Figure 28a). In order to determine if neurofibromin regulates the migration, proliferation and adhesion of macrophages, which are cellular functions critical for the recruitment and retention of macrophages in the vessel wall, we isolated and purified macrophages from the bone marrow of $Nf1^{+/-}$ and WT mice. Stimulation of the macrophages with macrophage colony stimulating factor (M-CSF), a growth factor critical in neointima formation, demonstrated that $Nf1^{+/-}$ macrophages had a two-fold increase in proliferation (Figure 28b) and migration (Figure 28c) compared to WT macrophages. Further, $Nf1^{+/-}$ macrophages showed significantly increased adhesion on fibronectin compared to WT macrophages (Figure 28d). Consistent with increased accumulation of $Nf1^{+/-}$ macrophages into the neointima *in vivo*, this data clearly demonstrates that heterozygous inactivation of *Nf1* increases macrophage migration, proliferation and adhesion *in vitro*. Collectively, this cellular and genetic data demonstrates that neointima formation in $Nf1^{+/-}$ mice is directly related to increased "vascular inflammation" and accumulation of BMDCs, especially macrophages, into the evolving neointima.
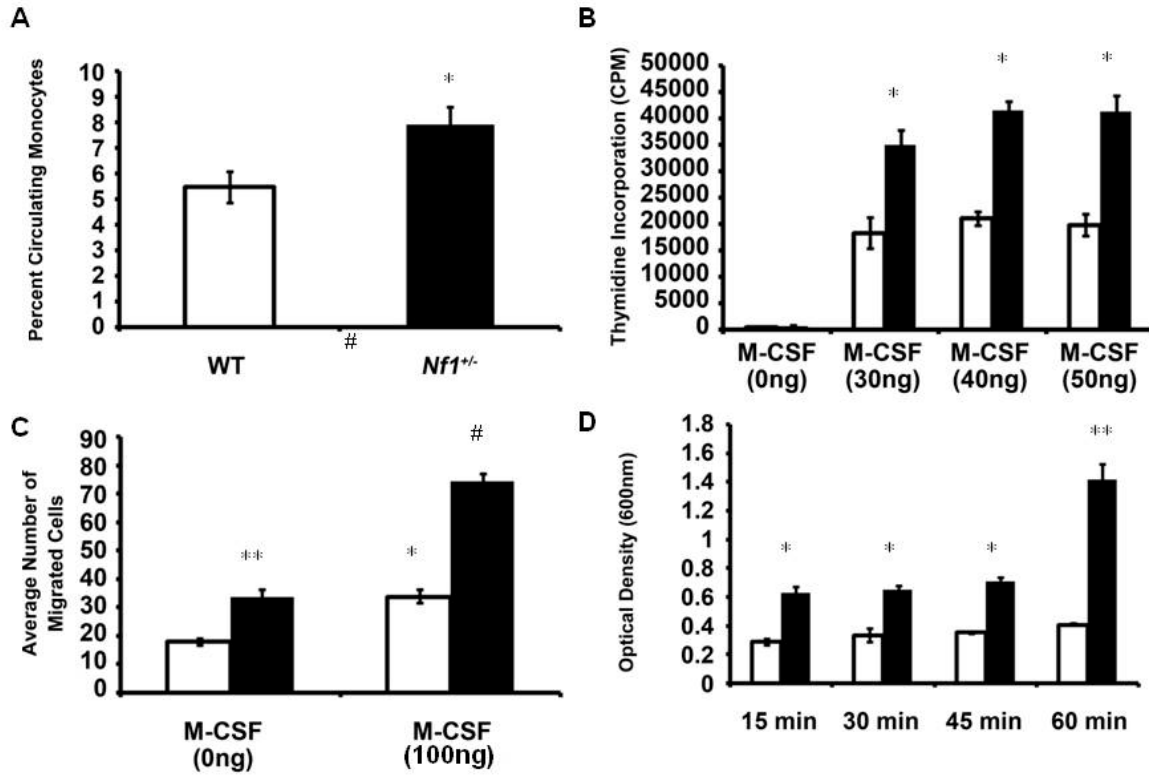
Figure 28. Effect of heterozygous inactivation of *Nf1* in macrophages *in vitro*. A) Complete blood analysis of percent monocytes in circulation from peripheral blood from WT (open bars) and *Nf1$^{+/-}$* mice (black bars). Data represents the average percentage ± SEM, n=8, *p=0.02 for *Nf1$^{+/-}$* vs. WT by Student's unpaired t test. B) Proliferation of WT (open bars) and *Nf1$^{+/-}$* (black bars) bone marrow derived macrophages in response to M-CSF stimulation. Data represents average CPM (thymidine counts per minute) ± SEM, n=4, *p<0.001 for WT macrophages 0 ng M-CSF vs. WT macrophages stimulated with 30ng, 40ng and 50ng M-CSF and **p<0.001 for *Nf1$^{+/-}$* macrophages stimulated with M-CSF vs. WT macrophages stimulated with M-CSF by one-way ANOVA with Tukey post-test. C) Haptotaxis of WT and *Nf1+/-* macrophages in response to 100ng M-CSF. Data represents average number of migrated cells ± SEM, *p<0.001 for WT macrophages stimulated with 0ng M-CSF vs. WT macrophages stimulated with 100ng M-CSF, **p<0.001 for WT macrophages stimulated with 0ng M-CSF vs. *Nf1$^{+/-}$* macrophages stimulated with 0ng M-CSF and #p<0.001 for *Nf1$^{+/-}$* macrophages stimulated with 0ng M-CSF vs. *Nf1$^{+/-}$* macrophages stimulated with 100ng M-CSF by one-way ANOVA with Tukey post-test. D) Adhesion of WT and *Nf1$^{+/-}$* macrophages to fibronectin. Data represents average optical density (600nm) ± SEM, n=4, *p<0.001 for WT macrophages vs. *Nf1$^{+/-}$* macrophages and **p<0.01 for *Nf1$^{+/-}$* macrophages at 60 min vs. *Nf1$^{+/-}$* macrophages at 15 min, 30 min and 45 min by one-way ANOVA with Tukey post-test.

Nf1$^{+/-}$ **Mice Do Not Have Evidence of Chronic Inflammation.**

The increased macrophage function observed *in vitro* suggests that *Nf1*$^{+/-}$ mice may exhibit chronic inflammation due to the increased function of *Nf1*$^{+/-}$ macrophages. To determine if *Nf1*$^{+/-}$ mice have evidence of chronic inflammation, we assayed for the presence of inflammatory cytokines and chemokines in plasma isolated from the peripheral blood of uninjured *Nf1*$^{+/-}$ mice and WT mice. Analysis of plasma samples demonstrated that there was no difference in circulating levels of the cytokines IL-1β, IL-6, IL-10 and TNFα, or the chemokines M-CSF and MCP-1 between *Nf1*$^{+/-}$ mice and WT mice (Figure 29). This is not a surprising observation given that *Nf1*$^{+/-}$ mice do not develop vascular lesions in the absence of an external challenge. Therefore, in order to determine the acute effects of carotid artery ligation in future studies, plasma samples need to be collected at early timepoints post-injury and assayed for increased levels of inflammatory cytokines. Preliminary data suggests that carotid artery ligation may increase the levels of circulating Cd11$^+$Gr-1$^+$ monocytes in *Nf1*$^{+/-}$ mice above baseline at 24 hours post-ligation compared to WT mice (Figure 30). However, in order to determine if there is a significant increase in circulating monocytes and increased levels of inflammatory cytokines and chemokines in *Nf1*$^{+/-}$ mice in response to injury, multiple studies need to be completed to analyze peripheral blood samples from injured mice at numerous timepoints. Studies will be continued in Dr. Ingram's lab to identify whether carotid artery ligation results in acute systemic inflammation in *Nf1*$^{+/-}$ mice by assaying for increased

inflammatory cytokines production as well as dissecting the role of $Nf1^{+/-}$

macrophages in neointima formation.
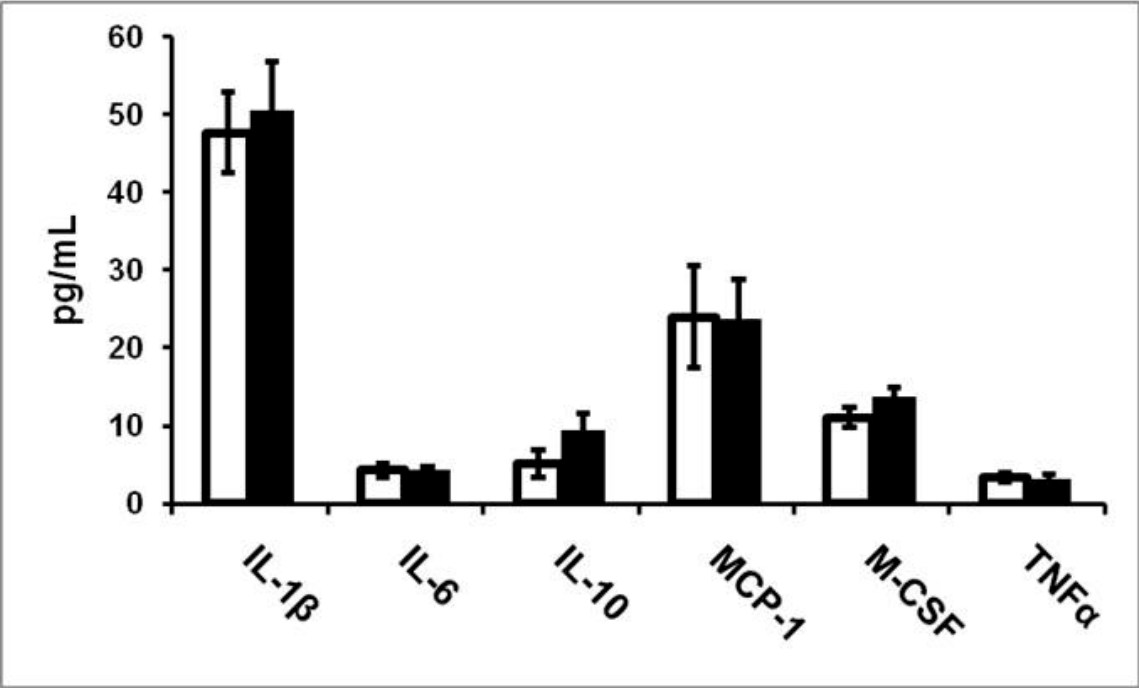
Figure 29. Analysis of circulating inflammatory cytokines and chemokines in *Nf1*^{+/-} and WT mice. Circulating levels of cytokines and chemokines in plasma samples isolated from uninjured WT (open bars) and *Nf1*^{+/-} (black bars) mice. Data represents the average pg/mL ± SEM, n=8.
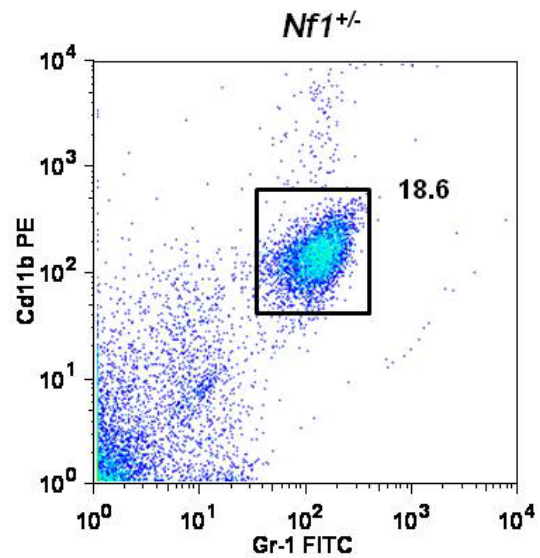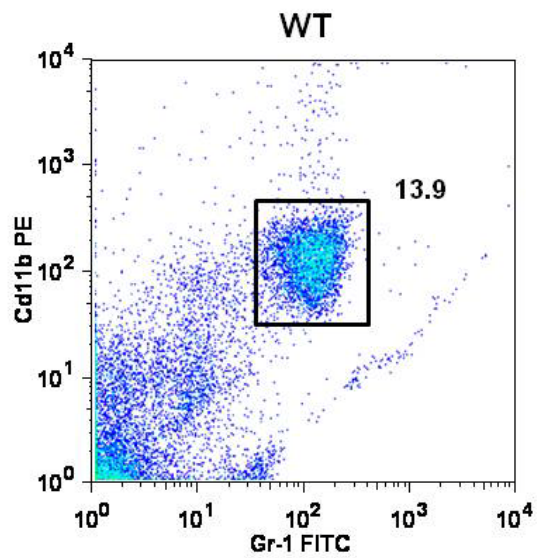
Figure 30. Flow cytometric analysis of circulating monocytes 24 hours post-ligation. Peripheral blood analysis of circulating Cd11b$^+$Gr-1$^+$ monocytes in WT (left panel) and *Nf1$^{+/-}$* (right panel) mice 24 hours post-ligation. Black box identifies the Cd11b$^+$Gr-1$^+$ population.

NF1 Patients Have Evidence of Chronic Inflammation

Given the observation of vascular inflammation in *Nf1*$^{+/-}$ mice *in vivo* in response to injury, we tested whether NF1 patients had cellular and cytokine evidence of vascular inflammation by assaying for previously established biomarkers linked to human vasoocclusive disease. Utilizing mulitparameter flow cytometry, we analyzed mononuclear cells isolated from the peripheral blood of NF1 patients and age and sex-matched healthy controls for inflammatory monocyte populations. The frequency of total circulating monocytes was initially determined by assaying total mononuclear cells for monocytes that co-expressed the cell surface antigens, CD45 and CD14 (185). NF1 patients had significantly increased frequencies of circulating monocytes compared with healthy controls (Figure 31a). We further measured specific circulating monocyte populations to identify pro-inflammatory monocytes, which co-express CD14 and CD16 (CD14$^+$CD16$^+$) (186). Pro-inflammatory monocytes have been identified in the peripheral blood of patients with coronary artery disease and atherosclerosis (102, 107) and have been shown to produce more inflammatory cytokines compared to classical monocytes (146, 186). Analysis of NF1 patient peripheral blood monocytes identified a population of monocytes that had increased CD16 expression (CD14^{dim}CD16^{bright}) compared to the traditional CD14$^+$CD16$^+$ population, a population that was not observed in peripheral blood samples from healthy controls (Figure 31b). Based on a side scatter profile, the population of CD14^{dim}CD16^{bright} monocytes is larger in size compared with other monocyte

populations, indicating the cells have increased granularity, a characteristic of

monocyte activation (187).
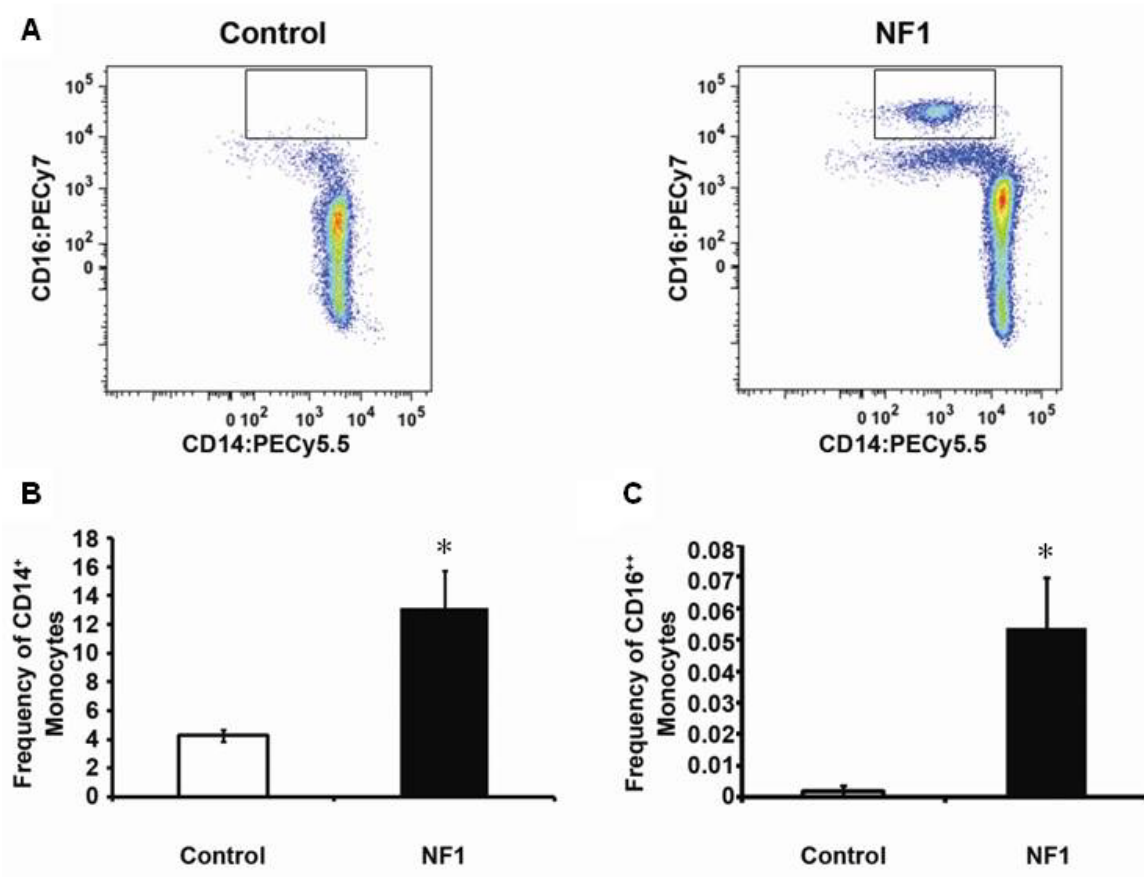
Figure 31. Identification of circulating monocytes from peripheral blood of healthy adult controls and NF1 patients. A) Representative PFC analysis of peripheral blood monocytes by CD14 and CD16 cell surface expression in healthy adult controls (left panel) and NF1 patients (right panel). Black box identifies CD14^{dim}CD16^{bright} monocyte population. Data represents 5 independent observations. B) Quantification of the frequency of CD45^{+}CD14^{+} monocytes in circulation from healthy adult control and NF1 patient peripheral blood MNCs. Data represents the mean frequency ± SEM, n=5, *p=0.024 by Student's unpaired t test with Welch correction. C) Quantification of the frequency of CD45^{+}CD14^{dim}CD16^{bright} monocytes in circulation from healthy adult control and NF1 patient peripheral blood MNCs. Data represents the mean frequency ± SEM, n=5, *p=0.0012 by Student's unpaired t test.

Pro-inflammatory monocytes produce a numerous inflammatory cytokines and chemokines that have been implicated in neointima formation. Therefore, based on the increased levels of circulating monocytes and the presence of an activated monocyte population, we hypothesized that NF1 patients would also have increased levels of inflammatory cytokines and chemokines in their peripheral blood, a correlation that has been made in other patient populations with the progression of vascular disease (100, 103, 188, 189). We analyzed plasma samples from NF1 patients and healthy controls for the presence of the specific pro-inflammatory cytokines IL-1β, IL-6, interferon-γ (IFN-γ) and TNFα. Analysis of plasma samples from NF1 patients with no known vascular disease (17±2 years, n=6) and healthy controls (18.5±3.4 years, n=7) showed a trend toward increased levels of IFN-γ (p=0.4399) and TNFα (p=0.17) as well as the growth factor GM-CSF (p=0.4228) but were not significant with the limited sample set (Figure 32). Further, the plasma samples showed no difference in levels of the chemoattractant protein MCP-1 between control and NF1 patient samples (Figure 32). However, significantly elevated levels of IL-1β and IL-6 were observed in the plasma samples from NF1 patients compared to controls (Figure 33). The production of pro-inflammatory cytokines has been linked to the activation of the endothelium and increased expression of chemokines involved in the recruitment of monocytes to the vessel wall (112, 143, 144, 151, 190). Interestingly, NF1 patient plasma samples had significantly elevated levels of soluble fractalkine (Figure 33), an adhesion molecule expressed on inflamed endothelium, which is involved in rapid, high-affinity binding of monocytes (151,

116

191, 192). The increased number of circulating monocytes and production of inflammatory cytokines provides direct evidence of chronic inflammation in NF1 and elevation of biomarkers previously identified as critical risk factors in other patient populations with vascular disease reminiscent of NF1 vasculopathy.
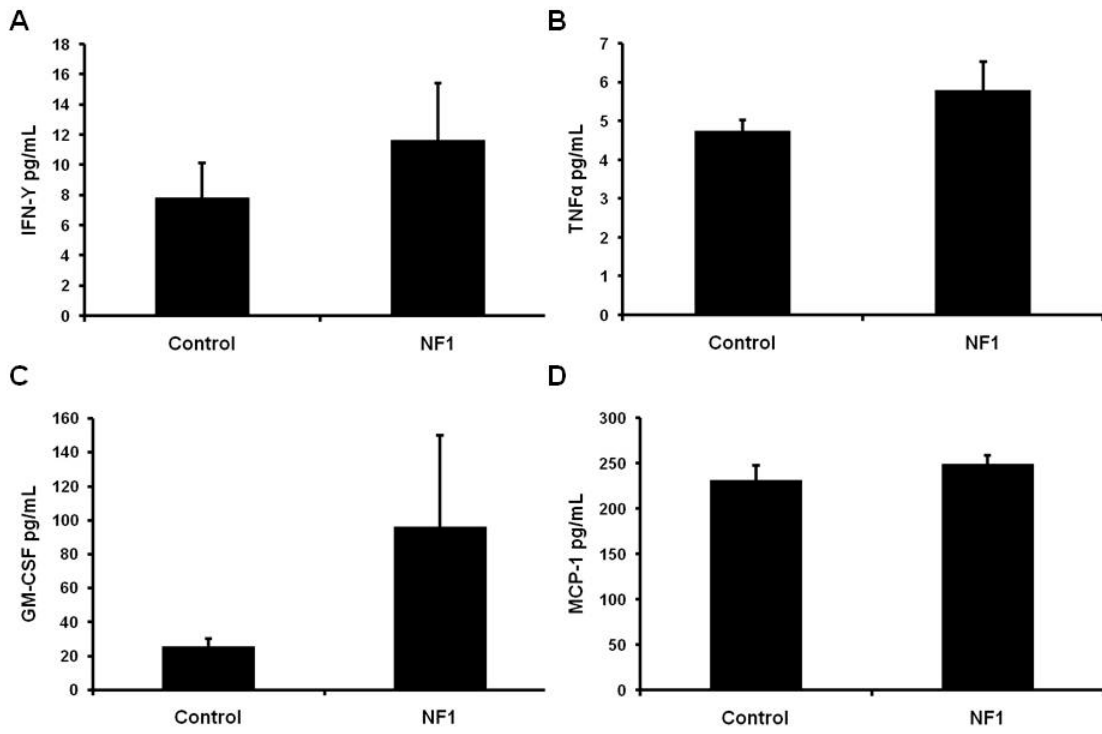
Figure 32. Analysis of inflammatory cytokines and chemokines from NF1 patient and healthy control plasma. Determination of cytokine levels in plasma isolated from control peripheral blood and NF1 patient peripheral blood. A) IFN-γ levels in pg/mL from control and NF1 patient plasma samples. Data represents the average pg/mL ± SEM, n=6. B) TNFα levels in pg/mL from control and NF1 patient plasma samples. Data represents the average pg/mL ± SEM, n=6. C) GM-CSF levels in pg/mL from control and NF1 plasma samples. Data represents the average pg/mL ± SEM, n=6. D) MCP-1 levels in pg/mL from control and NF1 plasma samples. Data represents the average pg/mL ± SEM, n=6.
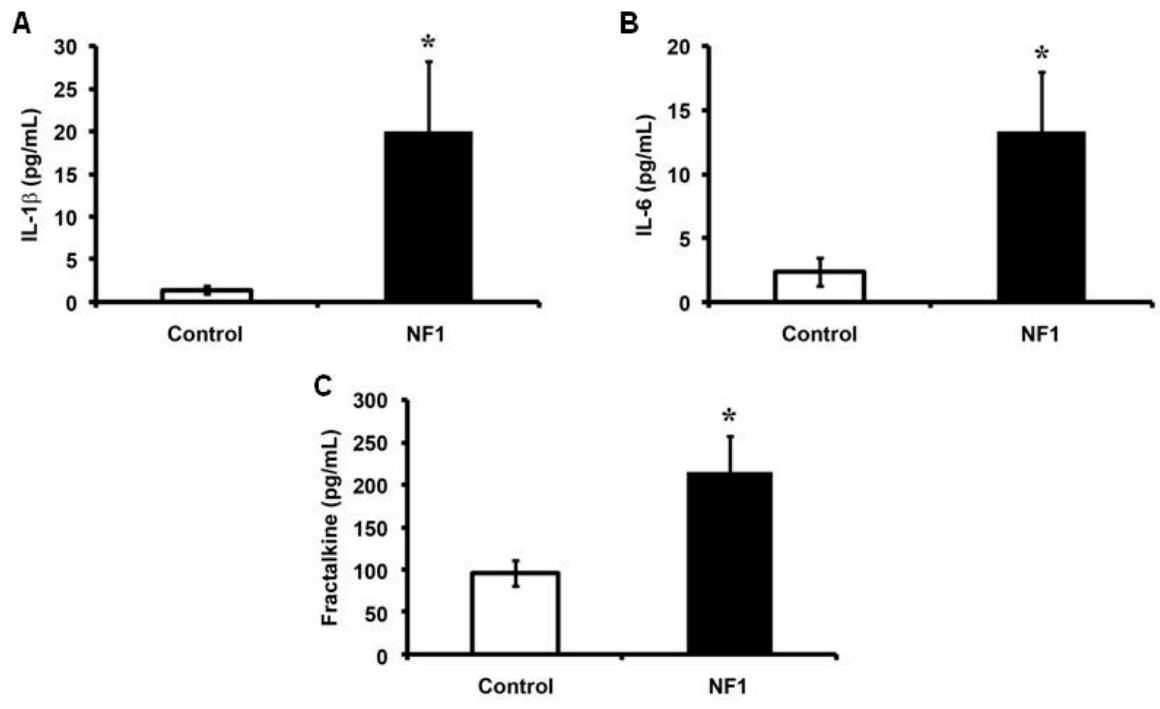
Figure 33. Analysis of inflammatory cytokines and chemokines from NF1 patient and healthy control plasma. Determination of cytokine levels in plasma isolated from control peripheral blood and NF1 patient peripheral blood. A) IL-1β levels in pg/mL. Data represents the average pg/mL ± SEM, n=6, *p=0.014 by Mann-Whitney test. B) IL-6 levels in pg/mL. Data represents the average pg/mL ± SEM, n=6, *p=0.046 by Student's unpaired t test of log transformed data. C) Fractalkine levels in pg/mL. Data represents the average pg/mL ± SEM, n=6-8, *p=0.0393 by Student's unpaired t test with Welch correction.

DISCUSSION

NF1 is an autosomal dominant genetic disorder with a wide range of both malignant and non-malignant clinical manifestations. In contrast to some NF1 cancers where loss of heterozygosity at the *NF1* allele is a prerequisite for tumor development, many of the non-malignant complications of NF1, including learning disorders, skeletal abnormalities and vascular disease occur secondary to aberrant *NF1*$^{+/-}$ cellular functions within a specific tissue microenvironment (21, 37, 38, 50, 126). Thus, study of the effects of *NF1* haploinsufficiency in different cell lineages is imperative for understanding the diverse morbidities associated with NF1. Vasculopathy associated with NF1 is an under-recognized complication of the disease and contributes to significant premature morbidity and mortality in patients. NF1 vasculopathy was first described in 1945 (21). Since the original report, multiple clinical studies demonstrate that different locations within the entire arterial tree may be affected in NF1 patients (15, 20). An important tool for understanding the pathogenesis of NF1 vasculopathy is the development of *in vivo* animal models, which accurately recapitulate some, if not all, aspects of the clinical disease.

An emerging paradigm in vascular biology is that neointima formation in response to injury is tightly controlled by the Ras-Mek-Erk signaling axis in resident cells within the vascular wall including endothelial cells and VSMCs (66, 68-71, 171). Specifically, prior animal studies indicate that increased Ras activation augments VSMC proliferation and migration, and the subsequent

122

development of vascular lesions (63, 65, 68, 72). These vascular lesions are characterized by intimal wall hyperplasia and neointima formation, which ultimately leads to occlusive vascular disease. In support of the importance of Ras in occlusive vascular disease, adenoviral mediated transfer of a dominant negative H-Ras into VSMCs prevents the development of stenotic lesions in rats after mechanical arterial injury by inhibiting the proliferation and migration of VSMCs (68). Similar results were obtained when animals were treated with a chemical Ras farnesyltransferase inhibitor prior to arterial mechanical injury (69).

Finally, when genetically engineered mice harboring constitutively active PDGF-βR only in VSMCs were intercrossed with low density lipoprotein receptor knockout mice, which have a predisposition to developing atherosclerosis, the mutant progeny developed aneurysms and a marked susceptibility to atherosclerosis (63). The mutant mice also showed hyperproliferation of VSMCs and increased Erk activation *in vivo* (63). Consistent with the central pathogenic role of hyperactivation of the PDGF-βR-Ras-Erk signaling pathway in controlling VSMC proliferation *in vivo*, mutant mice treated with imatinib mesylate, an inhibitor of PDGF-βR signaling, did not develop atherosclerosis or aneurysms (63). Collectively, these studies provide a paradigm where hyperactivation of Ras and the PDGF-βR signaling pathway activates a discrete set of biochemical effectors which potentiates VSMC proliferation and migration *in vivo.*

Recent genetic and biochemical studies from Dr. Ingram's laboratory demonstrated that neurofibromin functions as a formal Ras GAP in both murine and human VSMCs *in vitro* (48). Specifically *Nf1$^{+/-}$* VSMCs have increased

migration and proliferation in response to PDGF-BB stimulation via hyperactivation of the Ras-Erk signaling pathway (48). Given the importance of PDGF-βR-Ras-Erk signaling in vascular lesion formation *in vivo* and the observation that *Nf1*^{+/-} VSMCs have increased proliferation and migration *in vitro* in response to PDGF-BB, we utilized a well-established model of arterial injury to develop an *in vivo* model of NF1 vasculopathy.

Development of an *in vivo* model of NF1 vasculopathy.

In order to develop a model that properly reflected human disease, we utilized *Nf1*^{+/-} mice, which are genetically similar to NF1 patients. To date, loss of heterozygosity has not been described in the vascular cells of NF1 patients and therefore haploinsufficiency of *Nf1* was appropriate for this model. *Nf1*^{+/-} mice do not develop vascular lesions in the absence of an external challenge. In order to induce vascular lesion formation, we utilized a carotid artery injury model which mimics arterial microinjury by denuding the endothelium (157). Loss of the endothelium, exposes the underlying matrix and collagen to the circulation, initiating a wound healing response. Initially, platelets are recruited to the exposed collagen followed by leukocyte recruitment (111, 157). Platelets are a potent source of PDGF (158, 159), which has been reported to be necessary to stimulate the migration of quiescent medial VSMCs into the intima area of the vessel (61, 62, 160). The migration and proliferation of VSMCs in the intima area continues until reendothelialization of the lumen has occurred.

Utilizing C57Bl/6 male mice, we demonstrated that $Nf1^{+/-}$ mice had enhanced neointima formation in response to carotid artery injury compared to WT mice (Figure 8). Specifically, $Nf1^{+/-}$ mice had a five-fold increase in neointima area compared to WT mice which resulted in approximately 35% lumen stenosis (Figure 8). Morphologically, the neointima of $Nf1^{+/-}$ mice was reminiscent of vascular lesions described in NF1 patients. Immunohistochemistry was used to determine the cellular content of the neointima and anti-α-SMA staining demonstrated that greater than 75% of the cells within the neointima of $Nf1^{+/-}$ mice were VSMCs, consistent with clinical reports from NF1 patients. Further, immunohistochemistry demonstrated that $Nf1^{+/-}$ mice had significantly increased cellular proliferation within the neointima 21 days post vascular injury compared to WT mice (Figure 11). Proliferation of VSMCs, a function known to be regulated *in vitro* by Ras-Erk signaling (48), suggests that arterial injury results in Ras activation in $Nf1^{+/-}$ mice. Using phospho-Erk as a marker of Ras activation, we determined that vascular injury results in hyperactivation of the Ras-Erk signaling axis in $Nf1^{+/-}$ mice, resulting in enhanced neointima formation (Figure 12). Consistent with our prior *in vitro* observations, we now provide data in the present study to demonstrate that haploinsufficiency at $Nf1$ in vascular wall resident cells leads to hyperactivation of Erk, increased VSMC proliferation, and formation of an enlarged neointima *in vivo* in response to injury. This observation is consistent with the concept that precise regulation of the Ras-Erk signaling axis is critical for maintenance of vascular wall homeostasis and lumen integrity.

Pharmacological Inhibition of Neointima Formation in *Nf1^{+/-}* Mice.

Imatinib mesylate is a potent inhibitor of both PDGF-*β*R-Ras-Erk signaling and C-kit receptor activation *in vivo* (195) and prevents neointima formation in other mouse models after arterial injury (63, 115). Based on these prior studies and the fact that *Nf1^{+/-}* VSMCs are hypersensitive to PDGF-BB stimulation *in vitro*, we tested whether imatinib mesylate could prevent or delay neointima formation in *Nf1^{+/-}* mice after vessel injury. In Figure 14, we demonstrated that treatment of *Nf1^{+/-}* mice with imatinib mesylate completely abrogates neointima formation in response to injury. The inhibition of neointima formation is accompanied by an inhibition of cell proliferation and Ras-Erk activation (Figure 15). In this model, mice were treated with imatinib mesylate daily for 10 days as previously described (115), beginning three days prior to injury to ensure a therapeutic, steady-state level of imatinib mesylate in circulation on the day of injury. The mice continued recovering from day 7 through day 21 with no imatinib mesylate administration. These observations indicate that the events necessary for neointima formation in *Nf1^{+/-}* mice occur within the first week after injury and are a result of either PDGF-*β*R or C-kit activation.

While we do detect inhibition of Erk activation and proliferation in VSMCs in the vessel wall with imatinib mesylate treatment *in vivo*, it is possible that imatinib mesylate also prevents the influx of BMDCs to the evolving neointima in *Nf1^{+/-}* mice to account for the observed treatment effect. In support of this concept, recent murine genetic studies demonstrate that activation of the C-kit receptor in BMDCs mobilizes either VSMCs or cells that express VSMC antigens

to enhance the progression of an evolving neointima by either direct cellular integration or paracrine stimulation of resident cells in the vessel wall (115, 196). This observation is especially intriguing since previous studies from our group demonstrate that $Nf1^{+/-}$ bone marrow derived cells have increased proliferation, migration, and survival in response to Kit ligand stimulation both *in vitro* and *in vivo*(125-127).

This model has established that arterial injury results in enhanced neointima formation in $Nf1^{+/-}$ mice, characterized by increased accumulation of VSMCs and hyperactive Ras-Erk signaling compared to WT mice. These observations are important since they recapitulate the phenotype of NF1 patients and are consistent with *in vitro* reports of hyperactive neurofibromin deficient VSMCs. While these studies establish that *Nf1* haploinsufficiency is sufficient to predispose mice to an enlarged neointima compared to WT controls *in vivo*, several questions remain. Blood vessels are composed primarily of a continuous monolayer of ECs surrounded by VSMCs. Dysfunction of either cell type can result in intimal hyperplasia, which can ultimately lead to occlusive vascular disease. Further, animal studies of arterial mechanical injury have now shown that mobilization and transmigration of BMDCs into the intima in response to vascular injury directly contributes to neointima formation (111, 115-117, 196). Therefore, based on the complex interaction between cells in response to arterial injury and the global control of Ras signaling, it is essential that the predominant cell lineage(s) involved in neointima formation in $Nf1^{+/-}$ mice be dissected in order to determine the optimal treatment and prevention of NF1 vasculopathy.

Dissecting the Cellular Contribution to NF1 Vasculopathy.

Vessel wall homeostasis requires a tightly regulated interaction between vascular cells and circulating BMDCs. The endothelium functions as a barrier between the VSMCs within the vessel wall and the blood, controlling the transmigration of circulating cells into the vessel and inhibiting the proliferation and migration of VSMCs within the vessel wall (56, 57). Endothelial dysfunction can be caused by a number of factors including oxidative stress, inflammatory cytokine activation, changes in shear stress or injury (113, 197-200). A hallmark of endothelial dysfunction is the reduced production of nitric oxide, a potent inhibitor of VSMC proliferation (201). Further, endothelial activation by inflammatory cytokines or changes in shear stress upregulates the expression of adhesion molecules on the surface of the endothelium, recruiting circulating inflammatory cells to the vessel wall (56, 112, 113, 202, 203). Endothelial activation is one of the first steps in vascular inflammation, initiating a cascade of events that, if unchecked, result in vascular lesion formation (105, 204). Neurofibromin is a known critical regulator of Ras activation in ECs, VSMCs and BMDCs, however it remains unclear whether endothelial dysfunction, hyperproliferation or migration of VSMCs or increased activation of circulating BMDCs is the predominant factor in neointima formation in $Nf1^{+/-}$ mice. Therefore, we interrogated the role of heterozygous inactivation of $Nf1$ in ECs, VSMCs and BMDCs to neointima formation.

In this study, we demonstrated that heterozygous inactivation of $Nf1$ in ECs or VSMCs alone was insufficient to recapitulate the enhanced neointima

formation observed in $Nf1^{+/-}$ mice in response to carotid ligation. Carotid ligation

was chosen for inducing neointima formation in these studies because of the

techniques reproducibility. Neointima formation in response to carotid ligation

results from changes in shear stress and the migration of leukocytes into the

vessel wall (108, 161). In our studies, morphometric analysis showed that WT,

$Nf1^{flox/+}$;Tie2cre and $Nf1^{flox/+}$;SM22cre had similar neointima formation in

response to ligation, and all were significantly lower than $Nf1^{+/-}$ mice (Figure 17

and 18). However, heterozygous inactivation of Nf1 in BMDCs alone was

sufficient for neointima formation in response to vascular injury (Figure 19 and

20). Specifically, we showed that both WT and $Nf1^{+/-}$ mice reconstituted with

$Nf1^{+/-}$ BMDCs had enhanced neointima formation characterized by an

accumulation of BMDCs in response to carotid ligation (Figure 18 and 19). At 28

days post-ligation, mice transplanted with WT bone marrow had minimal

neointima formation, suggesting that heterozygous inactivation of Nf1 results in

increased recruitment and accumulation of BMDCs. Specifically,

immunohistochemistry demonstrated that in WT and $Nf1^{+/-}$ mice reconstituted

with $Nf1^{+/-}$ BM, 25-30% of the cells within the neointima were bone marrow

derived determined by GFP expression (Figure 23). The presence of $Nf1^{+/-}$

BMDCs within the neointima at 28 days post-ligation suggests inflammation is a

predominant factor in neointima formation given that in the original report of

carotid artery ligation, Kumar et al. described that at 28 days post-ligation,

inflammatory cells were not present in the neointima of WT mice and the majority

of the cells were VSMCs (161).

The attachment and transmigration of BMDCs has been reported by others to be essential for neointima formation (108, 110, 111). BMDCs contribute to neointima formation through the production of cytokines and growth factors to stimulate VSMC growth and proliferation as well as the addition of cellular mass to the neointima (108, 111, 150, 205, 206). It has previously been reported that BMDCs transmigrate into the neointima in response to arterial injury and differentiate into α-SMA positive VSMCs (118). To determine the origin of VSMCs within the neointima of both WT and $Nf1^{+/-}$ mice reconstituted with either WT or $Nf1^{+/-}$ BMDCs, arterial cross-sections were co-stained with an anti-GFP antibody, to identify BMDCs, and an anti-α-SMA antibody, to identify VSMCs. Analysis of co-stained arterial cross-sections under high-powered magnification determined that anti-GFP positive cells and anti-α-SMA positive cells did not colocalize (Figure 23), indicating that the VSMCs within the neointima and vessel wall were locally derived and not bone marrow derived VSMCs. These results are consistent with other reports utilizing adoptive hematopoietic stem cell transfer in models of vascular lesion formation (207). In order to fully understand the mechanism of neointima formation it is essential to determine the lineage of the BMDCs within the neointima in response to arterial injury.

Therefore, we analyzed arterial cross-sections from WT and $Nf1^{+/-}$ mice transplanted with either WT or $Nf1^{+/-}$ BMDCs utilizing immunohistochemistry to identify the lineage(s) of BMDCs within the neointima. Anti-CD45 staining of arterial cross-sections showed the same staining pattern as anti-GFP staining, indicating that the BMDCs within the neointima were of myeloid origin (Figure

25). Leukocytes, specifically lymphocytes and monocytes, have been shown to contribute to neointima formation in response to injury. Staining of arterial cross-sections to identify lymphocytes, CD3 positive cells, showed that lymphocytes did significantly accumulate within the neointima and 28 days post arterial ligation (Figure 26). Studies of lymphocyte infiltration in response to endothelial denudation have shown that lymphocytes are present at the vessel wall as early as 1 hour post-injury (172). Further, *in vivo* studies using lymphocyte deficient mice demonstrate that the infiltration of lymphocytes in response to injury have a protective effect, inhibiting the proliferation of VSMCs (172). Therefore, the role of lymphocytes in neointima formation in $Nf1^{+/-}$ mice cannot be discarded without determining if there are differences in lymphocyte infiltration at earlier timepoints in response to arterial injury compared to WT mice. Assaying for the presence of macrophages, using anti-Mac3 immunohistochemistry, demonstrated that greater than 85% of the $Nf1^{+/-}$ BMDCs within the neointima were macrophages (Figure 27). Mac3 is a glycoprotein that is produced and expressed by macrophages, but not lymphocytes or monocytes (208). Therefore, if there are immature macrophages within the vessel wall, they will not be identified by anti-Mac3 staining, which could account for the 10-15% of GFP positive cells that are not CD3 or Mac3 positive. These studies identify $Nf1^{+/-}$ BMDCs as necessary and sufficient for neointima formation and determine a new role for neurofibromin as an important regulator of macrophage function *in vivo* and *in vitro*. Further, this data provides a novel paradigm of "vascular inflammation" as the major

determinant of vessel occlusion despite the role of neurofibromin in regulating EC and VSMC function.

The Role of Macrophages in Neointima Formation.

The accumulation of macrophages in the vessel wall in response to arterial injury suggests that inflammation has a direct contribution to neointima formation in $Nf1^{+/-}$ mice. Macrophages play an important role in neointima formation through the production of growth factors and cytokines that activate ECs and stimulate VSMC migration and proliferation (209-211). Further, macrophages are a source of matrix proteases, which cleave collagen within the vessel wall (212, 213) and activation of matrix metalloproteinases, specifically the gelatinases MMP-2 and MMP-9, breaks down collagen within the vessel wall allowing VSMCs to migrate from the media into the intima in response to chemotactic agents generated by arterial injury (137, 214, 215). MMPs are expressed by macrophages and VSMCs and their expression can be induced by a number of cytokines and growth factors, including TNFα, IL-1β and PDGF-BB (138, 140, 141). MMP-9 expression has been shown to be induced in response to arterial injury and genetic deletion significantly impaired VSMC migration *in vitro* and *in vivo* (216). The expression and activation of the MMPs has not been described in neurofibromin deficient VSMCs or macrophages, however based on *in vitro* data that demonstrates that $Nf1^{+/-}$ VSMCs are hyperresponsive to PDGF-BB and our *in vivo* observations of increased macrophage function, we hypothesize that arterial injury in $Nf1^{+/-}$ mice would enhance MMP activation,

132

contributing to neointima formation. Along with cellular migration and proliferation, matrix remodeling significantly contributes to neointima formation. It has previously been reported that cellular proliferation is drastically reduced after 2 weeks post-injury although the neointima continues to develop due to the accumulation and remodeling of matrix (161, 217). The continued growth of the neointima in the absence of VSMC proliferation suggests a mechanism by which the WT mice transplanted with $Nf1^{+/-}$ bone marrow had equivalent neointima formation to $Nf1^{+/-}$ mice transplanted with $Nf1^{+/-}$ bone marrow 28 days post-injury (Figure 21 and 22) despite the observation that $Nf1^{+/-}$ mice had significantly more BMDCs within the neointima (Figure 23). These observations suggest that $Nf1^{+/-}$ vascular cells secrete increased levels of chemokines, which results in increased recruitment, retention or survival of BMDCs in the neointima compared to WT vascular cells. We predict that $Nf1^{+/-}$ mice reconstituted with $Nf1^{+/-}$ bone marrow will have increased neointima formation compared to WT mice with $Nf1^{+/-}$ bone marrow at earlier time points (i.e. 1-2 weeks) due to the increased accumulation of BMDCs in response to injury.

In order to fully understand the role of $Nf1^{+/-}$ macrophages in neointima formation, functional studies need to be completed. There are multiple mechanisms that could account for increased accumulation of $Nf1^{+/-}$ macrophages in the evolving neointima including: 1) increased recruitment to the site of injury, 2) increased proliferation within the neointima, 3) increased retention in the neointima or 4) increased survival. Recent *in vitro* studies completed in Dr. Kapur's lab indicate that bone marrow derived $Nf1^{+/-}$

macrophages have increased migration and proliferation in response to M-CSF

stimulation (Figure 28). M-CSF is a pro-inflammatory cytokine that regulates

macrophage function and is upregulated *in vivo* in response to arterial injury(211,

218). Further, exogenous administration of M-CSF significantly enhanced

neointima formation through the increased recruitment of BMDCs to the site of

injury(211). These observations suggest that $Nf1^{+/-}$ bone marrow derived

macrophages may have increased recruitment to the site of arterial injury in

response to M-CSF production. Further, once emigrated into the emerging

neointima, $Nf1^{+/-}$ macrophages may have increased proliferation in response to

M-CSF and other growth factors produced in response to injury, furthering the

accumulation of BMDCs within the neointima. However, it is not known whether

$Nf1^{+/-}$ vascular cells produce increased levels of M-CSF or other chemokines (i.e.

MCP-1) in response to arterial injury that are involved in monocyte recruitment.

Functional *in vitro* studies need to be completed to determine if heterozygous

inactivation of *Nf1* in VSMCs promotes the migration and proliferation of

macrophages. Along with increased recruitment and proliferation, M-CSF

stimulation has also been shown to promote the survival of monocytes and

macrophages.

Increased survival of $Nf1^{+/-}$ macrophages within the neointima would

enhance neointima formation through prolonged production of growth factors and

matrix remodeling. In addition to M-CSF, the multifunctional protein osteopontin

(OPN) has also been shown to promote the survival of macrophages by inhibiting

apoptosis (219). *In vivo*, OPN is upregulated in response to arterial injury (220-

222) and overexpression of OPN results in increased medial thickening and neointima formation (223), while genetic ablation of *OPN* results in protection against aneurysm formation (224). In a recent report on bone malformation and NF1, Li et al. (225) demonstrated that *Nf1*^{+/-} mice have increased serum levels of OPN compared with WT controls. Given the multiple effects of OPN, this is an important finding. In addition to its anti-apoptotic effects, OPN also stimulates VSMC proliferation and migration (226) and activates MMP-2 and MMP-9 activity, suggesting a role of OPN in vascular lesion formation in *Nf1*^{+/-} mice. While these observations suggest potential mechanisms, further characterization of neointima formation in *Nf1*^{+/-} mice needs to be completed in order to identify initiating factors. Specifically, *in vitro* studies of *Nf1*^{+/-} ECs, VSMCs and macrophages need to be completed to determine the role of neurofibromin in the production of cytokines and growth factors involved in neointima formation. Further, the expression and activity of MMPs needs to be characterized in *Nf1*^{+/-} VSMCs and macrophages. Information gathered from these studies can be applied to the expandable *in vivo* model that was developed in this study. Utilizing *cre/lox* technology and immunohistochemistry the direct role of cytokines and growth factors at early timepoints in neointima formation can be dissected.

Evidence of Vascular Inflammation in NF1 Patients.

The direct role of *Nf1*^{+/-} BMDCs and the accumulation of macrophages within the neointima of mice reconstituted with *Nf1*^{+/-} bone marrow suggests that vascular inflammation contributes to neointima formation. This observation is

intriguing given that inflammation is linked to vascular disease in patient

populations including atherosclerosis and coronary artery disease (107, 227-

229). In vascular inflammation, increased expression of adhesion molecules by

the endothelium and the production of chemokines lead to a recruitment of

BMDCs, specifically monocytes, to the site of injury initiating an inflammatory

response (112, 143, 144, 151, 190). In this study, we determined that NF1

patients, with no overt vascular disease, have increased numbers of circulating

monocytes compared to healthy controls (Figure 31). Further, we identified a

population of monocytes in NF1 patients that has characteristics of an activated

state, including increased CD16 expression and increased size (187). Increased

levels of the pro-inflammatory cytokines IL-1β and IL-6 in plasma samples from

NF1 patients (Figure 33) supports our observation that NF1 patients have

increased activated monocytes in circulation given that, in peripheral blood,

monocytes are the main producers of IL-1β and IL-6 (230, 231). IL-1β

stimulation of ECs increases the production of inflammatory cytokines, including

IL-1β and IL-6 as well as the production of chemokines which recruit monocytes

to the vessel wall, amplifying the inflammatory response (231, 232). IL-1β has

also been shown to induce the production of IL-6 in VSMCs (233). *In vitro*

studies have indicated that IL-6 stimulation of VSMCs results in increased

proliferation through the production of PDGF (234, 235). These observations

identify a mechanism by which increased circulating monocytes and increased

levels of inflammatory cytokines predispose NF1 patients to vasculopathy given

that neurofibromin deficient VSMCs are hyperproliferative in response to PDGF.

Along with endothelial activation, cytokines have been described to affect arterial endothelial dependent vasodilation. Iversen et al. demonstrated that the cytokines TNFα, IL-6 and IL-10 induced arterial contraction in an endothelial dependent manner (236). In studies completed by our collaborator, Dr. Jan Friedman, NF1 patients showed decreased endothelial dependent dilation compared to normal standards with no difference detected in smooth muscle dependent dilation. An important observation to this study was that reduced endothelial dependent dilation was observed in patients with no known vascular disease. In our study, we tested endothelial dependent vasodilation and analyzed plasma samples of NF1 patients (17±2 years of age) with no known vascular disease and showed that our patient population did not have impaired endothelial dependent vasodilation but did have increased levels of the pro-inflammatory cytokines IL-1β and IL-6. Based on these observations, inflammation precedes endothelial dysfunction in NF1 patients. Chronic inflammation results in endothelial dysfunction through the stimulation of the endothelium to produce adhesion molecules and chemokines that attract monocytes to the vessel wall. The attachment of monocytes to the vessel wall further exacerbates endothelial dysfunction through the production of activating cytokines and reactive oxygen species, which result in premature senescence. Therefore, the findings of this study suggest that all NF1 patients may have sub-clinical vascular disease. We are currently conducting studies to determine the incidence of subclinical vascular disease in NF1 patients along with identifying

potential biomarkers that correlate to the progression of vascular disease in patients.

In addition to increased levels of inflammatory cytokines, we identified that NF1 patients have increased levels the potent chemokine and adhesion molecule fractalkine (Figure 33). Membrane-bound fractalkine is an adhesion molecule expressed on an inflamed endothelium when activated by pro-inflammatory cytokines, such as TNFα and IL-1β (143, 152). Fractalkine produces a high-affinity interaction with CX3CR1 expressing cells, including inflammatory monocytes, which allows cells to rapidly bind to the endothelium under normal flow conditions (151, 191, 192). Fractalkine is cleaved from the cell membrane, resulting in soluble fractalkine which functions as a potent chemoattractant for monocytes (143). CD14$^+$CD16$^+$ monocytes preferentially express CX3CR1 and their interaction with fractalkine induces the expression of IL-6 and MMP-9 *in vitro*, further perpetuating the inflammatory response and subsequent neointima formation (153, 154, 237). *In vivo*, arterial injury upregulates the expression of fractalkine and genetic ablation of *CX3CR1* abrogates neointima formation through impaired monocyte recruitment (155). Further, single nucleotide polymorphisms within *CX3CR1* have been described in humans with a reduced incidence of atherosclerosis and cardiovascular disease (238-240). Taken together, upregulation of fractalkine expression in NF1 patients in response to increased inflammatory cytokines would result in increased recruitment and attachment of monocytes to the vessel wall leading to endothelial dysfunction and subsequent vascular disease.

In this study, we have developed an *in vivo* model of NF1 vasculopathy. We have demonstrated that $Nf1^{+/-}$ mice have increased neointima formation in response to injury and that the neointima is composed primarily of VSMCs, reminiscent of the patient phenotype. Further, we identified hyperactive Ras signaling through either the PDGF-βR or C-kit activation as potential mechanisms for increased neointima formation. The use of *cre/lox* technology and adoptive hematopoietic stem cell transfer techniques allowed us to interrogate the individual contribution of $Nf1^{+/-}$ ECs, VSMCs and BMDCs to neointima formation. The studies reported here demonstrated that heterozygous inactivation of *Nf1* in BMDCs alone is necessary and sufficient for neointima formation in response to arterial injury. The neointima of mice reconstituted with $Nf1^{+/-}$ bone marrow was characterized by an accumulation of macrophages, while mice transplanted with WT bone marrow showed minimal neointima formation. These observations demonstrate that neurofibromin is a critical regulator of macrophage function and that vascular inflammation is a leading factor in neointima formation. Further, the increased levels of circulating monocytes and increased expression of inflammatory cytokines observed in NF1 patients provide evidence of chronic inflammation associated with NF1. In sum, these studies provide the first genetic and cellular evidence of vascular inflammation in $Nf1^{+/-}$ mice and NF1 patients, and provide a framework for understanding the pathogenesis of NF1 vasculopathy and potential therapeutic and diagnostic interventions.

REFERENCES

1.   Theos, A., and Korf, B.R. 2006. Pathophysiology of neurofibromatosis type 1. *Ann Intern Med* 144:842-849.

2.   Xu, G., O'Connell, P., Viskochil, D., Cawthon, R., Robertson, M., Culver, M., Dunn, D., Stevens, J., Gesteland, R., White, R., et al. 1990. The Neurofibromatosis type 1 gene encodes a protein related to GAP. *Cell* 62:599-608.

3.   Wallace, M.R., Marchuk, D.A., Andersen, L.B., Letcher, R., Odeh, H.M., Saulino, A.M., Fountain, J.W., Brereton, A., Nicholson, J., Mitchell, A.L., et al. 1990. Type 1 neurofibromatosis gene: identification of a large transcript disrupted in three NF1 patients. *Science* 249:181-186.

4.   Viskochil, D., Buchberg, A.M., Xu, G., Cawthon, R.M., Stevens, J., Wolff, R.K., Culver, M., Carey, J.C., Copeland, N.G., Jenkins, N.A., et al. 1990. Deletions and a translocation interrupt a cloned gene at the neurofibromatosis type 1 locus. *Cell* 62:187-192.

5.   Cawthon, R.M., O'Connell, P., Buchberg, A.M., Viskochil, D., Weiss, R.B., Culver, M., Stevens, J., Jenkins, N.A., Copeland, N.G., and White, R. 1990. Identification and characterization of transcripts from the neurofibromatosis 1 region: the sequence and genomic structure of EVI2 and mapping of other transcripts. *Genomics* 7:555-565.

6.   Li, Y., O'Connell, P., Breidenbach, H.H., Cawthon, R., Stevens, J., Xu, G., Neil, S., Robertson, M., White, R., and Viskochil, D. 1995. Genomic organization of the neurofibromatosis 1 gene (NF1). *Genomics* 25:9-18.

7.   Ars, E., Kruyer, H., Morell, M., Pros, E., Serra, E., Ravella, A., Estivill, X., and Lazaro, C. 2003. Recurrent mutations in the NF1 gene are common among neurofibromatosis type 1 patients. *J Med Genet* 40:e82.

8.   Huson, S.M., Compston, D.A., Clark, P., and Harper, P.S. 1989. A genetic study of von Recklinghausen neurofibromatosis in south east Wales. I. Prevalence, fitness, mutation rate, and effect of parental transmission on severity. *J Med Genet* 26:704-711.

9.   Rasmussen, S.A., and Friedman, J.M. 2000. NF1 gene and neurofibromatosis 1. *Am J Epidemiol* 151:33-40.

10.   Upadhyaya, M., Shaw, D.J., and Harper, P.S. 1994. Molecular basis of neurofibromatosis type 1 (NF1): mutation analysis and polymorphisms in the NF1 gene. *Hum Mutat* 4:83-101.

11.   Ward, B.A., and Gutmann, D.H. 2005. Neurofibromatosis 1: from lab bench to clinic. *Pediatr Neurol* 32:221-228.

12.   Legius, E., Marchuk, D.A., Collins, F.S., and Glover, T.W. 1993. Somatic deletion of the neurofibromatosis type 1 gene in a neurofibrosarcoma supports a tumour suppressor gene hypothesis. *Nature Genet* 3:122-126.

13.   1988. Neurofibromatosis. Conference statement. National Institutes of Health Consensus Development Conference. *Arch Neurol* 45:575-578.

14. Friedman, J.M., Arbiser, J., Epstein, J.A., Gutmann, D.H., Huot, S.J., Lin, A.E., McManus, B., and Korf, B.R. 2002. Cardiovascular disease in neurofibromatosis 1: report of the NF1 Cardiovascular Task Force. *Genet Med* 4:105-111.
15. Lehrnbecher, T., Gassel, A.M., Rauh, V., Kirchner, T., and Huppertz, H.I. 1994. Neurofibromatosis presenting as a severe systemic vasculopathy. *Eur J Pediatr* 153:107-109.
16. Rasmussen, S.A., Yang, Q., and Friedman, J.M. 2001. Mortality in neurofibromatosis 1: an analysis using U.S. death certificates. *Am J Hum Genet* 68:1110-1118.
17. Rosser, T.L., Vezina, G., and Packer, R.J. 2005. Cerebrovascular abnormalities in a population of children with neurofibromatosis type 1. *Neurology* 64:553-555.
18. Reubi, F. 1945. Neurofibromatose et lesions vasculaires. *Schweizerische Medizinishe Wochenschrift* 75:463-465.
19. Salyer, W.R., and Salyer, D.C. 1974. The vascular lesions of neurofibromatosis. *Angiology* 25:510-519.
20. Greene, J.F., Jr., Fitzwater, J.E., and Burgess, J. 1974. Arterial lesions associated with neurofibromatosis. *Am J Clin Pathol* 62:481-487.
21. Hamilton, S.J., and Friedman, J.M. 2000. Insights into the pathogenesis of neurofibromatosis 1 vasculopathy. *Clin Genet* 58:341-344.
22. Kanter, R.J., Graham, M., Fairbrother, D., and Smith, S.V. 2006. Sudden cardiac death in young children with neurofibromatosis type 1. *J Pediatr* 149:718-720.
23. Marchuk, D.A., Saulino, A.M., Tavakkol, R., Swaroop, M., Wallace, M.R., Andersen, L.B., Mitchell, A.L., Gutmann, D.H., Boguski, M., and Collins, F.S. 1991. cDNA cloning of the type 1 neurofibromatosis gene: complete sequence of the NF1 gene product. *Genomics* 11:931-940.
24. Daston, M.M., Scrable, H., Nordlund, M., Sturbaum, A.K., Nissen, L.M., and Ratner, N. 1992. The protein product of the neurofibromatosis type 1 gene is expressed at highest abundance in neurons, Schwann cells, and oligodendrocytes. *Neuron* 8:415-428.
25. Boyer, M.J., Gutmann, D.H., Collins, F.S., and Bar-Sagi, D. 1994. Crosslinking of the surface immunoglobulin receptor in B lymphocytes induces a redistribution of neurofibromin but not p120-GAP. *Oncogene* 9:349-357.
26. DeClue, J.E., Cohen, B.D., and Lowy, D.R. 1991. Identification and characterization of the neurofibromatosis type 1 protein product. *Proc Natl Acad Sci U S A* 88:9914-9918.
27. Gutmann, D.H., Wood, D.L., and Collins, F.S. 1991. Identification of the neurofibromatosis type 1 gene product. *Proc Natl Acad Sci U S A* 88:9658-9662.
28. Norton, K.K., Xu, J., and Gutmann, D.H. 1995. Expression of the neurofibromatosis I gene product, neurofibromin, in blood vessel endothelial cells and smooth muscle. *Neurobiol Dis* 2:13-21.

29. Brannan, C.I., Perkins, A.S., Vogel, K.S., Ratner, N., Nordlund, M.L., Reid, S.W., Buchberg, A.M., Jenkins, N.A., Parada, L.F., and Copeland, N.G. 1994. Targeted disruption of the neurofibromatosis type-1 gene leads to developmental abnormalities in heart and various neural crest-derived tissues. *Genes Dev* 8:1019-1029.

30. Jacks, T., Shih, T.S., Schmitt, E.M., Bronson, R.T., Bernards, A., and Weinberg, R.A. 1994. Tumour predisposition in mice heterozygous for a targeted mutation in Nf1. *Nat Genet* 7:353-361.

31. Seizinger, B.R. 1993. NF1: a prevalent cause of tumorigenesis in human cancers? *Nat Genet* 3:97-99.

32. Shannon, K.M., O'Connell, P., Martin, G.A., Paderanga, D., Olson, K., Dinndorf, P., and McCormick, F. 1994. Loss of the normal NF1 allele from the bone marrow of children with type 1 neurofibromatosis and malignant myeloid disorders. *N Engl J Med* 330:597-601.

33. Xu, W., Mulligan, L.M., Ponder, M.A., Liu, L., Smith, B.A., Mathew, C.G., and Ponder, B.A. 1992. Loss of NF1 alleles in phaeochromocytomas from patients with type I neurofibromatosis. *Genes Chromosomes Cancer* 4:337-342.

34. Colman, S.D., Williams, C.A., and Wallace, M.R. 1995. Benign neurofibromas in type 1 neurofibromatosis (NF1) show somatic deletions of the NF1 gene. *Nat Genet* 11:90-92.

35. Gutmann, D.H., Loehr, A., Zhang, Y., Kim, J., Henkemeyer, M., and Cashen, A. 1999. Haploinsufficiency for the neurofibromatosis 1 (NF1) tumor suppressor results in increased astrocyte proliferation. *Oncogene* 18:4450-4459.

36. Le, L.Q., and Parada, L.F. 2007. Tumor microenvironment and neurofibromatosis type I: connecting the GAPs. *Oncogene* 26:4609-4616.

37. Silva, A.J., Frankland, P.W., Marowitz, Z., Friedman, E., Lazlo, G., Cioffi, D., Jacks, T., and Bourtchuladze, R. 1997. A mouse model for the learning and memory deficits associated with neurofibromatosis type I. *Nat Genet* 15:281-284.

38. Yang, F.C., Chen, S., Robling, A.G., Yu, X., Nebesio, T.D., Yan, J., Morgan, T., Li, X., Yuan, J., Hock, J., et al. 2006. Hyperactivation of p21ras and PI3K cooperate to alter murine and human neurofibromatosis type 1-haploinsufficient osteoclast functions. *J Clin Invest* 116:2880-2891.

39. Zhu, Y., Ghosh, P., Charnay, P., Burns, D.K., and Parada, L.F. 2002. Neurofibromas in NF1: Schwann cell origin and role of tumor environment. *Science* 296:920-922.

40. Ballaster, R., Marchuk, D., Boguski, M., Saulino, A., Letcher, R., Wigler, M., and Collins, F. 1990. The NF1 locus encodes a protein functionally related to mammalian GAP and yeast IRA proteins. *Cell* 63:851-859.

41. Buchberg, A.M., Cleveland, L.S., Jenkins, N.A., and Copeland, N.G. 1990. Sequence homology shared by neurofibromatosis type-1 gene and IRA-1 and IRA-2 negative regulators of the RAS cyclic AMP pathway. *Nature* 347:291-294.

42. Martin, G.A., Viskochil, D., Bollag, G., McCabe, P.C., Crosier, W.J., Haubruck, H., Conroy, L., Clark, R., O'Connell, P., Cawthon, R.M., et al. 1990. The GAP-related domain of the neurofibromatosis type 1 gene product interacts with ras p21. *Cell* 63:843-849.

43. Boguski, M.S., and McCormick, F. 1993. Proteins regulating Ras and its relatives. *Nature* 366:643-654.

44. Clark, C.J., Drugan, J.K., Terrell, R.S., Bradham, C., Der, C.J., Bell, R.M., and Campbell, S. 1996. Peptides containing a consensus RAS binding sequence from Raf-1 and GTPase activating protein NF1 Ras function. *Pro. Natl. Acad. Sci. USA* 93:1577-1581.

45. Hall, J.G. 1992. Genomic imprinting and its clinical implications. *N Engl J Med* 326:827-829.

46. DeClue, J.E., Papageorge, A.G., Fletcher, J.A., Diehl, S.R., Ratner, N., Vaas, W.C., and Lowry, D.R. 1992. Abnormal regulation of mammalian p21 ras contributes to malignant tumor growth in von Recklinghausen (Type 1) neurofibromatosis. *Cell* 69:265-273.

47. Viskochil, D., White, R., and Cawthon, R. 1993. The neurofibromatosis type 1 gene. *Annu Rev Neurosci* 16:183-205.

48. Li, F., Munchhof, A.M., White, H.A., Mead, L.E., Krier, T.R., Fenoglio, A., Chen, S., Wu, X., Cai, S., Yang, F.C., et al. 2006. Neurofibromin is a novel regulator of RAS-induced signals in primary vascular smooth muscle cells. *Hum Mol Genet* 15:1921-1930.

49. Munchhof, A.M., Li, F., White, H.A., Mead, L.E., Krier, T.R., Fenoglio, A., Li, X., Yuan, J., Yang, F.C., and Ingram, D.A. 2006. Neurofibroma-associated growth factors activate a distinct signaling network to alter the function of neurofibromin-deficient endothelial cells. *Hum Mol Genet* 15:1858-1869.

50. Cichowski, K., and Jacks, T. 2001. NF1 tumor suppressor gene function: narrowing the GAP. *Cell* 104:593-604.

51. The, I., Hannigan, G.E., Cowley, G.S., Reginald, S., Zhong, Y., Gusella, J.F., Hariharan, I.K., and Bernards, A. 1997. Rescue of a Drosophila NF1 mutant phenotype by protein kinase A. *Science* 276:791-794.

52. Tong, J., Hannan, F., Zhu, Y., Bernards, A., and Zhong, Y. 2002. Neurofibromin regulates G protein-stimulated adenylyl cyclase activity. *Nat Neurosci* 5:95-96.

53. Tong, J.J., Schriner, S.E., McCleary, D., Day, B.J., and Wallace, D.C. 2007. Life extension through neurofibromin mitochondrial regulation and antioxidant therapy for neurofibromatosis-1 in Drosophila melanogaster. *Nat Genet* 39:476-485.

54. Dasgupta, B., Dugan, L.L., and Gutmann, D.H. 2003. The neurofibromatosis 1 gene product neurofibromin regulates pituitary adenylate cyclase-activating polypeptide-mediated signaling in astrocytes. *J Neurosci* 23:8949-8954.

55. Kim, H.A., Ratner, N., Roberts, T.M., and Stiles, C.D. 2001. Schwann cell proliferative responses to cAMP and Nf1 are mediated by cyclin D1. *J Neurosci* 21:1110-1116.

56. Mombouli, J.V., and Vanhoutte, P.M. 1999. Endothelial dysfunction: from physiology to therapy. *J Mol Cell Cardiol* 31:61-74.

57. Rubanyi, G.M. 1993. The role of endothelium in cardiovascular homeostasis and diseases. *J Cardiovasc Pharmacol* 22 Suppl 4:S1-14.

58. Chen, J., and Goligorsky, M.S. 2006. Premature senescence of endothelial cells: Methusaleh's dilemma. *Am J Physiol Heart Circ Physiol* 290:H1729-1739.

59. Buetow, B.S., Tappan, K.A., Crosby, J.R., Seifert, R.A., and Bowen-Pope, D.F. 2003. Chimera analysis supports a predominant role of PDGFRbeta in promoting smooth-muscle cell chemotaxis after arterial injury. *Am J Pathol* 163:979-984.

60. Ferns, G.A., Raines, E.W., Sprugel, K.H., Motani, A.S., Reidy, M.A., and Ross, R. 1991. Inhibition of neointimal smooth muscle accumulation after angioplasty by an antibody to PDGF. *Science* 253:1129-1132.

61. Jackson, C.L., Raines, E.W., Ross, R., and Reidy, M.A. 1993. Role of endogenous platelet-derived growth factor in arterial smooth muscle cell migration after balloon catheter injury. *Arterioscler Thromb* 13:1218-1226.

62. Jawien, A., Bowen-Pope, D.F., Lindner, V., Schwartz, S.M., and Clowes, A.W. 1992. Platelet-derived growth factor promotes smooth muscle migration and intimal thickening in a rat model of balloon angioplasty. *J Clin Invest* 89:507-511.

63. Boucher, P., Gotthardt, M., Li, W.P., Anderson, R.G., and Herz, J. 2003. LRP: role in vascular wall integrity and protection from atherosclerosis. *Science* 300:329-332.

64. Bowen-Pope, D.F., Ross, R., and Seifert, R.A. 1985. Locally acting growth factors for vascular smooth muscle cells: endogenous synthesis and release from platelets. *Circulation* 72:735-740.

65. Chen, K.H., Guo, X., Ma, D., Guo, Y., Li, Q., Yang, D., Li, P., Qiu, X., Wen, S., Xiao, R.P., et al. 2004. Dysregulation of HSG triggers vascular proliferative disorders. *Nat Cell Biol* 6:872-883.

66. Chien, K.R., and Hoshijima, M. 2004. Unravelling Ras signals in cardiovascular disease. *Nat Cell Biol* 6:807-808.

67. Indolfi, C., Chiariello, M., and Avvedimento, E.V. 1996. Selective gene therapy for proliferative disorders: sense and antisense. *Nat Med* 2:634-635.

68. Jin, G., Chieh-Hsi Wu, J., Li, Y.S., Hu, Y.L., Shyy, J.Y., and Chien, S. 2000. Effects of active and negative mutants of Ras on rat arterial neointima formation. *J Surg Res* 94:124-132.

69. Kouchi, H., Nakamura, K., Fushimi, K., Sakaguchi, M., Miyazaki, M., Ohe, T., and Namba, M. 1999. Manumycin A, inhibitor of ras farnesyltransferase, inhibits proliferation and migration of rat vascular smooth muscle cells. *Biochem Biophys Res Commun* 264:915-920.

70. Ueno, H., Yamamoto, H., Ito, S., Li, J.J., and Takeshita, A. 1997. Adenovirus-mediated transfer of a dominant-negative H-ras suppresses neointimal formation in balloon-injured arteries in vivo. *Arterioscler Thromb Vasc Biol* 17:898-904.

71. Wu, C.H., Lin, C.S., Hung, J.S., Wu, C.J., Lo, P.H., Jin, G., Shyy, Y.J., Mao, S.J., and Chien, S. 2001. Inhibition of neointimal formation in porcine coronary artery by a Ras mutant. *J Surg Res* 99:100-106.

72. Zhang, S., Ren, J., Khan, M.F., Cheng, A.M., Abendschein, D., and Muslin, A.J. 2003. Grb2 is required for the development of neointima in response to vascular injury. *Arterioscler Thromb Vasc Biol* 23:1788-1793.

73. Bourne, H., Sanders, D., and McCormick, F. 1990. The GTPase superfamily: a conserved switch for diverse cell functions. *Nature* 348:125-132.

74. Bourne, H.R., Sanders, D.A., and McCormick, F. 1991. The GTPase superfamily: conserved structure and molecular mechanism. *Nature* 349:117-127.

75. Hall, A. 1990. The cellular functions of small GTP-Binding proteins. *Science* 249:635-640.

76. Hill, C., and Treisman, R. 1995. Transcriptional regulation by extracellular signals: Mechanisms and specificity. *Cell* 80:199-211.

77. Raines, E.W. 2004. PDGF and cardiovascular disease. *Cytokine Growth Factor Rev* 15:237-254.

78. Xu, J., Ismat, F.A., Wang, T., Yang, J., and Epstein, J.A. 2007. NF1 regulates a Ras-dependent vascular smooth muscle proliferative injury response. *Circulation* 116:2148-2156.

79. Gennaro, G., Menard, C., Michaud, S.E., Deblois, D., and Rivard, A. 2004. Inhibition of vascular smooth muscle cell proliferation and neointimal formation in injured arteries by a novel, oral mitogen-activated protein kinase/extracellular signal-regulated kinase inhibitor. *Circulation* 110:3367-3371.

80. Gitler, A.D., Zhu, Y., Ismat, F.A., Lu, M.M., Yamauchi, Y., Parada, L.F., and Epstein, J.A. 2003. Nf1 has an essential role in endothelial cells. *Nat Genet* 33:75-79.

81. Spyridopoulos, I., Isner, J.M., and Losordo, D.W. 2002. Oncogenic ras induces premature senescence in endothelial cells: role of p21(Cip1/Waf1). *Basic Res Cardiol* 97:117-124.

82. Erusalimsky, J.D., and Kurz, D.J. 2005. Cellular senescence in vivo: its relevance in ageing and cardiovascular disease. *Exp Gerontol* 40:634-642.

83. Counter, C.M., Avilion, A.A., LeFeuvre, C.E., Stewart, N.G., Greider, C.W., Harley, C.B., and Bacchetti, S. 1992. Telomere shortening associated with chromosome instability is arrested in immortal cells which express telomerase activity. *Embo J* 11:1921-1929.

84. Campisi, J., Kim, S.H., Lim, C.S., and Rubio, M. 2001. Cellular senescence, cancer and aging: the telomere connection. *Exp Gerontol* 36:1619-1637.

85. Chiu, C.P., and Harley, C.B. 1997. Replicative senescence and cell immortality: the role of telomeres and telomerase. *Proc Soc Exp Biol Med* 214:99-106.

86. Foreman, K.E., and Tang, J. 2003. Molecular mechanisms of replicative senescence in endothelial cells. *Exp Gerontol* 38:1251-1257.

87. Minamino, T., Miyauchi, H., Yoshida, T., Tateno, K., Kunieda, T., and Komuro, I. 2004. Vascular cell senescence and vascular aging. *J Mol Cell Cardiol* 36:175-183.

88. Matsushita, H., Chang, E., Glassford, A.J., Cooke, J.P., Chiu, C.P., and Tsao, P.S. 2001. eNOS activity is reduced in senescent human endothelial cells: Preservation by hTERT immortalization. *Circ Res* 89:793-798.

89. Sato, I., Morita, I., Kaji, K., Ikeda, M., Nagao, M., and Murota, S. 1993. Reduction of nitric oxide producing activity associated with in vitro aging in cultured human umbilical vein endothelial cell. *Biochem Biophys Res Commun* 195:1070-1076.

90. Munzel, T., Daiber, A., Ullrich, V., and Mulsch, A. 2005. Vascular consequences of endothelial nitric oxide synthase uncoupling for the activity and expression of the soluble guanylyl cyclase and the cGMP-dependent protein kinase. *Arterioscler Thromb Vasc Biol* 25:1551-1557.

91. Zou, M.H., Shi, C., and Cohen, R.A. 2002. Oxidation of the zinc-thiolate complex and uncoupling of endothelial nitric oxide synthase by peroxynitrite. *J Clin Invest* 109:817-826.

92. Uematsu, M., Ohara, Y., Navas, J.P., Nishida, K., Murphy, T.J., Alexander, R.W., Nerem, R.M., and Harrison, D.G. 1995. Regulation of endothelial cell nitric oxide synthase mRNA expression by shear stress. *Am J Physiol* 269:C1371-1378.

93. Burrig, K.F. 1991. The endothelium of advanced arteriosclerotic plaques in humans. *Arterioscler Thromb* 11:1678-1689.

94. Deanfield, J.E., Halcox, J.P., and Rabelink, T.J. 2007. Endothelial function and dysfunction: testing and clinical relevance. *Circulation* 115:1285-1295.

95. Moncada, S., Palmer, R.M., and Higgs, E.A. 1991. Nitric oxide: physiology, pathophysiology, and pharmacology. *Pharmacol Rev* 43:109-142.

96. Radomski, M.W., Palmer, R.M., and Moncada, S. 1987. The role of nitric oxide and cGMP in platelet adhesion to vascular endothelium. *Biochem Biophys Res Commun* 148:1482-1489.

97. Radomski, M.W., Palmer, R.M., and Moncada, S. 1987. Endogenous nitric oxide inhibits human platelet adhesion to vascular endothelium. *Lancet* 2:1057-1058.

98. Shelton, D.N., Chang, E., Whittier, P.S., Choi, D., and Funk, W.D. 1999. Microarray analysis of replicative senescence. *Curr Biol* 9:939-945.

99. Barath, P., Fishbein, M.C., Cao, J., Berenson, J., Helfant, R.H., and Forrester, J.S. 1990. Detection and localization of tumor necrosis factor in human atheroma. *Am J Cardiol* 65:297-302.

100. Lindmark, E., Diderholm, E., Wallentin, L., and Siegbahn, A. 2001. Relationship between interleukin 6 and mortality in patients with unstable coronary artery disease: effects of an early invasive or noninvasive strategy. *Jama* 286:2107-2113.

101. Porsch-Oezcueruemez, M., Kunz, D., Kloer, H.U., and Luley, C. 1999. Evaluation of serum levels of solubilized adhesion molecules and cytokine receptors in coronary heart disease. *J Am Coll Cardiol* 34:1995-2001.
102. Schlitt, A., Heine, G.H., Blankenberg, S., Espinola-Klein, C., Dopheide, J.F., Bickel, C., Lackner, K.J., Iz, M., Meyer, J., Darius, H., et al. 2004. CD14+CD16+ monocytes in coronary artery disease and their relationship to serum TNF-alpha levels. *Thromb Haemost* 92:419-424.
103. Skoog, T., Dichtl, W., Boquist, S., Skoglund-Andersson, C., Karpe, F., Tang, R., Bond, M.G., de Faire, U., Nilsson, J., Eriksson, P., et al. 2002. Plasma tumour necrosis factor-alpha and early carotid atherosclerosis in healthy middle-aged men. *Eur Heart J* 23:376-383.
104. Szmitko, P.E., Wang, C.H., Weisel, R.D., de Almeida, J.R., Anderson, T.J., and Verma, S. 2003. New markers of inflammation and endothelial cell activation: Part I. *Circulation* 108:1917-1923.
105. Rao, R.M., Yang, L., Garcia-Cardena, G., and Luscinskas, F.W. 2007. Endothelial-dependent mechanisms of leukocyte recruitment to the vascular wall. *Circ Res* 101:234-247.
106. Charo, I.F., and Ransohoff, R.M. 2006. The many roles of chemokines and chemokine receptors in inflammation. *N Engl J Med* 354:610-621.
107. Hansson, G.K. 2005. Inflammation, atherosclerosis, and coronary artery disease. *N Engl J Med* 352:1685-1695.
108. Kumar, A., Hoover, J.L., Simmons, C.A., Lindner, V., and Shebuski, R.J. 1997. Remodeling and neointimal formation in the carotid artery of normal and P-selectin-deficient mice. *Circulation* 96:4333-4342.
109. Oguchi, S., Dimayuga, P., Zhu, J., Chyu, K.Y., Yano, J., Shah, P.K., Nilsson, J., and Cercek, B. 2000. Monoclonal antibody against vascular cell adhesion molecule-1 inhibits neointimal formation after periadventitial carotid artery injury in genetically hypercholesterolemic mice. *Arterioscler Thromb Vasc Biol* 20:1729-1736.
110. Schober, A., Zernecke, A., Liehn, E.A., von Hundelshausen, P., Knarren, S., Kuziel, W.A., and Weber, C. 2004. Crucial role of the CCL2/CCR2 axis in neointimal hyperplasia after arterial injury in hyperlipidemic mice involves early monocyte recruitment and CCL2 presentation on platelets. *Circ Res* 95:1125-1133.
111. Simon, D.I., Dhen, Z., Seifert, P., Edelman, E.R., Ballantyne, C.M., and Rogers, C. 2000. Decreased neointimal formation in Mac-1(-/-) mice reveals a role for inflammation in vascular repair after angioplasty. *J Clin Invest* 105:293-300.
112. Davies, M.J., Gordon, J.L., Gearing, A.J., Pigott, R., Woolf, N., Katz, D., and Kyriakopoulos, A. 1993. The expression of the adhesion molecules ICAM-1, VCAM-1, PECAM, and E-selectin in human atherosclerosis. *J Pathol* 171:223-229.
113. Gimbrone, M.A., Jr., Topper, J.N., Nagel, T., Anderson, K.R., and Garcia-Cardena, G. 2000. Endothelial dysfunction, hemodynamic forces, and atherogenesis. *Ann N Y Acad Sci* 902:230-239; discussion 239-240.

114. Sata, M., Saiura, A., Kunisato, A., Tojo, A., Okada, S., Tokuhisa, T., Hirai, H., Makuuchi, M., Hirata, Y., and Nagai, R. 2002. Hematopoietic stem cells differentiate into vascular cells that participate in the pathogenesis of atherosclerosis. *Nat Med* 8:403-409.

115. Wang, C.H., Anderson, N., Li, S.H., Szmitko, P.E., Cherng, W.J., Fedak, P.W., Fazel, S., Li, R.K., Yau, T.M., Weisel, R.D., et al. 2006. Stem cell factor deficiency is vasculoprotective: unraveling a new therapeutic potential of imatinib mesylate. *Circ Res* 99:617-625.

116. Roque, M., Fallon, J.T., Badimon, J.J., Zhang, W.X., Taubman, M.B., and Reis, E.D. 2000. Mouse model of femoral artery denudation injury associated with the rapid accumulation of adhesion molecules on the luminal surface and recruitment of neutrophils. *Arterioscler Thromb Vasc Biol* 20:335-342.

117. Tanaka, H., Sukhova, G.K., Swanson, S.J., Clinton, S.K., Ganz, P., Cybulsky, M.I., and Libby, P. 1993. Sustained activation of vascular cells and leukocytes in the rabbit aorta after balloon injury. *Circulation* 88:1788-1803.

118. Tanaka, K., Sata, M., Hirata, Y., and Nagai, R. 2003. Diverse contribution of bone marrow cells to neointimal hyperplasia after mechanical vascular injuries. *Circ Res* 93:783-790.

119. Welt, F.G., Edelman, E.R., Simon, D.I., and Rogers, C. 2000. Neutrophil, not macrophage, infiltration precedes neointimal thickening in balloon-injured arteries. *Arterioscler Thromb Vasc Biol* 20:2553-2558.

120. Egashira, K., Zhao, Q., Kataoka, C., Ohtani, K., Usui, M., Charo, I.F., Nishida, K., Inoue, S., Katoh, M., Ichiki, T., et al. 2002. Importance of monocyte chemoattractant protein-1 pathway in neointimal hyperplasia after periarterial injury in mice and monkeys. *Circ Res* 90:1167-1172.

121. Domen, J., and Weissman, I.L. 2000. Hematopoietic stem cells need two signals to prevent apoptosis; BCL-2 can provide one of these, Kitl/c-Kit signaling the other. *J Exp Med* 192:1707-1718.

122. Fleming, W.H., Alpern, E.J., Uchida, N., Ikuta, K., and Weissman, I.L. 1993. Steel factor influences the distribution and activity of murine hematopoietic stem cells in vivo. *Proc Natl Acad Sci U S A* 90:3760-3764.

123. Leary, A.G., Zeng, H.Q., Clark, S.C., and Ogawa, M. 1992. Growth factor requirements for survival in G0 and entry into the cell cycle of primitive human hemopoietic progenitors. *Proc Natl Acad Sci U S A* 89:4013-4017.

124. Linnekin, D. 1999. Early signaling pathways activated by c-Kit in hematopoietic cells. *Int J Biochem Cell Biol* 31:1053-1074.

125. Ingram, D.A., Hiatt, K., King, A.J., Fisher, L., Shivakumar, R., Derstine, C., Wenning, M.J., Diaz, B., Travers, J.B., Hood, A., et al. 2001. Hyperactivation of p21^{ras} and the hematopoietic-specific Rho GTPase, Rac2, cooperate to alter the proliferation of neurofibromin deficient mast cells *in vivo* and *in vitro*. *J Exp Med* 194:57-70.

126. Ingram, D.A., Yang, F.C., Travers, J.B., Wenning, M.J., Hiatt, K., New, S., Hood, A., Shannon, K., Williams, D.A., and Clapp, D.W. 2000. Genetic and biochemical evidence that haploinsufficiency of the *Nf1* tumor suppressor gene modulates melanocyte and mast cell fates *in vivo. J Exp Med* 191:181-188.

127. Zhang, Y.Y., Vik, T.A., Ryder, J.W., Srour, E.F., Jacks, T., Shannon, K., and Clapp, D.W. 1998. *Nf1* regulates hematopoietic progenitor cell growth and ras signaling in response to multiple cytokines. *J Exp Med* 187:1893-1902.

128. Bollag, G., Clapp, D.W., Shih, S., Adler, F., Zhang, Y.Y., Thompson, P., Lange, B.J., Freedman, M.H., McCormick, F., Jacks, T., et al. 1996. Loss of NF1 results in activation of the Ras signaling pathway and leads to aberrant growth in haematopoietic cells. *Nat Genet* 12:144-148.

129. Largaespada, D.A., Brannan, C.I., Jenkins, N.A., and Copeland, N.G. 1996. Nf1 deficiency causes Ras-mediated granulocyte/macrophage colony stimulating factor hypersensitivity and chronic myeloid leukaemia. *Nat Genet* 12:137-143.

130. Zhang, Y., Taylor, B., Shannon, K., and Clapp, D.W. 2001. Quantitative effects of *Nf1* inactivation on in vivo hematopoiesis. *J. Clin. Invest.* 108:709-715.

131. Fu, Y.X., Cai, J.P., Chin, Y.H., Watson, G.A., and Lopez, D.M. 1992. Regulation of leukocyte binding to endothelial tissues by tumor-derived GM-CSF. *Int J Cancer* 50:585-588.

132. Gamble, J.R., Elliott, M.J., Jaipargas, E., Lopez, A.F., and Vadas, M.A. 1989. Regulation of human monocyte adherence by granulocyte-macrophage colony-stimulating factor. *Proc Natl Acad Sci U S A* 86:7169-7173.

133. Bergamini, A., Bolacchi, F., Bongiovanni, B., Cepparulo, M., Ventura, L., Capozzi, M., Sarrecchia, C., and Rocchi, G. 2000. Granulocyte-macrophage colony-stimulating factor regulates cytokine production in cultured macrophages through CD14-dependent and -independent mechanisms. *Immunology* 101:254-261.

134. Harris, A.K., Shen, J., Radford, J., Bao, S., and Hambly, B.D. 2009. GM-CSF deficiency delays neointima formation in a normolipidemic mouse model of endoluminal endothelial damage. *Immunol Cell Biol* 87:122-130.

135. Myllarniemi, M., Calderon, L., Lemstrom, K., Buchdunger, E., and Hayry, P. 1997. Inhibition of platelet-derived growth factor receptor tyrosine kinase inhibits vascular smooth muscle cell migration and proliferation. *Faseb J* 11:1119-1126.

136. Yamasaki, Y., Miyoshi, K., Oda, N., Watanabe, M., Miyake, H., Chan, J., Wang, X., Sun, L., Tang, C., McMahon, G., et al. 2001. Weekly dosing with the platelet-derived growth factor receptor tyrosine kinase inhibitor SU9518 significantly inhibits arterial stenosis. *Circ Res* 88:630-636.

137. Bendeck, M.P., Zempo, N., Clowes, A.W., Galardy, R.E., and Reidy, M.A. 1994. Smooth muscle cell migration and matrix metalloproteinase expression after arterial injury in the rat. *Circ Res* 75:539-545.

138. Galis, Z.S., Muszynski, M., Sukhova, G.K., Simon-Morrissey, E., Unemori, E.N., Lark, M.W., Amento, E., and Libby, P. 1994. Cytokine-stimulated human vascular smooth muscle cells synthesize a complement of enzymes required for extracellular matrix digestion. *Circ Res* 75:181-189.

139. Hibbs, M.S., Hoidal, J.R., and Kang, A.H. 1987. Expression of a metalloproteinase that degrades native type V collagen and denatured collagens by cultured human alveolar macrophages. *J Clin Invest* 80:1644-1650.

140. Saren, P., Welgus, H.G., and Kovanen, P.T. 1996. TNF-alpha and IL-1beta selectively induce expression of 92-kDa gelatinase by human macrophages. *J Immunol* 157:4159-4165.

141. Dollery, C.M., McEwan, J.R., and Henney, A.M. 1995. Matrix metalloproteinases and cardiovascular disease. *Circ Res* 77:863-868.

142. Godin, D., Ivan, E., Johnson, C., Magid, R., and Galis, Z.S. 2000. Remodeling of carotid artery is associated with increased expression of matrix metalloproteinases in mouse blood flow cessation model. *Circulation* 102:2861-2866.

143. Bazan, J.F., Bacon, K.B., Hardiman, G., Wang, W., Soo, K., Rossi, D., Greaves, D.R., Zlotnik, A., and Schall, T.J. 1997. A new class of membrane-bound chemokine with a CX3C motif. *Nature* 385:640-644.

144. Bevilacqua, M.P., and Gimbrone, M.A., Jr. 1987. Inducible endothelial functions in inflammation and coagulation. *Semin Thromb Hemost* 13:425-433.

145. Murao, K., Ohyama, T., Imachi, H., Ishida, T., Cao, W.M., Namihira, H., Sato, M., Wong, N.C., and Takahara, J. 2000. TNF-alpha stimulation of MCP-1 expression is mediated by the Akt/PKB signal transduction pathway in vascular endothelial cells. *Biochem Biophys Res Commun* 276:791-796.

146. Belge, K.U., Dayyani, F., Horelt, A., Siedlar, M., Frankenberger, M., Frankenberger, B., Espevik, T., and Ziegler-Heitbrock, L. 2002. The proinflammatory CD14+CD16+DR++ monocytes are a major source of TNF. *J Immunol* 168:3536-3542.

147. Clausell, N., de Lima, V.C., Molossi, S., Liu, P., Turley, E., Gotlieb, A.I., Adelman, A.G., and Rabinovitch, M. 1995. Expression of tumour necrosis factor alpha and accumulation of fibronectin in coronary artery restenotic lesions retrieved by atherectomy. *Br Heart J* 73:534-539.

148. Jovinge, S., Hultgardh-Nilsson, A., Regnstrom, J., and Nilsson, J. 1997. Tumor necrosis factor-alpha activates smooth muscle cell migration in culture and is expressed in the balloon-injured rat aorta. *Arterioscler Thromb Vasc Biol* 17:490-497.

149. Rus, H.G., Niculescu, F., and Vlaicu, R. 1991. Tumor necrosis factor-alpha in human arterial wall with atherosclerosis. *Atherosclerosis* 89:247-254.

150. Zimmerman, M.A., Selzman, C.H., Reznikov, L.L., Miller, S.A., Raeburn, C.D., Emmick, J., Meng, X., and Harken, A.H. 2002. Lack of TNF-alpha attenuates intimal hyperplasia after mouse carotid artery injury. *Am J Physiol Regul Integr Comp Physiol* 283:R505-512.
151. Fong, A.M., Robinson, L.A., Steeber, D.A., Tedder, T.F., Yoshie, O., Imai, T., and Patel, D.D. 1998. Fractalkine and CX3CR1 mediate a novel mechanism of leukocyte capture, firm adhesion, and activation under physiologic flow. *J Exp Med* 188:1413-1419.
152. Umehara, H., Bloom, E.T., Okazaki, T., Nagano, Y., Yoshie, O., and Imai, T. 2004. Fractalkine in vascular biology: from basic research to clinical disease. *Arterioscler Thromb Vasc Biol* 24:34-40.
153. Ancuta, P., Rao, R., Moses, A., Mehle, A., Shaw, S.K., Luscinskas, F.W., and Gabuzda, D. 2003. Fractalkine preferentially mediates arrest and migration of CD16+ monocytes. *J Exp Med* 197:1701-1707.
154. Geissmann, F., Jung, S., and Littman, D.R. 2003. Blood monocytes consist of two principal subsets with distinct migratory properties. *Immunity* 19:71-82.
155. Liu, P., Patil, S., Rojas, M., Fong, A.M., Smyth, S.S., and Patel, D.D. 2006. CX3CR1 deficiency confers protection from intimal hyperplasia after arterial injury. *Arterioscler Thromb Vasc Biol* 26:2056-2062.
156. Ferns, G.A., Stewart-Lee, A.L., and Anggard, E.E. 1992. Arterial response to mechanical injury: balloon catheter de-endothelialization. *Atherosclerosis* 92:89-104.
157. Lindner, V., Fingerle, J., and Reidy, M.A. 1993. Mouse model of arterial injury. *Circ Res* 73:792-796.
158. Heldin, C.H., Westermark, B., and Wasteson, A. 1981. Platelet-derived growth factor. Isolation by a large-scale procedure and analysis of subunit composition. *Biochem J* 193:907-913.
159. Ross, R. 1987. Platelet-derived growth factor. *Annu Rev Med* 38:71-79.
160. Lewis, C.D., Olson, N.E., Raines, E.W., Reidy, M.A., and Jackson, C.L. 2001. Modulation of smooth muscle proliferation in rat carotid artery by platelet-derived mediators and fibroblast growth factor-2. *Platelets* 12:352-358.
161. Kumar, A., and Lindner, V. 1997. Remodeling with neointima formation in the mouse carotid artery after cessation of blood flow. *Arterioscler Thromb Vasc Biol* 17:2238-2244.
162. Asakura, T., and Karino, T. 1990. Flow patterns and spatial distribution of atherosclerotic lesions in human coronary arteries. *Circ Res* 66:1045-1066.
163. Ku, D.N., Giddens, D.P., Zarins, C.K., and Glagov, S. 1985. Pulsatile flow and atherosclerosis in the human carotid bifurcation. Positive correlation between plaque location and low oscillating shear stress. *Arteriosclerosis* 5:293-302.
164. Harmon, K.J., Couper, L.L., and Lindner, V. 2000. Strain-dependent vascular remodeling phenotypes in inbred mice. *Am J Pathol* 156:1741-1748.

165. Kuhel, D.G., Zhu, B., Witte, D.P., and Hui, D.Y. 2002. Distinction in genetic determinants for injury-induced neointimal hyperplasia and diet-induced atherosclerosis in inbred mice. *Arterioscler Thromb Vasc Biol* 22:955-960.

166. Tolbert, T., Thompson, J.A., Bouchard, P., and Oparil, S. 2001. Estrogen-induced vasoprotection is independent of inducible nitric oxide synthase expression: evidence from the mouse carotid artery ligation model. *Circulation* 104:2740-2745.

167. Werner, N., Junk, S., Laufs, U., Link, A., Walenta, K., Bohm, M., and Nickenig, G. 2003. Intravenous transfusion of endothelial progenitor cells reduces neointima formation after vascular injury. *Circ Res* 93:e17-24.

168. Burke, G.L., Evans, G.W., Riley, W.A., Sharrett, A.R., Howard, G., Barnes, R.W., Rosamond, W., Crow, R.S., Rautaharju, P.M., and Heiss, G. 1995. Arterial wall thickness is associated with prevalent cardiovascular disease in middle-aged adults. The Atherosclerosis Risk in Communities (ARIC) Study. *Stroke* 26:386-391.

169. Huang, J., and Kontos, C.D. 2002. Inhibition of vascular smooth muscle cell proliferation, migration, and survival by the tumor suppressor protein PTEN. *Arterioscler Thromb Vasc Biol* 22:745-751.

170. Mourani, P.M., Garl, P.J., Wenzlau, J.M., Carpenter, T.C., Stenmark, K.R., and Weiser-Evans, M.C. 2004. Unique, highly proliferative growth phenotype expressed by embryonic and neointimal smooth muscle cells is driven by constitutive Akt, mTOR, and p70S6K signaling and is actively repressed by PTEN. *Circulation* 109:1299-1306.

171. Zhan, Y., Kim, S., Izumi, Y., Izumiya, Y., Nakao, T., Miyazaki, H., and Iwao, H. 2003. Role of JNK, p38, and ERK in platelet-derived growth factor-induced vascular proliferation, migration, and gene expression. *Arterioscler Thromb Vasc Biol* 23:795-801.

172. Zhu, B., Reardon, C.A., Getz, G.S., and Hui, D.Y. 2002. Both apolipoprotein E and immune deficiency exacerbate neointimal hyperplasia after vascular injury in mice. *Arterioscler Thromb Vasc Biol* 22:450-455.

173. Regan, C.P., Adam, P.J., Madsen, C.S., and Owens, G.K. 2000. Molecular mechanisms of decreased smooth muscle differentiation marker expression after vascular injury. *J Clin Invest* 106:1139-1147.

174. Scholzen, T., and Gerdes, J. 2000. The Ki-67 protein: from the known and the unknown. *J Cell Physiol* 182:311-322.

175. Kisanuki, Y.Y., Hammer, R.E., Miyazaki, J., Williams, S.C., Richardson, J.A., and Yanagisawa, M. 2001. Tie2-Cre transgenic mice: a new model for endothelial cell-lineage analysis in vivo. *Dev Biol* 230:230-242.

176. Holtwick, R., Gotthardt, M., Skryabin, B., Steinmetz, M., Potthast, R., Zetsche, B., Hammer, R.E., Herz, J., and Kuhn, M. 2002. Smooth muscle-selective deletion of guanylyl cyclase-A prevents the acute but not chronic effects of ANP on blood pressure. *Proc Natl Acad Sci U S A* 99:7142-7147.

177. Soriano, P. 1999. Generalized lacZ expression with the ROSA26 Cre reporter strain. *Nat Genet* 21:70-71.
178. Chamberlain, J., Evans, D., King, A., Dewberry, R., Dower, S., Crossman, D., and Francis, S. 2006. Interleukin-1beta and signaling of interleukin-1 in vascular wall and circulating cells modulates the extent of neointima formation in mice. *Am J Pathol* 168:1396-1403.
179. Galli, S.J. 1993. New concepts about the mast cell. *N Engl J Med* 328:257-265.
180. Libby, P., and Shi, G.P. 2007. Mast cells as mediators and modulators of atherogenesis. *Circulation* 115:2471-2473.
181. Murayama, H., Takahashi, M., Takamoto, M., Shiba, Y., Ise, H., Koyama, J., Tagawa, Y., Iwakura, Y., and Ikeda, U. 2008. Deficiency of tumour necrosis factor-alpha and interferon-gamma in bone marrow cells synergistically inhibits neointimal formation following vascular injury. *Cardiovasc Res* 80:175-180.
182. Rectenwald, J.E., Moldawer, L.L., Huber, T.S., Seeger, J.M., and Ozaki, C.K. 2000. Direct evidence for cytokine involvement in neointimal hyperplasia. *Circulation* 102:1697-1702.
183. Tennant, G.M., Wadsworth, R.M., and Kennedy, S. 2008. PAR-2 mediates increased inflammatory cell adhesion and neointima formation following vascular injury in the mouse. *Atherosclerosis* 198:57-64.
184. Ingram, D.A., Zhang, L., McCarthy, J., Wenning, M.J., Fisher, L., Yang, F.C., Clapp, D.W., and Kapur, R. 2002. Lymphoproliferative defects in mice lacking the expression of neurofibromin: functional and biochemical consequences of Nf1 deficiency in T-cell development and function. *Blood* 100:3656-3662.
185. Todd, R.F., 3rd, Van Agthoven, A., Schlossman, S.F., and Terhorst, C. 1982. Structural analysis of differentiation antigens Mo1 and Mo2 on human monocytes. *Hybridoma* 1:329-337.
186. Grage-Griebenow, E., Flad, H.D., and Ernst, M. 2001. Heterogeneity of human peripheral blood monocyte subsets. *J Leukoc Biol* 69:11-20.
187. Abel, P.M., McSharry, C., Galloway, E., Ross, C., Severn, A., Toner, G., Gruer, L., and Wilkinson, P.C. 1992. Heterogeneity of peripheral blood monocyte populations in human immunodeficiency virus-1 seropositive patients. *FEMS Microbiol Immunol* 5:317-323.
188. Cesari, M., Penninx, B.W., Newman, A.B., Kritchevsky, S.B., Nicklas, B.J., Sutton-Tyrrell, K., Rubin, S.M., Ding, J., Simonsick, E.M., Harris, T.B., et al. 2003. Inflammatory markers and onset of cardiovascular events: results from the Health ABC study. *Circulation* 108:2317-2322.
189. Luc, G., Bard, J.M., Juhan-Vague, I., Ferrieres, J., Evans, A., Amouyel, P., Arveiler, D., Fruchart, J.C., and Ducimetiere, P. 2003. C-reactive protein, interleukin-6, and fibrinogen as predictors of coronary heart disease: the PRIME Study. *Arterioscler Thromb Vasc Biol* 23:1255-1261.
190. Mantovani, A., Bussolino, F., and Dejana, E. 1992. Cytokine regulation of endothelial cell function. *Faseb J* 6:2591-2599.

191. Goda, S., Imai, T., Yoshie, O., Yoneda, O., Inoue, H., Nagano, Y., Okazaki, T., Imai, H., Bloom, E.T., Domae, N., et al. 2000. CX3C-chemokine, fractalkine-enhanced adhesion of THP-1 cells to endothelial cells through integrin-dependent and -independent mechanisms. *J Immunol* 164:4313-4320.

192. Imai, T., Hieshima, K., Haskell, C., Baba, M., Nagira, M., Nishimura, M., Kakizaki, M., Takagi, S., Nomiyama, H., Schall, T.J., et al. 1997. Identification and molecular characterization of fractalkine receptor CX3CR1, which mediates both leukocyte migration and adhesion. *Cell* 91:521-530.

193. 1988. Neurofibromatosis. Conference statement. National Institutes of Health Consensus Development Conference. *Arch Neurol* 45:575-578.

194. Yoder, M.C., Mead, L.E., Prater, D., Krier, T.R., Mroueh, K.N., Li, F., Krasich, R., Temm, C.J., Prchal, J.T., and Ingram, D.A. 2007. Redefining endothelial progenitor cells via clonal analysis and hematopoietic stem/progenitor cell principals. *Blood* 109:1801-1809.

195. Buchdunger, E., Cioffi, C.L., Law, N., Stover, D., Ohno-Jones, S., Druker, B.J., and Lydon, N.B. 2000. Abl protein-tyrosine kinase inhibitor STI571 inhibits in vitro signal transduction mediated by c-kit and platelet-derived growth factor receptors. *J Pharmacol Exp Ther* 295:139-145.

196. Zernecke, A., Schober, A., Bot, I., von Hundelshausen, P., Liehn, E.A., Mopps, B., Mericskay, M., Gierschik, P., Biessen, E.A., and Weber, C. 2005. SDF-1alpha/CXCR4 axis is instrumental in neointimal hyperplasia and recruitment of smooth muscle progenitor cells. *Circ Res* 96:784-791.

197. Cai, H., and Harrison, D.G. 2000. Endothelial dysfunction in cardiovascular diseases: the role of oxidant stress. *Circ Res* 87:840-844.

198. Cleland, S.J., Sattar, N., Petrie, J.R., Forouhi, N.G., Elliott, H.L., and Connell, J.M. 2000. Endothelial dysfunction as a possible link between C-reactive protein levels and cardiovascular disease. *Clin Sci (Lond)* 98:531-535.

199. De Keulenaer, G.W., Chappell, D.C., Ishizaka, N., Nerem, R.M., Alexander, R.W., and Griendling, K.K. 1998. Oscillatory and steady laminar shear stress differentially affect human endothelial redox state: role of a superoxide-producing NADH oxidase. *Circ Res* 82:1094-1101.

200. Ross, R. 1993. The pathogenesis of atherosclerosis: a perspective for the 1990s. *Nature* 362:801-809.

201. Davignon, J., and Ganz, P. 2004. Role of endothelial dysfunction in atherosclerosis. *Circulation* 109:III27-32.

202. Chappell, D.C., Varner, S.E., Nerem, R.M., Medford, R.M., and Alexander, R.W. 1998. Oscillatory shear stress stimulates adhesion molecule expression in cultured human endothelium. *Circ Res* 82:532-539.

203. Nagel, T., Resnick, N., Atkinson, W.J., Dewey, C.F., Jr., and Gimbrone, M.A., Jr. 1994. Shear stress selectively upregulates intercellular adhesion molecule-1 expression in cultured human vascular endothelial cells. *J Clin Invest* 94:885-891.

204. Kofler, S., Nickel, T., and Weis, M. 2005. Role of cytokines in cardiovascular diseases: a focus on endothelial responses to inflammation. *Clin Sci (Lond)* 108:205-213.

205. Han, C.I., Campbell, G.R., and Campbell, J.H. 2001. Circulating bone marrow cells can contribute to neointimal formation. *J Vasc Res* 38:113-119.

206. Moreno, P.R., Bernardi, V.H., Lopez-Cuellar, J., Newell, J.B., McMellon, C., Gold, H.K., Palacios, I.F., Fuster, V., and Fallon, J.T. 1996. Macrophage infiltration predicts restenosis after coronary intervention in patients with unstable angina. *Circulation* 94:3098-3102.

207. Bentzon, J.F., Weile, C., Sondergaard, C.S., Hindkjaer, J., Kassem, M., and Falk, E. 2006. Smooth muscle cells in atherosclerosis originate from the local vessel wall and not circulating progenitor cells in ApoE knockout mice. *Arterioscler Thromb Vasc Biol* 26:2696-2702.

208. Ho, M.K., and Springer, T.A. 1983. Tissue distribution, structural characterization, and biosynthesis of Mac-3, a macrophage surface glycoprotein exhibiting molecular weight heterogeneity. *J Biol Chem* 258:636-642.

209. Danenberg, H.D., Welt, F.G., Walker, M., 3rd, Seifert, P., Toegel, G.S., and Edelman, E.R. 2002. Systemic inflammation induced by lipopolysaccharide increases neointimal formation after balloon and stent injury in rabbits. *Circulation* 105:2917-2922.

210. Hanke, H., Hassenstein, S., Ulmer, A., Kamenz, J., Oberhoff, M., Haase, K.K., Baumbach, A., Gown, A.M., and Karsch, K.R. 1994. Accumulation of macrophages in the arterial vessel wall following experimental balloon angioplasty. *Eur Heart J* 15:691-698.

211. Shiba, Y., Takahashi, M., Yoshioka, T., Yajima, N., Morimoto, H., Izawa, A., Ise, H., Hatake, K., Motoyoshi, K., and Ikeda, U. 2007. M-CSF accelerates neointimal formation in the early phase after vascular injury in mice: the critical role of the SDF-1-CXCR4 system. *Arterioscler Thromb Vasc Biol* 27:283-289.

212. Ikeda, U., and Shimada, K. 2003. Matrix metalloproteinases and coronary artery diseases. *Clin Cardiol* 26:55-59.

213. Matrisian, L.M. 1992. The matrix-degrading metalloproteinases. *Bioessays* 14:455-463.

214. Cho, A., and Reidy, M.A. 2002. Matrix metalloproteinase-9 is necessary for the regulation of smooth muscle cell replication and migration after arterial injury. *Circ Res* 91:845-851.

215. Kuzuya, M., Kanda, S., Sasaki, T., Tamaya-Mori, N., Cheng, X.W., Itoh, T., Itohara, S., and Iguchi, A. 2003. Deficiency of gelatinase a suppresses smooth muscle cell invasion and development of experimental intimal hyperplasia. *Circulation* 108:1375-1381.

216. Galis, Z.S., Johnson, C., Godin, D., Magid, R., Shipley, J.M., Senior, R.M., and Ivan, E. 2002. Targeted disruption of the matrix metalloproteinase-9 gene impairs smooth muscle cell migration and geometrical arterial remodeling. *Circ Res* 91:852-859.

217. Clowes, A.W., Reidy, M.A., and Clowes, M.M. 1983. Kinetics of cellular proliferation after arterial injury. I. Smooth muscle growth in the absence of endothelium. *Lab Invest* 49:327-333.

218. Finkelstein, A., Makkar, R., Doherty, T.M., Vegesna, V.R., Tripathi, P., Liu, M., Bergman, J., Fishbein, M., Hausleiter, J., Takizawa, K., et al. 2002. Increased expression of macrophage colony-stimulating factor after coronary artery balloon injury is inhibited by intracoronary brachytherapy. *Circulation* 105:2411-2415.

219. Burdo, T.H., Wood, M.R., and Fox, H.S. 2007. Osteopontin prevents monocyte recirculation and apoptosis. *J Leukoc Biol* 81:1504-1511.

220. Corjay, M.H., Diamond, S.M., Schlingmann, K.L., Gibbs, S.K., Stoltenborg, J.K., and Racanelli, A.L. 1999. alphavbeta3, alphavbeta5, and osteopontin are coordinately upregulated at early time points in a rabbit model of neointima formation. *J Cell Biochem* 75:492-504.

221. Giachelli, C., Bae, N., Lombardi, D., Majesky, M., and Schwartz, S. 1991. Molecular cloning and characterization of 2B7, a rat mRNA which distinguishes smooth muscle cell phenotypes in vitro and is identical to osteopontin (secreted phosphoprotein I, 2aR). *Biochem Biophys Res Commun* 177:867-873.

222. Srivatsa, S.S., Fitzpatrick, L.A., Tsao, P.W., Reilly, T.M., Holmes, D.R., Jr., Schwartz, R.S., and Mousa, S.A. 1997. Selective alpha v beta 3 integrin blockade potently limits neointimal hyperplasia and lumen stenosis following deep coronary arterial stent injury: evidence for the functional importance of integrin alpha v beta 3 and osteopontin expression during neointima formation. *Cardiovasc Res* 36:408-428.

223. Isoda, K., Nishikawa, K., Kamezawa, Y., Yoshida, M., Kusuhara, M., Moroi, M., Tada, N., and Ohsuzu, F. 2002. Osteopontin plays an important role in the development of medial thickening and neointimal formation. *Circ Res* 91:77-82.

224. Bruemmer, D., Collins, A.R., Noh, G., Wang, W., Territo, M., Arias-Magallona, S., Fishbein, M.C., Blaschke, F., Kintscher, U., Graf, K., et al. 2003. Angiotensin II-accelerated atherosclerosis and aneurysm formation is attenuated in osteopontin-deficient mice. *J Clin Invest* 112:1318-1331.

225. Li, H., Liu, Y., Zhang, Q., Jing, Y., Chen, S., Song, Z., Yan, J., Li, Y., Wu, X., Zhang, X., et al. 2009. Ras dependent paracrine secretion of osteopontin by Nf1+/- osteoblasts promote osteoclast activation in a neurofibromatosis type I murine model. *Pediatr Res* 65:613-618.

226. Liaw, L., Skinner, M.P., Raines, E.W., Ross, R., Cheresh, D.A., Schwartz, S.M., and Giachelli, C.M. 1995. The adhesive and migratory effects of osteopontin are mediated via distinct cell surface integrins. Role of alpha v beta 3 in smooth muscle cell migration to osteopontin in vitro. *J Clin Invest* 95:713-724.

227. Libby, P., Ridker, P.M., and Maseri, A. 2002. Inflammation and atherosclerosis. *Circulation* 105:1135-1143.

228. Packard, R.R., and Libby, P. 2008. Inflammation in atherosclerosis: from vascular biology to biomarker discovery and risk prediction. *Clin Chem* 54:24-38.
229. Ross, R. 1999. Atherosclerosis--an inflammatory disease. *N Engl J Med* 340:115-126.
230. Dinarello, C.A., and Wolff, S.M. 1993. The role of interleukin-1 in disease. *N Engl J Med* 328:106-113.
231. Sironi, M., Breviario, F., Proserpio, P., Biondi, A., Vecchi, A., Van Damme, J., Dejana, E., and Mantovani, A. 1989. IL-1 stimulates IL-6 production in endothelial cells. *J Immunol* 142:549-553.
232. Shalaby, M.R., Waage, A., and Espevik, T. 1989. Cytokine regulation of interleukin 6 production by human endothelial cells. *Cell Immunol* 121:372-382.
233. Loppnow, H., and Libby, P. 1990. Proliferating or interleukin 1-activated human vascular smooth muscle cells secrete copious interleukin 6. *J Clin Invest* 85:731-738.
234. Ikeda, U., Ikeda, M., Oohara, T., Oguchi, A., Kamitani, T., Tsuruya, Y., and Kano, S. 1991. Interleukin 6 stimulates growth of vascular smooth muscle cells in a PDGF-dependent manner. *Am J Physiol* 260:H1713-1717.
235. Raines, E.W., Dower, S.K., and Ross, R. 1989. Interleukin-1 mitogenic activity for fibroblasts and smooth muscle cells is due to PDGF-AA. *Science* 243:393-396.
236. Iversen, P.O., Nicolaysen, A., Kvernebo, K., Benestad, H.B., and Nicolaysen, G. 1999. Human cytokines modulate arterial vascular tone via endothelial receptors. *Pflugers Arch* 439:93-100.
237. Ancuta, P., Wang, J., and Gabuzda, D. 2006. CD16+ monocytes produce IL-6, CCL2, and matrix metalloproteinase-9 upon interaction with CX3CL1-expressing endothelial cells. *J Leukoc Biol* 80:1156-1164.
238. McDermott, D.H., Fong, A.M., Yang, Q., Sechler, J.M., Cupples, L.A., Merrell, M.N., Wilson, P.W., D'Agostino, R.B., O'Donnell, C.J., Patel, D.D., et al. 2003. Chemokine receptor mutant CX3CR1-M280 has impaired adhesive function and correlates with protection from cardiovascular disease in humans. *J Clin Invest* 111:1241-1250.
239. McDermott, D.H., Halcox, J.P., Schenke, W.H., Waclawiw, M.A., Merrell, M.N., Epstein, N., Quyyumi, A.A., and Murphy, P.M. 2001. Association between polymorphism in the chemokine receptor CX3CR1 and coronary vascular endothelial dysfunction and atherosclerosis. *Circ Res* 89:401-407.
240. Moatti, D., Faure, S., Fumeron, F., Amara Mel, W., Seknadji, P., McDermott, D.H., Debre, P., Aumont, M.C., Murphy, P.M., de Prost, D., et al. 2001. Polymorphism in the fractalkine receptor CX3CR1 as a genetic risk factor for coronary artery disease. *Blood* 97:1925-1928.

CURRICULUM VITAE

Elisabeth A. Lasater

EDUCATION:

Undergraduate

2000-2004	Western Washington University, Bellingham, WA	B.S.: Biochemistry

Graduate

2004-12/2009	Indiana University, Indianapolis, IN	Ph.D: Biochemistry Minor:Pharmacology

RESEARCH EXPERIENCE:

Indiana University School of Medicine
Graduate Student, Department of Biochemistry and Cellular Biology, 2004-2009.
Dr. David Ingram, MD
Dissertation title: *Dissecting Neurofibromatosis Type 1 Related Vasculopathy.*

Western Washington University
Undergraduate Research, Department of Chemistry, 2003-2004.
Dr. Salvatore Russo, Ph.D.
Use of HPLC to determine binding affinity between GAPDH and trehalose.

SKILLS and LAB TECHNIQUES:

Endothelial cell culture, isolation of endothelial cells from cord blood and adult peripheral blood, shRNA technology, flow cytometry, *cre/lox* technology, histology, immunohistochemistry, gel electrophoresis and Western blot, cellular phenotyping by FACs analysis

HONORS and AWARDS:

2009	Indiana University School of Medicine Travel Award
2008	Indiana University School of Medicine Department of Biochemistry Poster Presentation Award
2008	Indiana University School of Medicine Travel Award

2002-2004	National Society of Collegiate Scholars member
Spring 2001	President's List
2000-2001	Charter Fund Scholarship
2000-2002	Presidential Scholarship, Western Washington University
2000-2004	L.S. Wood Charitable Trust Scholarship
2000-2004	Jessie Deardorff Memorial Scholarship
2000	Valedictorian, Rifle High School, Rifle, CO

GRANTS AND FELLOWSHIPS:

PRIOR SUPPORT:

"Development of an *In Vivo* Model to Assess the Pathogenesis of Neurofibromatosis Type 1 Associated Vasculopathy", Indiana University School of Medicine, 7/01/06-6/30/07.

"Dissecting Neurofibromatosis Type 1 Related Vasculopathy", American Heart Association Greater Midwest Affiliate Predoctoral Fellowship, 7/01/07-6/30/09.

"Dissecting Neurofibromatosis Type 1 Related Vasculopathy", Children's Tumor Foundation Young Investigator Award, 7/01/07, Declined Award Due to Alternate Funding.

PEER REVIEWED PUBLICATIONS:

Lasater EA, Bessler WK, Mead LE, Horn WE, Clapp DW, Conway SJ, Ingram DA, Li F. *Nf1*$^{+/-}$ Mice Have Increased Neointima Formation via Hyperactivation of a Gleevec Sensitive Pathway. *Human Molecular Genetics* 17:2336-2344 2008 (Selected as cover image).

Lasater EA, Li F, Bessler WK, Estes ML, Vemula S, Hingtgen CM, Kapur R, Conway SJ, Ingram DA. Genetic and Cellular Evidence of Vascular Inflammation in Neurofibromin Deficient Mice and Humans. *Journal of Clinical Investigation* In Press 2010.

INVITED LECTURES:

2007	"Neurofibromatosis Type 1 Related Vasculopathy", Department of Biochemistry, Indiana University School of Medicine.
2007	"Dissecting Neurofibromatosis Type 1 Related Vasculopathy", Herman B Wells Center for Pediatric Research, Indiana University School of Medicine.

2008   "*Nf1$^{+/-}$* Mice Have Enhance Neointima Formation via Hyperactivation of a Gleevec Sensitive Pathway and Complex Interactions of Multiple Vascular Cell Lineages", Department of Biochemistry, Indiana University School of Medicine.

2009   "Use of Mouse Models to Dissect Neurofibromatosis Type 1 Related Vasculopathy", Herman B Wells Center for Pediatric Research, Indiana University School of Medicine.

2009   "Dissecting Neurofibromatosis Type 1 Related Vasculopathy", Novartis Institutes for BioMedical Research, Emeryville, CA.

2009   "Use of Mouse Models to Dissect Neurofibromatosis Type 1 Related Vasculopathy", University of California-San Francisco.

ABSTRACTS:

2008   "*Nf1$^{+/-}$* Mice Have Enhanced Neointima Formation via Hyperactivation of a Gleevec Sensitive Pathway and Complex Interactions of Multiple Vascular Cell Lineages", Children's Tumor Foundation NF Conference 2008 (oral presentation).

2009   "Neurofibromatosis Type 1 Vasculopathy Results from Interaction Between Vascular Cells and Bone Marrow Derived Cells", Arteriosclerosis Thrombosis and Vascular Biology Scientific Sessions.

2009   "Vascular Inflammation Contributes to Neointima Formation in *Nf1$^{+/-}$* Mice", Children's Tumor Foundation NF Conference.